Journal of Computational Physics 228 (2009) 6629–6669

Contents lists available at ScienceDirect

Journal of Computational Physics

journal homepage: www.elsevier.com/locate/jcp

Numerical approximation of the Vlasov–Poisson–Fokker–Planck system in two dimensions

Stephen Wollman *, Ercument Ozizmir

The College of Staten Island, CUNY, 2800 Victory Boulevard, Staten Island, NY 10314, USA

ARTICLE INFO

Article history:
Received 7 April 2008
Received in revised form 27 April 2009
Accepted 11 May 2009
Available online 22 May 2009

MSC:
65M06
65M25
82D10

Keywords:
Collisional plasma
Two-dimensional Vlasov–Poisson–Fokker–Planck system
Deterministic particle method

ABSTRACT

A numerical method is developed for approximating the solution to the Vlasov–Poisson–Fokker–Planck system in two spatial dimensions. The method generalizes the approximation for the system in one dimension given in [S. Wollman, E. Ozizmir, Numerical approximation of the Vlasov–Poisson–Fokker–Planck system in one dimension, J. Comput. Phys. 202 (2005) 602–644]. The numerical procedure is based on a change of variables that puts the convection–diffusion equation into a form so that finite difference methods for parabolic type partial differential equations can be applied. The computational cycle combines a type of deterministic particle method with a periodic interpolation of the solution along particle trajectories onto a fixed grid. computational work is done to demonstrate the accuracy and effectiveness of the approximation method. Parts of the numerical procedure are adapted to run on a parallel computer.

1. Introduction

The purpose of this paper is to develop a numerical method for approximating the Vlasov–Poisson–Fokker–Planck system in two spatial dimension, i.e., in a four dimensional phase space. Let $x = (x_1, x_2)$, $v = (v_1, v_2)$

$$\nabla_x = \left(\frac{\partial}{\partial x_1}, \frac{\partial}{\partial x_2}\right), \quad \nabla_v = \left(\frac{\partial}{\partial v_1}, \frac{\partial}{\partial v_2}\right), \quad \Delta_x = \frac{\partial^2}{\partial x_1^2} + \frac{\partial^2}{\partial x_2^2}.$$

The set $\mathcal{A} \in R^4$ is defined as $\mathcal{A} = \{(x, v)/0 \leqslant x_1, x_2 \leqslant L, -\infty < v_1, v_2 < \infty\}$. For $(x, v) \in \mathcal{A}$ and $t \in [0, T]$ the equations with periodic boundary conditions are given as

$$\begin{aligned} &\frac{\partial f}{\partial t} + v \cdot \nabla_x f + E(x,t) \cdot \nabla_v f = \nabla_v \cdot (\beta v f + q \nabla_v f), \quad f(x, v, 0) = f_0(x, v), \\ &f(0, x_2, v, t) = f(L, x_2, v, t), \quad f(x_1, 0, v, t) = f(x_1, L, v, t). \end{aligned} \tag{1.1}$$

Also it is assumed that $\lim_{|v|\to\infty} f(x, v, t) = 0$. Eq. (1.1) is combined with

$$E(x,t) = -\nabla_x \phi$$

* Corresponding author. Tel.: +1 718 982 3614.
E-mail address: wollman@math.csi.cuny.edu (S. Wollman).

0021-9991/$ - see front matter © 2009 Elsevier Inc. All rights reserved.
doi:10.1016/j.jcp.2009.05.027

where

$$\begin{aligned} &\Delta_x \phi = -\rho(x,t) \\ &\phi(0,x_2,t) = \phi(L,x_2,t), \quad \phi(x_1,0,t) = \phi(x_1,L,t) \end{aligned} \tag{1.2}$$

and

$$\rho(x,t) = \int f(x,v,t)dv - h(x).$$

The Eqs. (1.1) and (1.2) are a mathematical model for a collisional, electrostatic plasma. The function, $f(x,v,t)$, is the phase space distribution function for a single species of charged particles in the presence of a fixed background charge density given by $h(x)$. In (1.1) $\beta > 0$ and $q > 0$ are constants. The parameter β relates to the viscosity, and q is a coefficient of diffusion. A brief description of the numerical method of the present paper is contained in [29].

The Fokker–Planck equation of the form (1.1) is derived by Chandrasekhar in [10] in connection with the theory of Brownian motion. The equation has been used as a model for small angle collisions in a plasma. Accordingly in papers [1,12,16,20] a one dimensional version of (1.1) and (1.2) is used to study collisional effects on Landau damping. In this application the function, f, is regarded as an electron distribution in a fixed background of opposite charge. Another application for a Fokker–Planck equation of type (1.1) is the momentum relaxation of a small admixture of a heavy gas in a light one [21]. The light gas is assumed to be in equilibrium. For such an application the function, f, can be regarded as a distribution of heavy positive ions [6]. The Eqs. (1.1) and (1.2) also find applications in the study of the statistical properties of laser light. A reference for the Fokker–Planck equation in this context is [24]. As a model for electron–electron and electron–ion collisions in a plasma the equation with β, q constant has its limitations as is pointed out in [20, footnote 3]. The more complete Fokker–Planck model for such collisions requires that β, q in (1.1) be respectively vector and tensor expressions in terms of velocity, v. In an equivalent form the equation is then referred to as the Fokker–Planck–Landau equation, [17].

In the collisionless case, $\beta = q = 0$, a numerical approximation is given for a 2-D periodic problem of this type by Shoucri and Gagne [26]. In [28] we develop a numerical method for the Vlasov–Poisson–Fokker–Planck system in 1-D. An analysis of the convergence and accuracy of the method as applied to a linear Vlasov–Fokker–Planck equation in 1-D is carried out in [30]. The goal of the present work is to extend the method of [28] to the Vlasov–Poisson–Fokker–Planck system in two dimensions. We also consider the system for which there is a constant magnetic field in the $z = x_3$ direction. In this case the force, $E(x,t)$, in (1.1) is replaced with $E(x,t) + v \times B$, and $B = (0,0,B_z)$ with B_z a constant. Letting $v = (v_1, v_2, v_3)$, $E = (E_1, E_2, 0)$ then $E(x,t) + v \times B = (E_1 + v_2 B_z, E_2 - v_1 B_z, 0)$. Our methods can apply to the system with the resulting $v \times B$ force included. A description of the electrostatic problem with the constant magnetic field for collisionless plasma is contained in [18].

A number of other papers have been written on the numerical approximation of the Vlasov–Poisson–Fokker–Planck system in higher dimensions. Random particle methods are considered in [1,15]. In [3,4] convergence analyses are carried out for types of finite element approximations. A type of deterministic particle method based on a splitting of operations between a convection step and a diffusion step is developed in [16]. Numerical solutions based on expanding the distribution function in terms of spherical harmonics are obtained in [5]. A numerical method for a Vlasov–Fokker–Planck system in 2-D with a self consistent electric and magnetic field is in [19]. Some papers on the approximation of the Fokker–Planck–Landau system are [7,11,23]. Additional related work is contained in [9,13,14].

2. Change of variables

2.1. Electrostatic case, $B_z = 0$

We start by considering the system (1.1) and (1.2) without the magnetic field. The numerical method is based on making a change of variables to put (1.1) into a form so that finite difference methods for parabolic type PDE's can be applied. To reformulate the system this way we first consider the transport Eq. (1.1) as an initial value problem in all space, i.e., $-\infty < x_1, x_2 < \infty$, and with $E(x,t)$ as a known function. The characteristic equations associated with the first order transport part of (1.1) in component form are

$$\begin{aligned} &\frac{dx_1}{dt} = v_1, \quad x_1(0) = \xi_1 \\ &\frac{dx_2}{dt} = v_2, \quad x_2(0) = \xi_2 \\ &\frac{dv_1}{dt} = E_1(x(t),t) - \beta v_1, \quad v_1(0) = \eta_1 \\ &\frac{dv_2}{dt} = E_2(x(t),t) - \beta v_2, \quad v_2(0) = \eta_2 \end{aligned} \tag{2.1}$$

The solution is written

$$x_1(t) = x_1(\xi_1,\xi_2,\eta_1,\eta_2,t), \quad x_2(t) = x_2(\xi_1,\xi_2,\eta_1,\eta_2,t),$$
$$v_1(t) = v_1(\xi_1,\xi_2,\eta_1,\eta_2,t), \quad v_2(t) = v_2(\xi_1,\xi_2,\eta_1,\eta_2,t). \tag{2.2}$$

The solution to (2.1) defines a transformation of $R_4 \to R_4$ as $(\xi,\eta) \to (x(\xi,\eta,t), v(\xi,\eta,t))$. The Jacobian of this transformation is $\partial(x,v)/\partial(\xi,\eta) = e^{-2\beta t} \neq 0$. Thus the transformation is invertible. Let the inverse transformation be given by

$$\xi_1 = \xi_1(x_1,x_2,v_1,v_2,t), \quad \xi_2 = \xi_2(x_1,x_2,v_1,v_2,t),$$
$$\eta_1 = \eta_1(x_1,x_2,v_1,v_2,t), \quad \eta_2 = \eta_2(x_1,x_2,v_1,v_2,t). \tag{2.3}$$

The functions (2.3) are independent integrals of the system (2.1). Following the procedure in [10] the Eq. (1.1) is written in terms of the variables (ξ,η).

$$\frac{\partial f}{\partial t} - 2\beta f - q\left[\left(\left(\frac{\partial\xi_1}{\partial v_1}\right)^2 + \left(\frac{\partial\xi_1}{\partial v_2}\right)^2\right)\frac{\partial^2 f}{\partial\xi_1^2} + \left(\left(\frac{\partial\xi_2}{\partial v_1}\right)^2 + \left(\frac{\partial\xi_2}{\partial v_2}\right)^2\right)\frac{\partial^2 f}{\partial\xi_2^2} + \left(\left(\frac{\partial\eta_1}{\partial v_1}\right)^2 + \left(\frac{\partial\eta_1}{\partial v_2}\right)^2\right)\frac{\partial^2 f}{\partial\eta_1^2}\right.$$
$$+\left(\left(\frac{\partial\eta_2}{\partial v_1}\right)^2 + \left(\frac{\partial\eta_2}{\partial v_2}\right)^2\right)\frac{\partial^2 f}{\partial\eta_2^2} + 2\left(\left[\left(\frac{\partial\xi_1}{\partial v_1}\right)\left(\frac{\partial\xi_2}{\partial v_1}\right) + \left(\frac{\partial\xi_1}{\partial v_2}\right)\left(\frac{\partial\xi_2}{\partial v_2}\right)\right]\frac{\partial^2 f}{\partial\xi_1\partial\xi_2} + \cdots + \left[\left(\frac{\partial\eta_1}{\partial v_1}\right)\left(\frac{\partial\eta_2}{\partial v_1}\right)\right.\right.$$
$$\left.\left.\left.+\left(\frac{\partial\eta_1}{\partial v_2}\right)\left(\frac{\partial\eta_2}{\partial v_2}\right)\right]\frac{\partial^2 f}{\partial\eta_1\partial\eta_2}\right) + \left(\frac{\partial^2\xi_1}{\partial v_1^2} + \frac{\partial^2\xi_1}{\partial v_2^2}\right)\frac{\partial f}{\partial\xi_1} + \cdots + \left(\frac{\partial^2\eta_2}{\partial v_1^2} + \frac{\partial^2\eta_2}{\partial v_2^2}\right)\frac{\partial f}{\partial\eta_2}\right] = 0$$

With a change of dependent variable $f(\xi,\eta,t) = e^{2\beta t} g(\xi,\eta,t)$ one obtains the initial value problem for g as

$$\frac{\partial g}{\partial t} = q\left(\sum_{i=1}^{2}\left(\left(\frac{\partial\xi_i}{\partial v_1}\right)^2 + \left(\frac{\partial\xi_i}{\partial v_2}\right)^2\right)\frac{\partial^2 g}{\partial\xi_i^2} + \sum_{j=1}^{2}\left(\left(\frac{\partial\eta_j}{\partial v_1}\right)^2 + \left(\frac{\partial\eta_j}{\partial v_2}\right)^2\right)\frac{\partial^2 g}{\partial\eta_j^2}\right.$$
$$+2\left[\left(\left(\frac{\partial\xi_1}{\partial v_1}\right)\left(\frac{\partial\xi_2}{\partial v_1}\right) + \left(\frac{\partial\xi_1}{\partial v_2}\right)\left(\frac{\partial\xi_2}{\partial v_2}\right)\right)\frac{\partial^2 g}{\partial\xi_1\partial\xi_2} + \sum_{i=1}^{2}\sum_{j=1}^{2}\left(\left(\frac{\partial\xi_i}{\partial v_1}\right)\left(\frac{\partial\eta_j}{\partial v_1}\right) + \left(\frac{\partial\xi_i}{\partial v_2}\right)\left(\frac{\partial\eta_j}{\partial v_2}\right)\right)\frac{\partial^2 g}{\partial\xi_i\partial\eta_j}\right.$$
$$\left.\left.+\left(\left(\frac{\partial\eta_1}{\partial v_1}\right)\left(\frac{\partial\eta_2}{\partial v_1}\right) + \left(\frac{\partial\eta_1}{\partial v_2}\right)\left(\frac{\partial\eta_2}{\partial v_2}\right)\right)\frac{\partial^2 g}{\partial\eta_1\partial\eta_2}\right] + \sum_{i=1}^{2}\left(\frac{\partial^2\xi_i}{\partial v_1^2} + \frac{\partial^2\xi_i}{\partial v_2^2}\right)\frac{\partial g}{\partial\xi_i} + \sum_{j=1}^{2}\left(\frac{\partial^2\eta_j}{\partial v_1^2} + \frac{\partial^2\eta_j}{\partial v_2^2}\right)\frac{\partial g}{\partial\eta_j}\right)$$
$$g(\xi,\eta,0) = f_0(\xi,\eta). \tag{2.4}$$

We need to write the coefficients of (2.4) as functions of ξ,η and t. This involves writing derivatives of ξ,η with respect to v_1, v_2 in terms of derivatives of $x(\xi,\eta,t), v(\xi,\eta,t)$ with respect to ξ,η. Let

$$Q = \begin{pmatrix} \frac{\partial x_1}{\partial\xi_1} & \cdots & & \frac{\partial x_1}{\partial\eta_2} \\ \vdots & \ddots & \ddots & \vdots \\ \frac{\partial v_2}{\partial\xi_1} & & \cdots & \frac{\partial v_2}{\partial\eta_2} \end{pmatrix}, \quad \bar{u} = \left[\frac{\partial\xi_1}{\partial v_1}, \frac{\partial\xi_2}{\partial v_1}, \frac{\partial\eta_1}{\partial v_1}, \frac{\partial\eta_2}{\partial v_1}\right], \quad \bar{b} = [0,0,1,0].$$

Here Q is the matrix for the Jacobian determinant $\partial(x,v)/\partial(\xi,\eta)$. Expressions for the first derivatives of ξ,η with respect to v_1 are obtained as solutions to

$$Q\bar{u} = \bar{b}. \tag{2.5}$$

Expressions for the first derivatives of ξ,η with respect to v_2 are obtained as the solution to (2.5) but with $\bar{u} = \left[\frac{\partial\xi_1}{\partial v_2}, \frac{\partial\xi_2}{\partial v_2}, \frac{\partial\eta_1}{\partial v_2}, \frac{\partial\eta_2}{\partial v_2}\right]$ and $\bar{b} = [0,0,0,1]$. Thus we let $\left(\frac{\partial\xi_1}{\partial v_1}\right)^2 + \left(\frac{\partial\xi_1}{\partial v_2}\right)^2 = c_1(\xi,\eta,t)$ as the coefficient of $\frac{\partial^2 g}{\partial\xi_1^2}$ in which $c_1(\xi,\eta,t)$ is an expression involving first derivatives of $x(\xi,\eta,t), v(\xi,\eta,t)$ with respect to ξ,η. Similarly one obtains coefficients $c_2(\xi,\eta,t),\ldots,c_{10}(\xi,\eta,t)$ of the other second partial terms in (2.4) of the form $\partial^2 g/(\partial\xi_1^{r_1}\partial\xi_2^{r_2}\partial\eta_1^{s_1}\partial\eta_2^{s_2})$, $0 \leqslant r_1, r_2, s_1, s_2 \leqslant 2$, $r_1 + r_2 + s_1 + s_2 = 2$.

The coefficients in (2.4) of the first partial terms with respect to ξ,η involve second derivatives of ξ,η with respect to v_1, v_2. Let $\bar{y} = \left[\frac{\partial^2\xi_1}{\partial v_1^2}, \frac{\partial^2\xi_2}{\partial v_1^2}, \frac{\partial^2\eta_1}{\partial v_1^2}, \frac{\partial^2\eta_2}{\partial v_1^2}\right]$. The vector $\bar{y}$ is obtained as the solution to

$$Q\bar{y} = -\bar{F} \tag{2.6}$$

where $\bar{F} = [F_1,F_2,F_3,F_4]^T$. Here $F_1 = \bar{u}A\bar{u}^T$ for which $\bar{u} = \left[\frac{\partial\xi_1}{\partial v_1}, \frac{\partial\xi_2}{\partial v_1}, \frac{\partial\eta_1}{\partial v_1}, \frac{\partial\eta_2}{\partial v_1}\right]$ and

$$A = \begin{pmatrix} \frac{\partial^2 x_1}{\partial\xi_1^2} & \frac{\partial^2 x_1}{\partial\xi_1\partial\xi_2} & \frac{\partial^2 x_1}{\partial\xi_1\partial\eta_1} & \frac{\partial^2 x_1}{\partial\xi_1\partial\eta_2} \\ \cdots & \frac{\partial^2 x_1}{\partial\xi_2^2} & \frac{\partial^2 x_1}{\partial\xi_2\partial\eta_1} & \frac{\partial^2 x_1}{\partial\xi_2\partial\eta_2} \\ \cdots & & \frac{\partial^2 x_1}{\partial\eta_1^2} & \frac{\partial^2 x_1}{\partial\eta_1\partial\eta_2} \\ \cdots & & \cdots & \frac{\partial^2 x_1}{\partial\eta_2^2} \end{pmatrix}.$$

The matrix A is symmetric so the lower triangular part is obtained from the symmetry. The components of $\bar{u}$ can be evaluated in terms of derivatives of $x(\xi,\eta,t), v(\xi,\eta,t)$ through the solution to (2.5). The second partial derivatives of $x_1(\xi,\eta,t)$ in the matrix A are obtained as the second derivatives of the solution to (2.1). The components F_2, F_3, F_4 are similarly expressed in which the second partials of x_1 in A are replaced by second partials of x_2, v_1, v_2, respectively. To obtain expressions for the second partial derivatives of ξ,η with respect to v_2 then (2.6) is solved but with $\bar{y} = \left[\frac{\partial^2\xi_1}{\partial v_2^2}, \frac{\partial^2\xi_2}{\partial v_2^2}, \frac{\partial^2\eta_1}{\partial v_2^2}, \frac{\partial^2\eta_2}{\partial v_2^2}\right]$. Also, for the component $F_1 = \bar{u}A\bar{u}^T$ of $\overline{F}$ let $\bar{u} = \left[\frac{\partial\xi_1}{\partial v_2}, \frac{\partial\xi_2}{\partial v_2}, \frac{\partial\eta_1}{\partial v_2}, \frac{\partial\eta_2}{\partial v_2}\right]$. The matrix A is the same as above for F_1, and the above stated changes to A are made to compute F_2, F_3, F_4. Thus the coefficient of $\frac{\partial g}{\partial\xi_1}$ is given as a function of ξ,η as $\left(\frac{\partial^2\xi_1}{\partial v_1^2} + \frac{\partial^2\xi_1}{\partial v_2^2}\right) = c_{11}(\xi,\eta,t)$ in which the quantities $\frac{\partial^2\xi_1}{\partial v_1^2}$, $\frac{\partial^2\xi_1}{\partial v_2^2}$ are expressed through the solutions to (2.5) and (2.6) in terms of first and second partial derivatives of $x(\xi,\eta,t), v(\xi,\eta,t)$. One similarly obtains the coefficients $c_{12}(\xi,\eta,t)$, $c_{13}(\xi,\eta,t), c_{14}(\xi,\eta,t)$ of the first partials derivatives $\frac{\partial g}{\partial\xi_2}, \frac{\partial g}{\partial\eta_1}, \frac{\partial g}{\partial\eta_2}$ in (2.4).

With the coefficients so derived the initial value problem (2.4) is of the form

$$\begin{aligned}\frac{\partial g}{\partial t} &= q\left[c_1(\xi,\eta,t)\frac{\partial^2 g}{\partial\xi_1^2} + \cdots + c_4(\xi,\eta,t)\frac{\partial^2 g}{\partial\eta_2^2} + 2\left(c_5(\xi,\eta,t)\frac{\partial^2 g}{\partial\xi_1\partial\xi_2} + \cdots + c_{10}(\xi,\eta,t)\frac{\partial^2 g}{\partial\eta_1\partial\eta_2}\right)\right.\\ &\quad \left. + c_{11}(\xi,\eta,t)\frac{\partial g}{\partial\xi_1} + \cdots + c_{14}(\xi,\eta,t)\frac{\partial g}{\partial\eta_2}\right] \qquad (2.7)\\ g(\xi,\eta,0) &= f_0(\xi,\eta).\end{aligned}$$

In terms of the solution to (2.7) and the inverse transformation (2.3) the solution to (1.1) as an initial value problem in all of phase space is $f(x,v,t) = e^{2\beta t}g(\xi(x,v,t),\eta(x,v,t),t)$.

To solve the initial, boundary value problem (1.1) and (1.2) defined on the domain $\mathcal{A}$ the periodic boundary condition in ξ is introduced with the assumption that $0 \leqslant \xi_1, \xi_2 \leqslant L$. Also, to deal with the infinite domain in η a further transformation of independent variable is made. Let $\eta(u) = (\eta_1,\eta_2)$ such that

$$\eta_1 = \eta_1(u_1) = \frac{cu_1}{\sqrt{1-u_1^2}}, \quad \eta_2 = \eta_2(u_2) = \frac{cu_2}{\sqrt{1-u_2^2}}, \quad -1 < u_1, u_2 < 1. \qquad (2.8)$$

Here c is a positive constant. Let $s_1(u_1) = \frac{1}{c}(1-u_1^2)^{3/2}$, $s_2(u_2) = \frac{1}{c}(1-u_2^2)^{3/2}$. In terms of variables $\xi_1, \xi_2, u_1, u_2, t$ the Eq. (2.7) is now put into the form of an initial, boundary value problem for $g(\xi_1,\xi_2,u_1,u_2,t)$ given as

$$\begin{aligned}\frac{\partial g}{\partial t} &= q\left[c_1(\xi,\eta(u),t)\frac{\partial^2 g}{\partial\xi_1^2} + c_2(\xi,\eta(u),t)\frac{\partial^2 g}{\partial\xi_2^2} + c_3(\xi,\eta(u),t)s_1(u_1)\frac{\partial}{\partial u_1}\left(s_1(u_1)\frac{\partial g}{\partial u_1}\right) + c_4(\xi,\eta(u),t)s_2(u_2)\frac{\partial}{\partial u_2}\left(s_2(u_2)\frac{\partial g}{\partial u_2}\right)\right.\\ &\quad + 2\left(c_5(\xi,\eta(u),t)\frac{\partial^2 g}{\partial\xi_1\partial\xi_2} + c_6(\xi,\eta(u),t)s_1(u_1)\frac{\partial^2 g}{\partial\xi_1\partial u_1} + \cdots + c_{10}(\xi,\eta(u),t)s_1(u_1)s_2(u_2)\frac{\partial^2 g}{\partial u_1\partial u_2}\right)\\ &\quad \left. + c_{11}(\xi,\eta(u),t)\frac{\partial g}{\partial\xi_1} + c_{12}(\xi,\eta(u),t)\frac{\partial g}{\partial\xi_2} + c_{13}(\xi,\eta(u),t)s_1(u_1)\frac{\partial g}{\partial u_1} + c_{14}(\xi,\eta(u),t)s_2(u_2)\frac{\partial g}{\partial u_2}\right],\\ g(\xi,u,0) &= f_0(\xi,\eta(u)), \quad g(0,\xi_2,u,t) = g(L,\xi_2,u,t), \quad g(\xi_1,0,u,t) = g(\xi_1,L,u,t),\\ g(\xi,-1,u_2,t) &= g(\xi,1,u_2,t) = g(\xi,u_1,-1,t) = g(\xi,u_1,1,t) = 0. \qquad (2.9)\end{aligned}$$

Through expressions of type (2.5) and (2.6) the coefficients $c_1,\ldots,c_{14}$ in (2.9) are obtained in terms of first and second partial derivatives with respect to ξ,η of functions

$$x_1(\xi,\eta(u),t), \quad x_2(\xi,\eta(u),t), \quad v_1(\xi,\eta(u),t), \quad v_2(\xi,\eta(u),t). \qquad (2.10)$$

These functions are the solution to

$$\begin{aligned}\frac{dx_1}{dt} &= v_1, \quad x_1(0) = \xi_1\\ \frac{dx_2}{dt} &= v_2, \quad x_2(0) = \xi_2\\ \frac{dv_1}{dt} &= E_1(x(\xi,\eta(u),t),t) - \beta v_1, \quad v_1(0) = \eta_1(u_1) \qquad (2.11)\\ \frac{dv_2}{dt} &= E_2(x(\xi,\eta(u),t),t) - \beta v_2, \quad v_2(0) = \eta_2(u_2).\end{aligned}$$

By periodicity the transformation defined by (2.2) and the inverse transformation (2.3) are now regarded as transformations from $\mathcal{A}$ to $\mathcal{A}$ with $\mathcal{A} = \{(x,v)/0 \leqslant x_1, x_2 \leqslant L, -\infty < v_1, v_2 < \infty\}$. In terms of the solution to (2.9) the solution to (1.1) is given as

$$f(x,v,t) = e^{2\beta t}g(\xi(x,v,t),u(\eta(x,v,t)),t). \qquad (2.12)$$

Here $u(\eta) = (u_1(\eta_1),u_2(\eta_2))$ where $u_1(\eta_1), u_2(\eta_2)$ are the inverses of (2.8), and $\xi(x,v,t),\eta(x,v,t)$ is the inverse transformation (2.3). The function $f(x,v,t)$ given by (2.12) is in turn used to obtain the charge density $\rho(x,t)$. Through the solution to (1.2)

one then obtains the internally consistent field $E(x,t)$ in (2.11). The system to be solved is thus the Eq. (2.9) for $g(\xi,u,t)$ combined with (1.2) for the self consistent field $E(x,t)$. In addition, the coefficients in (2.9) are derived from derivatives of solutions to (2.11).

The derivatives of the functions (2.10) with respect to ξ,η needed for the coefficients in (2.9) are obtained by differentiating (2.11) with respect to ξ,η and solving the resulting system of ODE's. There are sixteen first partial derivatives with respect to ξ,η. Derivatives with respect to ξ_1 are obtained as follows: let $\bar{y} = \left[\frac{\partial x_1}{\partial \xi_1}, \frac{\partial x_2}{\partial \xi_1}, \frac{\partial v_1}{\partial \xi_1}, \frac{\partial v_2}{\partial \xi_1}\right]^T$ and

$$A = \begin{pmatrix} 0 & 0 & 1 & 0 \\ 0 & 0 & 0 & 1 \\ \frac{\partial E_1}{\partial x_1} & \frac{\partial E_1}{\partial x_2} & -\beta & 0 \\ \frac{\partial E_2}{\partial x_1} & \frac{\partial E_2}{\partial x_2} & 0 & -\beta \end{pmatrix}. \tag{2.13}$$

Then $\bar{y}$ is the solution to

$$\frac{d}{dt}\bar{y} = A\bar{y}, \quad \bar{y}(0) = [1,0,0,0]^T. \tag{2.14}$$

The remaining first partial derivatives of the functions (2.10) are obtained by replacing derivatives with respect to ξ_1 in the vector $\bar{y}$ with derivatives with respect to ξ_2,η_1, and η_2 and then solving (2.14) with conditions $\bar{y}(0) = [0,1,0,0]^T$, $[0,0,1,0]^T$, $[0,0,0,1]^T$, respectively. In the matrix A the functions $\frac{\partial E_i}{\partial x_j}$, $i,j = 1,2$ are evaluated along characteristic trajectories which are the solutions to (2.11). For example, $\frac{\partial E_1}{\partial x_1} = \frac{\partial E_1}{\partial x_1}(x_1(\xi,\eta(u),t), x_2(\xi,\eta(u),t),t)$.

There are a total of forty second partial derivatives of the functions (2.10) with respect to ξ,η. That is, there are four functions to be differentiated, x_1,x_2,v_1,v_2, and for each function there are ten second derivatives with respect to $\xi_1,\xi_2,\eta_1,\eta_2$ in which the order of differentiation is not distinguished. The form of the system for second derivatives is demonstrated by considering second partials with respect to ξ_1,ξ_2 given as follows: let $\bar{y} = \left[\frac{\partial^2 x_1}{\partial \xi_1 \partial \xi_2}, \frac{\partial^2 x_2}{\partial \xi_1 \partial \xi_2}, \frac{\partial^2 v_1}{\partial \xi_1 \partial \xi_2}, \frac{\partial^2 v_2}{\partial \xi_1 \partial \xi_2}\right]^T$. Then $\bar{y}$ is the solution to

$$\frac{d}{dt}\bar{y} = A\bar{y} + \overline{G}, \quad \bar{y}(0) = [0,0,0,0]^T. \tag{2.15}$$

Here A is the matrix (2.13) and $\overline{G} = [0,0,G_1,G_2]^T$ in which

$$G_1 = \frac{\partial^2 E_1}{\partial x_1^2}\left(\frac{\partial x_1}{\partial \xi_1}\right)\left(\frac{\partial x_1}{\partial \xi_2}\right) + \frac{\partial^2 E_1}{\partial x_1 \partial x_2}\left(\frac{\partial x_1}{\partial \xi_1}\frac{\partial x_2}{\partial \xi_2} + \frac{\partial x_1}{\partial \xi_2}\frac{\partial x_2}{\partial \xi_1}\right) + \frac{\partial^2 E_1}{\partial x_2^2}\left(\frac{\partial x_2}{\partial \xi_1}\right)\left(\frac{\partial x_2}{\partial \xi_2}\right)$$

$$G_2 = \frac{\partial^2 E_2}{\partial x_1^2}\left(\frac{\partial x_1}{\partial \xi_1}\right)\left(\frac{\partial x_1}{\partial \xi_2}\right) + \frac{\partial^2 E_2}{\partial x_1 \partial x_2}\left(\frac{\partial x_1}{\partial \xi_1}\frac{\partial x_2}{\partial \xi_2} + \frac{\partial x_1}{\partial \xi_2}\frac{\partial x_2}{\partial \xi_1}\right) + \frac{\partial^2 E_2}{\partial x_2^2}\left(\frac{\partial x_2}{\partial \xi_1}\right)\left(\frac{\partial x_2}{\partial \xi_2}\right).$$

In G_1,G_2 the functions $\frac{\partial x_i}{\partial \xi_j}$, $i,j = 1,2$ are obtained as solutions to systems for the first partial derivatives of which (2.14) is repesentative. The second partials of E are evaluated along characteristic trajectories as $\frac{\partial^2 E_1}{\partial x_1^2} = \frac{\partial^2 E_1}{\partial x_1^2}(x_1(\xi,\eta(u),t), x_2(\xi,\eta(u),t),t)$. The system (2.15) accounts for four second partial derivatives of $x(\xi,\eta(u),t)$, $v(\xi,\eta(u),t),t)$. The remaining thirty six second partial derivatives are derived as solutions to nine similar systems for other second derivative combinations of $\xi_1,\xi_2,\eta_1,\eta_2$.

2.2. Constant magnetic field, $B_z \neq 0$

If a constant magnetic field is introduced in the x_3 direction, i.e., perpendicular to the plane of x_1,x_2 then the electric field E in (1.1) is replaced with $E + v \times B$ with B the magnetic field. The form of $E + v \times B$ in two dimensions is given in the Introduction. For $B = (0,0,B_z)$ with $B_z = b$, constant, then $E + v \times B = (E_1 + v_2 b, E_2 - v_1 b, 0)$. Thus Eq. (1.1) is replaced with

$$\frac{\partial f}{\partial t} + v \cdot \nabla_x f + (E_1 + v_2 b, E_2 - v_1 b) \cdot \nabla_v f = \nabla_v \cdot (\beta v f + q \nabla_v f), \quad f(x,v,0) = f_0(x,v). \tag{2.16}$$

Eq. (1.2) remains the same, and the system to be solved is (2.16) and (1.2) along with periodic boundary conditions in x.

The characteristic equations associated with the first order transport part of (2.16) are

$$\begin{aligned} \frac{dx_1}{dt} &= v_1, \quad x_1(0) = \xi_1 \\ \frac{dx_2}{dt} &= v_2, \quad x_2(0) = \xi_2 \\ \frac{dv_1}{dt} &= E_1(x(t),t) + b v_2 - \beta v_1, \quad v_1(0) = \eta_1 \\ \frac{dv_2}{dt} &= E_2(x(t),t) - b v_1 - \beta v_2, \quad v_2(0) = \eta_2 \end{aligned} \tag{2.17}$$

As with the solution to (2.1) the solution to (2.17) is written

$$x_1(t) = x_1(\xi_1,\xi_2,\eta_1,\eta_2,t), \quad x_2(t) = x_2(\xi_1,\xi_2,\eta_1,\eta_2,t),$$
$$v_1(t) = v_1(\xi_1,\xi_2,\eta_1,\eta_2,t), \quad v_2(t) = v_2(\xi_1,\xi_2,\eta_1,\eta_2,t). \tag{2.18}$$

These functions define the transformation $(\xi,\eta) \to (x,v)$ of $R_4 \to R_4$ with nonzero Jacobian. In fact, the Jacobian for the transformation based on (2.17) is the same as that based on (2.1). Thus the inverse transformation and change of variables is defined as with (2.3). One then exactly proceeds with the development following (2.3) to put Eq. (2.16) into the form (2.7). The only difference in this reformulation of system (2.16) and (1.2) from that of (1.1) and (1.2) is that the coefficients in (2.7) depend on the partial derivatives of the solution to (2.17) instead of on the derivatives of the solution to (2.1). With coefficients based on the solutions to (2.17) the Eq. (2.7) is further transformed to the form (2.9). The characteristic system (2.17) is written as for (2.11) with initial points $v_1(0) = \eta_1(u_1) = cu_1/\sqrt{1-u_1^2},\ v_2(0) = \eta_2(u_2) = cu_2/\sqrt{1-u_2^2}$.

To obtain the derivatives of the solutions to (2.17) with respect to ξ,η needed for the coefficients in (2.9) the matrix A given by (2.13) is replaced with

$$A = \begin{pmatrix} 0 & 0 & 1 & 0 \\ 0 & 0 & 0 & 1 \\ \frac{\partial E_1}{\partial x_1} & \frac{\partial E_1}{\partial x_2} & -\beta & b \\ \frac{\partial E_2}{\partial x_1} & \frac{\partial E_2}{\partial x_2} & -b & -\beta \end{pmatrix}. \tag{2.19}$$

With this change one then proceeds with the development following (2.13). Solving the systems of type (2.14) and (2.15) with the matrix A given by (2.19) then provides the required derivatives of the solutions to (2.17).

The numerical procedure for solving (1.1) and (1.2) is a type of deterministic particle method which is a generalization of the method given in [28] for the 1-D Vlasov–Poisson–Fokker–Planck system. The approach is to obtain the solution to (1.1) and (1.2) by means of a sequence of solutions to (2.9) and (1.2). This is done in the following way: given the time interval $[0,T]$ let T_1 be such that $T/T_1 = M$ an integer. The interval $[0,T]$ is divided into subintervals $[mT_1,(m+1)T_1]$ for $m = 0,1,\ldots M-1$. Let $f(x,v,\bar{t})$ be the solution to (1.1) and (1.2) for $0 \leqslant \bar{t} \leqslant T$. On the time interval $mT_1 \leqslant \bar{t} \leqslant (m+1)T_1$ let $t = \bar{t} - mT_1$. Then

$$f(x,v,\bar{t}) = e^{2\beta t} g(\xi(x,v,t), u(\eta(x,v,t)),t), \quad t \in [0,T_1] \tag{2.20}$$

and such that $g(\xi,u,t)$ is the solution to (2.9) and (1.2) with $g(\xi,u,0) = f(\xi,\eta(u),mT_1)$. If $m = 0$ then $f(x,v,mT_1) = f_0(x,v)$. If $m > 0$ then $f(x,v,mT_1) = e^{2\beta T_1} g(\xi(x,v,T_1), u(\eta(x,v,T_1)),T_1)$ such that $g(\xi,u,t)$ is the solution to (2.9) and (1.2) for $t \in [0,T_1]$ with $g(\xi,u,0) = f(\xi,\eta(u),(m-1)T_1)$. The numerical method discretizes this procedure. The path of a particle in phase space is obtained from a discrete approximation of (2.11). In accordance with (2.12) the solution g of (2.9) provides the value of f of (1.1) along the particle trajectory given by the solution to (2.11). Hence, the charge along the approximate trajectory is determined at each time step from the solution to (2.9). The Eq. (2.9) is approximated by a finite difference equation which is solved on a fixed grid by either an iterative SOR type algorithm or by a direct Douglas–Rachford method. To get the coefficients in (2.9) one solves discretized versions of equations (2.14) and (2.15) for the first and second partial derivatives with respect to ξ,η of a trajectory $x(\xi,\eta(u),t), v(\xi,\eta(u),t)$. This provides the approximation to matrices Q and A, and the coefficients are then derived from the solutions to (2.5) and (2.6). The field $E(x,t)$ is approximated by a 2-D particle-in-cell method. At time $t = T_1$ the solution along trajectories is interpolated onto the fixed grid as initial data for (2.9). The solution to (2.9) for g is restarted and the particle computation is then repeated for the time interval $[(m+1)T_1,(m+2)T_1]$. This regriding of the solution greatly improves the long term stability and accuracy of the numerical method. With some relatively minor changes the numerical method for solving (1.1) and (1.2) is adapted to the system (2.16) and (1.2). A more detailed description of the numerical method is given in the next section.

3. The numerical method

The description of the discrete method for approximating solutions to (1.1) and (1.2) or (2.16) and (1.2) generalizes to two dimensions the description of the discrete approximation for the one dimensional system given in [28], Section 2. We will first outline the method as it applies to system (1.1) and (1.2) and then point out the changes needed to apply the method to the system (2.16) and (1.2).

3.1. Partition of phase space and time interval

Several domains of definition for functions are defined. Phase space is the (x,v) domain given by

$$\mathcal{A} = \{(x,v)/0 \leqslant x_1,x_2 \leqslant L, -\infty < v_1,v_2 < \infty\}.$$

The system (1.1) and (1.2) is defined on $\mathcal{A}$. The set $\mathcal{A}_0$ is defined by

$$\mathcal{A}_0 = \{(\xi,\eta)/0 \leqslant \xi_1,\xi_2 \leqslant L, -\infty < \eta_1,\eta_2 < \infty\}$$

in which (ξ,η) are defined by the inverse transformation (2.3) as applied to the problem with periodic boundary conditions. The points $(\xi,\eta)\in\mathcal{A}_0$ are initial points for the solution to (2.11). The domain Ω is defined as

$$\Omega=\{(\xi,u)/0\leqslant\xi_1,\xi_2\leqslant L,-1<u_1,u_2<1\}$$

and such that $\eta_1=\frac{cu_1}{\sqrt{1-u_1^2}}$, $\eta_2=\frac{cu_2}{\sqrt{1-u_2^2}}$. The Eq. (2.9) is defined on Ω.

The domain Ω is partitioned as follows: given integers N_x,N_v let $\Delta\xi=L/N_x$, $\Delta u=2/(N_v+1)$. We define multiindices, i,j, as $i=(i_1,i_2)$, $j=(j_1,j_2)$. Then $\xi_i=(\xi_{1,i_1},\xi_{2,i_2})$ and $u_j=(u_{1,j_1},u_{2,j_2})$ such that

$$\xi_{1,i_1}=(i_1-1/2)\Delta\xi,\quad \xi_{2,i_2}=(i_2-1/2)\Delta\xi,\quad i_1,i_2=1,\ldots,N_x, \tag{3.1}$$

$$u_{1,j_1}=-1+j_1\Delta u,\quad u_{2,j_2}=-1+j_2\Delta u,\quad j_1,j_2=1,\ldots,N_v. \tag{3.2}$$

Thus the region

$$\left\{(\xi,u)/\ 0\leqslant\xi_1,\xi_2\leqslant L,\ -\frac{N_v}{N_v+1}\leqslant u_1,u_2\leqslant\frac{N_v}{N_v+1}\right\}$$

is subdivided into a uniform rectangular type grid with the point (ξ_i,u_j) the center of the i,j "rectangle" on the grid. The region

$$\left\{(\xi,u)/\ 0\leqslant\xi_1,\xi_2\leqslant L,\ -1<u_1\text{ or }u_2<-\frac{N_v}{N_v+1}\ \text{ or }\ \frac{N_v}{N_v+1}<u_1\text{ or }u_2<1\right\}$$

is the part of Ω associated with points at infinity at which the distribution function is zero.

Let $\eta_j=\eta(u_j)=(\eta_{1,j_1},\eta_{2,j_2})$ such that

$$\eta_{1,j_1}=\frac{cu_{1,j_1}}{\sqrt{1-u_{1,j_1}^2}},\quad \eta_{2,j_2}=\frac{cu_{2,j_2}}{\sqrt{1-u_{2,j_2}^2}},\quad j_1,j_2=1,\ldots,N_v. \tag{3.3}$$

The points (ξ_i,u_j) in Ω then correspond to points (ξ_i,η_j) in $\mathcal{A}_0$.

The partition of the time interval $[0,T]$ is the same as in [28], Section 2.1. Let $T_1<T$ be such that $MT_1=T$ for a positive integer M. For a positive integer N_g let $\Delta t=T_1/N_g$. Then $t_n=n\Delta t$, $n=0,1,\ldots,N_g$ is a partition of the interval $[0,T_1]$. Let $\tau_m=mT_1$, $m=0,1,\ldots,M$ and $\bar{t}_k=\tau_m+t_n$ for $k=mN_g+n$. The deterministic particle method is carried out on the time interval $[0,T_1]$ with discrete time variable t_n. This involves discretizing Eq. (2.9) and the systems of ODE's for the particle trajectories and partial derivatives. The reconstruction of the distribution function on the fixed grid from the solution along particle trajectories is done at times τ_m, $m=1,2,\ldots,M$. The actual time of the discrete approximation is given by $\bar{t}_k$, $k=0,1,\ldots,N_t$ for $N_t=MN_g$.

3.2. The deterministic particle method on $[0,T_1]$

3.2.1. The initial data

On the time interval $[mT_1,(m+1)T_1]$, $m=0,1,\ldots,M-1$, the solution to (1.1) and (1.2) is obtained by approximating the solution to (2.9) along with approximations to (2.11) and to equations for partial derivatives of type (2.14) and (2.15). The initial function for (2.9) is $g(\xi,u,0)=f(\xi,\eta(u),mT_1)$ where $f(x,v,\bar{t})$ is the solution to (1.1) and (1.2). If $m=0$ then $f(\xi,\eta(u),0)=f_0(\xi,\eta(u))$. It is assumed that $\int_{\mathcal{A}}f_0(x,v)dvdx=K$. The notation is for $x=(x_1,x_2)$ then $dx=dx_1dx_2$ and similarly for dv. Thus, in terms of variables ξ,η and ξ,u then

$$\begin{aligned}\int_{\mathcal{A}_0}f_0(\xi,\eta)d\xi d\eta&=\int_\Omega f_0(\xi,\eta(u))\left|\frac{\partial(\xi,\eta)}{\partial(\xi,u)}\right|d\xi du\\&=\int_0^L\int_0^L\int_{-1}^1\int_{-1}^1 f_0\left(\xi_1,\xi_2,\frac{cu_1}{\sqrt{1-u_1^2}},\frac{cu_2}{\sqrt{1-u_2^2}}\right)\frac{c^2}{(1-u_1^2)^{3/2}(1-u_2^2)^{3/2}}dud\xi=K.\end{aligned}$$

Therefore for $m=0$

$$\int_\Omega g(\xi,u,0)\frac{c^2}{(1-u_1^2)^{3/2}(1-u_2^2)^{3/2}}dud\xi=\int_\Omega f_0(\xi,\eta(u))\frac{c^2}{(1-u_1^2)^{3/2}(1-u_2^2)^{3/2}}dud\xi=K.$$

If $g(\xi,u,t)$ is the solution to (2.9) for $\bar{t}\in[\tau_m,\tau_{m+1}]$, $t=\bar{t}-\tau_m$, then let $g_{i,j}^{m,n}=g_{i_1,i_2,j_1,j_2}^{m,n}$ be the approximation to $g(\xi_i,u_j,t_n)$, $t_n\in[0,T_1]$. The initial data at $t_n=0$ is then denoted $g_{i,j}^{m,0}$. For $m=0,n=0$, that is $\tau_m=0$, $t_n=0$ and $\bar{t}_k=0$ let

$$\bar{g}_{ij}^0=f_0(\xi_i,\eta_j),\quad i_1,i_2=1,\ldots,N_x,\quad j_1,j_2=1,\ldots,N_v,$$

with $\eta_j=\eta(u_j)$ given by (3.3). Let

$$\lambda=\frac{1}{K}\sum_{i,j}\bar{g}_{ij}^0\frac{c^2}{\left(1-u_{1,j_1}^2\right)^{3/2}\left(1-u_{2,j_2}^2\right)^{3/2}}(\Delta u\Delta\xi)^2.$$

Then $g^{0,0}_{i,j} = \bar{g}^0_{i,j}/\lambda$. Thus

$$\sum_{i,j} g^{0,0}_{i,j} \frac{c^2}{\left(1-u^2_{1,j_1}\right)^{3/2}\left(1-u^2_{2,j_2}\right)^{3/2}}(\Delta u \Delta\xi)^2 = K$$

and the grid function $g^{m,n}_{i,j}$ is normalized at $\bar{t}_k = 0$ to preserve the L_1 norm of the initial data or total charge.

For $m > 0$ the initial function for (2.9) is $g(\xi, u, 0) = f(\xi, \eta(u), \tau_m)$ with $f(x, v, \bar{t})$ the solution to (1.1) and (1.2). In this case the initial grid function $g^{m,0}_{i,j}$ is obtained from the regriding process described in Section 3.3. That is the solution computed by the deterministic method for the time interval $[\tau_{m-1}, \tau_m]$ is reconstructed on the fixed grid at time τ_m to provide the approximation to $f(\xi, \eta(u), \tau_m)$.

3.2.2. The approximation of (2.9), the transformed Vlasov–Fokker–Planck equation

The approximate solution to (2.9) on the time interval $\bar{t} \in [\tau_m, \tau_{m+1}]$ with $t_n \in [0, T_1]$ is $g^{m,n}_{i,j}$, $n = 0, 1, \ldots, N_g$. If $n = 0$ then $g^{m,0}_{i,j}$ is given in Section 3.2.1. Let $c_1(i,j,t_n), \ldots, c_{14}(i,j,t_n)$ be the approximation to coefficients $c_1(\xi_i, \eta(u_j), t_n), \ldots, c_{14}(\xi_i, \eta(u_j), t_n)$ in (2.9). For simplicity we let $g^{m,n}_{i,j} = g^n_{i,j}$. Then given $g^n_{i,j}$ the grid function $g^{n+1}_{i,j}$ is compute as follows. We first introduce some notation. Let

$$s_{l,j_l} = \frac{(1-u^2_{l,j_l})^{3/2}}{c}, \quad s^0_{l,j_l} = \frac{(1-(u_{l,j_l}-.5\Delta u)^2)^{3/2}}{c},$$
$$s^1_{l,j_l} = \frac{(1-(u_{l,j_l}+.5\Delta u)^2)^{3/2}}{c}, \quad l = 1, 2.$$

The quantity $s_1(u_1)\frac{\partial}{\partial u_1}\left(s_1(u_1)\frac{\partial g}{\partial u_1}\right)$ is approximated by

$$\frac{s_{1,j_1}\left[s^1_{1,j_1}\left(\frac{g_{i,j_1+1,j_2}-g_{i,j_1,j_2}}{\Delta u}\right) - s^0_{1,j_1}\left(\frac{g_{i,j_1,j_2}-g_{i,j_1-1,j_2}}{\Delta u}\right)\right]}{\Delta u} = \frac{s_{1,j_1}\left(s^1_{1,j_1}g_{i,j_1+1,j_2} - \left(s^1_{1,j_1}+s^0_{1,j_1}\right)g_{i,j_1,j_2} + s^0_{1,j_1}g_{i,j_1-1,j_2}\right)}{(\Delta u)^2}.$$

The centered difference approximation to $s_1(u_1)\frac{\partial g}{\partial u_1}$ is

$$\frac{s_{1,j_1}(g_{i,j_1+1,j_2} - g_{i,j_1-1,j_2})}{2\Delta u}.$$

The quantities $s_2(u_2)\frac{\partial}{\partial u_2}\left(s_2(u_2)\frac{\partial g}{\partial u_2}\right)$ and $s_2(u_2)\frac{\partial g}{\partial u_2}$ are similarly approximated. The notation for a finite difference approximation to (2.9) is

$$D^2_{\xi_1} g_{i,j} = \frac{g_{i_1+1,i_2,j} - 2g_{i_1,i_2,j} + g_{i_1-1,i_2,j}}{(\Delta\xi)^2}, \quad D^2_{\xi_2} g_{i,j} = \frac{g_{i_1,i_2+1,j} - 2g_{i_1,i_2,j} + g_{i_1,i_2-1,j}}{(\Delta\xi)^2},$$
$$D^2_{u_1} g_{i,j} = \frac{s_{1,j_1}(s^1_{1,j_1}g_{i,j_1+1,j_2} - (s^1_{1,j_1}+s^0_{1,j_1})g_{i,j_1,j_2} + s^0_{1,j_1}g_{i,j_1-1,j_2})}{(\Delta u)^2},$$
$$D^2_{u_2} g_{i,j} = \frac{s_{2,j_2}\left(s^1_{2,j_2}g_{i,j_1,j_2+1} - \left(s^1_{2,j_2}+s^0_{2,j_2}\right)g_{i,j_1,j_2} + s^0_{2,j_2}g_{i,j_1,j_2-1}\right)}{(\Delta u)^2},$$
$$D_{0,\xi_1} g_{i,j} = \frac{g_{i_1+1,i_2,j} - g_{i_1-1,i_2,j}}{2\Delta\xi}, \quad D_{0,\xi_2} g_{i,j} = \frac{g_{i_1,i_2+1,j} - g_{i_1,i_2-1,j}}{2\Delta\xi},$$
$$D_{0,u_1} g_{i,j} = \frac{s_{1,j_1}(g_{i,j_1+1,j_2} - g_{i,j_1-1,j_2})}{2\Delta u}, \quad D_{0,u_2} g_{i,j} = \frac{s_{2,j_2}(g_{i,j_1,j_2+1} - g_{i,j_1,j_2-1})}{2\Delta u}.$$

It is also convenient to define the difference operators for $l = 1, 2$ as

$$\delta^2_{\xi_l} = (\Delta\xi)^2 D^2_{\xi_l}, \quad \delta^2_{u_l} = (\Delta u)^2 D^2_{u_l}, \quad \delta_{0,\xi_l} = (2\Delta\xi) D_{0,\xi_l}, \quad \delta_{0,u_l} = (2\Delta u) D_{0,u_l}.$$

So, for example, $\delta^2_{\xi_1} g_{i,j} = g_{i_1+1,i_2,j} - 2g_{i_1,i_2,j} + g_{i_1-1,i_2,j}$.

Let $c_l = c_l(i,j,t_n)$. The grid function $\bar{g}^{n+1}_{i,j}$ is obtained as the solution to the semi-implicit difference equation

$$\bar{g}^{n+1}_{i,j} = g^n_{i,j} + q\Delta t\Big[\left(c_1 D^2_{\xi_1} + c_2 D^2_{\xi_2} + c_3 D^2_{u_1} + c_4 D^2_{u_2}\right)\bar{g}^{n+1}_{i,j} + 2\big(c_5 D_{0,\xi_1} D_{0,\xi_2} + c_6 D_{0,\xi_1} D_{0,u_1} + c_7 D_{0,\xi_1} D_{0,u_2}$$
$$+ c_8 D_{0,\xi_2} D_{0,u_1} + c_9 D_{0,\xi_2} D_{0,u_2} + c_{10} D_{0,u_1} D_{0,u_2}\big) g^n_{i,j} + \left(c_{11} D_{0,\xi_1} + c_{12} D_{0,\xi_2} + c_{13} D_{0,u_1} + c_{14} D_{0,u_2}\right) g^n_{i,j}\Big] \tag{3.4}$$

If $i_1 = 1$ then $\bar{g}^{n+1}_{i_1-1,i_2,j} = \bar{g}^{n+1}_{N_x,i_2,j}$, if $i_1 = N_x$ then $\bar{g}^{n+1}_{i_1+1,i_2,j} = \bar{g}^{n+1}_{1,i_2,j}$. If $i_2 = 1$ then $\bar{g}^{n+1}_{i_1,i_2-1,j} = \bar{g}^{n+1}_{i_1,N_x,j}$, if $i_2 = N_x$ then $\bar{g}^{n+1}_{i_1,i_2+1,j} = \bar{g}^{n+1}_{i_1,1,j}$. This is the periodic boundary condition in ξ. If $j_1 = 1$ then $\bar{g}^{n+1}_{i,j_1-1,j_2} = 0$, if $j_1 = N_v$ then $\bar{g}^{n+1}_{i,j_1+1,j_2} = 0$. If $j_2 = 1$ then $\bar{g}^{n+1}_{i,j_1,j_2-1} = 0$, if $j_2 = N_v$ then $\bar{g}^{n+1}_{i,j_1,j_2+1} = 0$. This is the zero boundary condition condition at $u_1, u_2 = ^+ \pm 1$.

Eq. (3.4) can be solved by an iterative procedure which is a direct generalization of the iterative procedure for the one dimensional Eq. (2.3) [28]. Let $r_1 = \Delta t/(\Delta\xi)^2$, $r2 = \Delta t/(\Delta u)^2$, $p_1 = \Delta t/(2\Delta\xi)$, $p_2 = \Delta t/(2\Delta u)$. Then (3.4) is written as

$$\left(1+2qc_1r_1+2qc_2r_1+qc_3r_2s_{1,j_1}\left(s^1_{1,j_1}+s^0_{1,j_1}\right)+qc_4r_2s_{2,j_2}\left(s^1_{2,j_2}+s^0_{2,j_2}\right)\right)\bar{g}^{n+1}_{i,j}$$
$$=qc_1r_1\left(\bar{g}^{n+1}_{i_1+1,i_2,j}+\bar{g}^{n+1}_{i_1-1,i_2,j}\right)+qc_2r_1\left(\bar{g}^{n+1}_{i_1,i_2+1,j}+\bar{g}^{n+1}_{i_1,i_2-1,j}\right)+qc_3r_2s_{1,j_1}\left(s^1_{1,j_1}\bar{g}^{n+1}_{i,j_1+1,j_2}+s^0_{1,j_1}\bar{g}^{n+1}_{i,j_1-1,j_2}\right)$$
$$+qc_4r_2s_{2,j_2}\left(s^1_{2,j_2}\bar{g}^{n+1}_{i,j_1,j_2+1}+s^0_{2,j_2}\bar{g}^{n+1}_{i,j_1,j_2-1}\right)+F^n_{i,j}$$

where $F^n_{i,j}$ is

$$F^n_{i,j}=g^n_{i,j}+\frac{1}{2}q\left[c_5r_1\delta_{0,\xi_1}\delta_{0,\xi_2}+c_6\sqrt{r_1r_2}\delta_{0,\xi_1}\delta_{0,u_1}+c_7\sqrt{r_1r_2}\delta_{0,\xi_1}\delta_{0,u_2}+c_8\sqrt{r_1r_2}\delta_{0,\xi_2}\delta_{0,u_1}+c_9\sqrt{r_1r_2}\delta_{0,\xi_2}\delta_{0,u_2}\right.$$
$$\left.+c_{10}r_2\delta_{0,u_1}\delta_{0,u_2}\right]g^n_{i,j}+q\left[c_{11}p_1\delta_{0,\xi_1}+c_{12}p_1\delta_{0,\xi_2}+c_{13}p_2\delta_{0,u_1}+c_{14}p_2\delta_{0,u_2}\right]g^n_{i,j}$$

Let

$$d_{i,j}=1+2qc_1r_1+2qc_2r_1+qc_3r_2s_{1,j_1}\left(s^1_{1,j_1}+s^0_{1,j_1}\right)+qc_4r_2s_{2,j_2}\left(s^1_{2,j_2}+s^0_{2,j_2}\right)$$

then

$$\bar{g}^{n+1}_{i,j}=\frac{qc_1r_1}{d_{i,j}}\left(\bar{g}^{n+1}_{i_1+1,i_2,j}+\bar{g}^{n+1}_{i_1-1,i_2,j}\right)+\frac{qc_2r_1}{d_{i,j}}\left(\bar{g}^{n+1}_{i_1,i_2+1,j}+\bar{g}^{n+1}_{i_1,i_2-1,j}\right)+\frac{qc_3r_2s_{1,j_1}}{d_{i,j}}\left(s^1_{1,j_1}\bar{g}^{n+1}_{i,j_1+1,j_2}+s^0_{1,j_1}\bar{g}^{n+1}_{i,j_1-1,j_2}\right)$$
$$+\frac{qc_4r_2s_{2,j_2}}{d_{i,j}}\left(s^1_{2,j_2}\bar{g}^{n+1}_{i,j_1,j_2+1}+s^0_{2,j_2}\bar{g}^{n+1}_{i,j_1,j_2-1}\right)+\frac{1}{d_{i,j}}F^n_{i,j}.$$

Given $g^n_{i,j}$ the Jacobi method for obtaining $\bar{g}^{n+1}_{i,j}$ is the extension to two dimensions of [28], (2.5). That is let $h^0_{i,j}=g^n_{i,j}$, then for $k=0,1,2,\ldots$

$$h^{k+1}_{i,j}=\frac{qc_1r_1}{d_{i,j}}\left(h^k_{i_1+1,i_2,j}+h^k_{i_1-1,i_2,j}\right)+\frac{qc_2r_1}{d_{i,j}}\left(h^k_{i_1,i_2+1,j}+h^k_{i_1,i_2-1,j}\right)+\frac{qc_3r_2s_{1,j_1}}{d_{i,j}}\left(s^1_{1,j_1}h^k_{i,j_1+1,j_2}+s^0_{1,j_1}h^k_{i,j_1-1,j_2}\right)$$
$$+\frac{qc_4r_2s_{2,j_2}}{d_{i,j}}\left(s^1_{2,j_2}h^k_{i,j_1,j_2+1}+s^0_{2,j_2}h^k_{i,j_1,j_2-1}\right)+\frac{1}{d_{i,j}}F^n_{i,j}. \tag{3.5}$$

Letting $\|h^k\|=\max_{i,j}|h^k_{i,j}|$ and

$$\Theta(t_n)=\max_{i,j}\left[\left(2qc_1r_1+2qc_2r_1+qc_3r_2s_{1,j_1}\left(s^1_{1,j_1}+s^0_{1,j_1}\right)+qc_4r_2s_{2,j_2}\left(s^1_{2,j_2}+s^0_{2,j_2}\right)\right)/d_{i,j}\right]$$

then $0<\Theta(t_n)<1$ and one can readily verify that $\|h^{k+1}-h^k\|\leqslant\Theta(t_n)\|h^k-h^{k-1}\|$. Therefore, the sequence $\{h^k_{i,j}\}$ converges uniformly in i,j and $\lim_{k\to\infty}h^k_{i,j}=\bar{g}^{n+1}_{i,j}$.

The convergence rate of the iterative procedure (3.5) is accelerated by the method of successive overrelaxation (SOR). Thus, for $i_l>1, j_l>1,\ l=1,2$ then (3.5) is replaced by

$$\bar{h}^{k+1}_{i,j}=\frac{qc_1r_1}{d_{i,j}}\left(h^k_{i_1+1,i_2,j}+h^{k+1}_{i_1-1,i_2,j}\right)+\frac{qc_2r_1}{d_{i,j}}\left(h^k_{i_1,i_2+1,j}+h^{k+1}_{i_1,i_2-1,j}\right)+\frac{qc_3r_2s_{1,j_1}}{d_{i,j}}\left(s^1_{1,j_1}h^k_{i,j_1+1,j_2}+s^0_{1,j_1}h^{k+1}_{i,j_1-1,j_2}\right)$$
$$+\frac{qc_4r_2s_{2,j_2}}{d_{i,j}}\left(s^1_{2,j_2}h^k_{i,j_1,j_2+1}+s^0_{2,j_2}h^{k+1}_{i,j_1,j_2-1}\right)+\frac{1}{d_{i,j}}F^n_{i,j} \tag{3.6}$$

and

$$h^{k+1}_{i,j}=\omega\bar{h}^{k+1}_{i,j}+(1-\omega)h^k_{i,j}. \tag{3.7}$$

Here $\omega>1$ is the overrelaxation parameter. According to theory in [2] to obtain an optimal ω one must determine the eigenvalues, λ, that are the solutions to

$$\frac{qc_1r_1}{d_{i,j}}\left(h_{i_1+1,i_2,j}+h_{i_1-1,i_2,j}\right)+\frac{qc_2r_1}{d_{i,j}}\left(h_{i_1,i_2+1,j}+h_{i_1,i_2-1,j}\right)+\frac{qc_3r_2s_{1,j_1}}{d_{i,j}}\left(s^1_{1,j_1}h_{i,j_1+1,j_2}+s^0_{1,j_1}h_{i,j_1-1,j_2}\right)$$
$$+\frac{qc_4r_2s_{2,j_2}}{d_{i,j}}\left(s^1_{2,j_2}h_{i,j_1,j_2+1}+s^0_{2,j_2}h_{i,j_1,j_2-1}\right)=\lambda h_{i,j} \tag{3.8}$$

The optimal ω for the SOR algorithm is derived from the maximal eigenvalue, $\lambda_{\max}$, according to the formula [2] (3–113). As in [28] we approximate the maximal eigenvalue of (3.8) by $\Theta(t_n)$ and compute

$$\omega_b=\frac{2}{1+\sqrt{1-(\Theta(t_n))^2}}.$$

It is also useful to have a direct method for solving (3.4). The Douglas–Rachford method described in [27] and applied in [28], Section 2.2.2 for the one dimensional problem can be generalized to the problem in two dimensions. Eq. (3.4) is put into the form

$$\left(1-qc_1r_1\delta_{\xi_1}^2-qc_2r_1\delta_{\xi_2}^2-qc_3r_2\delta_{u_1}^2-qc_4r_2\delta_{u_2}^2\right)\bar{g}_{i,j}^{n+1}=F_{i,j}^n. \tag{3.9}$$

Eq. (3.9) is then replaced with

$$\begin{aligned}&\left(1-qc_1r_1\delta_{\xi_1}^2-qc_3r_2\delta_{u_1}^2\right)\left(1-qc_2r_1\delta_{\xi_2}^2-qc_4r_2\delta_{u_2}^2\right)\bar{g}_{i,j}^{n+1}\\&\quad=\left[\left(qc_1r_1\delta_{\xi_1}^2\right)\left(qc_2r_1\delta_{\xi_2}^2\right)+\left(qc_1r_1\delta_{\xi_1}^2\right)\left(qc_4r_2\delta_{u_2}^2\right)+\left(qc_3r_2\delta_{u_1}^2\right)\left(qc_2r_1\delta_{\xi_2}^2\right)+\left(qc_3r_2\delta_{u_1}^2\right)\left(qc_4r_2\delta_{u_2}^2\right)\right]g_{i,j}^n+F_{i,j}^n.\end{aligned} \tag{3.10}$$

The products of operators on the left side at time t_{n+1}, for example, $\left(qc_1r_1\delta_{\xi_1}^2\right)\left(qc_2r_1\delta_{\xi_2}^2\right)\bar{g}_{i,j}^{n+1}$, are balanced by the products on the right side at time t_n, for the example $\left(qc_1r_1\delta_{\xi_1}^2\right)\left(qc_2r_1\delta_{\xi_2}^2\right)g_{i,j}^n$. The Eq. (3.10) is equivalent to

$$\left(1-qc_1r_1\delta_{\xi_1}^2-qc_3r_2\delta_{u_1}^2\right)g_{i,j}^*=\left(qc_2r_1\delta_{\xi_2}^2+qc_4r_2\delta_{u_2}^2\right)g_{i,j}^n+F_{i,j}^n, \tag{3.11}$$

$$\left(1-qc_2r_1\delta_{\xi_2}^2-qc_4r_2\delta_{u_2}^2\right)\bar{g}_{i,j}^{n+1}=g_{i,j}^*-\left(qc_2r_1\delta_{\xi_2}^2+qc_4r_2\delta_{u_2}^2\right)g_{i,j}^n. \tag{3.12}$$

Eqs. (3.11) and (3.12) are then replaced with

$$\left(1-qc_1r_1\delta_{\xi_1}^2\right)\left(1-qc_3r_2\delta_{u_1}^2\right)g_{i,j}^*=\left(qc_1r_1\delta_{\xi_1}^2\right)\left(qc_3r_2\delta_{u_1}^2\right)g_{i,j}^n+\left(qc_2r_1\delta_{\xi_2}^2+qc_4r_2\delta_{u_2}^2\right)g_{i,j}^n+F_{i,j}^n, \tag{3.13}$$

$$\left(1-qc_2r_1\delta_{\xi_2}^2\right)\left(1-qc_4r_2\delta_{u_2}^2\right)\bar{g}_{i,j}^{n+1}=\left(qc_2r_1\delta_{\xi_2}^2\right)\left(qc_4r_2\delta_{u_2}^2\right)g_{i,j}^n+g_{i,j}^*-\left(qc_2r_1\delta_{\xi_2}^2+qc_4r_2\delta_{u_2}^2\right)g_{i,j}^n. \tag{3.14}$$

Eqs. (3.13) and (3.14) are then further divided as

$$\left(1-qc_1r_1\delta_{\xi_1}^2\right)\tilde{g}_{i,j}=\left(qc_3r_2\delta_{u_1}^2+qc_2r_1\delta_{\xi_2}^2+qc_4r_2\delta_{u_2}^2\right)g_{i,j}^n+F_{i,j}^n, \tag{3.15}$$

$$\left(1-qc_3r_2\delta_{u_1}^2\right)g_{i,j}^*=-\left(qc_3r_2\delta_{u_1}^2\right)g_{i,j}^n+\tilde{g}_{i,j}, \tag{3.16}$$

$$\left(1-qc_2r_1\delta_{\xi_2}^2\right)\hat{g}_{i,j}=-\left(qc_2r_1\delta_{\xi_2}^2\right)g_{i,j}^n+g_{i,j}^*, \tag{3.17}$$

$$\left(1-qc_4r_2\delta_{u_2}^2\right)\bar{g}_{i,j}^{n+1}=-\left(qc_4r_2\delta_{u_2}^2\right)g_{i,j}^n+\hat{g}_{i,j}. \tag{3.18}$$

The Eqs. (3.15)–(3.17) and (3.18) constitute the Douglas–Rachford method in the four dimensional phase space. Thus for each of indices i_2,j_1,j_2 the system (3.15) is solved in the index i_1. Then given $\tilde{g}_{i,j}$ the system (3.16) is solved in j_1 for each i_1,i_2,j_2. Given $g_{i,j}^*$ the system (3.17) is solved in i_2 for each i_1,j_1,j_2. Then (3.18) is solved in j_2 for each i_1,i_2,j_1 which gives the array $\bar{g}_{i,j}^{n+1}$. Eqs. (3.15) and (3.17) require periodic boundary conditions in ξ_1,ξ_2. Eqs. (3.16) and (3.18) require zero boundary conditions at $u_1,u_2=\pm1$.

The solution to (1.1) preserves the L_1 norm or total charge, that is, $\int_{\mathcal{A}}f(x,v,\bar{t})dvdx=K$ for $\bar{t}\in[0,T]$. For $\bar{t}\in[mT_1,(m+1)T_1]$ and $t=\bar{t}-mT_1$, $t\in[0,T_1]$ the function $f(x,v,\bar{t})$ is represented in terms of the solution to (2.9) by (2.20). Therefore, a change of variables in the integral is carried out from $(x,v)\to(\xi,\eta)$ and then $(\xi,\eta)\to(\xi,u)$. The respective Jacobian determinants for these change of variables are $|\partial(x,v)/\partial(\xi,\eta)|=e^{-2\beta t}$ and $|\partial(\xi,\eta)/\partial(\xi,u)|=c^2/\left(\left(1-u_1^2\right)^{3/2}\left(1-u_2^2\right)^{3/2}\right)$. The L_1 norm in terms of the function $g(\xi,u,t)$ which is the solution to (2.9) is given as

$$\int_\Omega g(\xi,u,t)\frac{c^2}{\left(1-u_1^2\right)^{3/2}\left(1-u_2^2\right)^{3/2}}dud\xi=K.$$

For the discrete approximation we let

$$\lambda=\frac{1}{K}\sum_{i,j}\bar{g}_{i,j}^{n+1}\frac{c^2}{\left(1-u_{1,j_1}^2\right)^{3/2}\left(1-u_{2,j_2}^2\right)^{3/2}}(\Delta u\Delta\xi)^2$$

and then $g_{i,j}^{n+1}=g_{i,j}^{m,n+1}=\bar{g}_{i,j}^{n+1}/\lambda$. Thus, the grid function $g_{i,j}^{m,n+1}$ has the property that

$$\sum_{i,j}g_{i,j}^{m,n+1}\frac{c^2}{\left(1-u_{1,j_1}^2\right)^{3/2}\left(1-u_{2,j_2}^2\right)^{3/2}}(\Delta u\Delta\xi)^2=K.$$

This renormalization of $g_{i,j}^{m,n}$ at each step preserves the discrete L_1 norm of the approximate solution.

As in [28] the iterative SOR procedure is most advantageous for relatively small values of the diffusion parameter, q. This is because for fixed values of the coefficients $c_1,\ldots,c_4$ the smaller the q value the smaller the quantity $\Theta(t_n)$, and the greater is the rate of convergence of the iterative procedure. For larger q values the iterative method may converge too slowly, and the preference can be to solve (3.4) by the direct Douglas–Rachford method.

3.2.3. The approximation of (2.11), particle trajectories

For $t_n\in[0,T_1]$ let $(x(\xi_i,\eta_j,t_n),v(\xi_i,\eta_j,t_n))$ be the solution to (2.11) with initial point $x(\xi_i,\eta_j,0)=\xi_i$, $v(\xi_i,\eta_j,0)=\eta_j$. Here $\xi_i=(\xi_{1,i_1},\xi_{2,i_2})$ and $\eta_j=\eta(u_j)=(\eta_{1,j_1},\eta_{2,j_2})$ where $\eta_{1,j_1}=cu_{1,j_1}\Big/\sqrt{1-u_{1,j_1}^2}$, $\eta_{2,j_2}=cu_{2,j_2}\Big/\sqrt{1-u_{2,j_2}^2}$. The approximation to this

trajectory where $i=(i_1,i_2)$, $j=(j_1,j_2)$ is denoted $(x(i,j,t_n),v(i,j,t_n))=(x_1(i,j,t_n),\dots,v_2(i,j,t_n))$. The approximation to the electric field $E(x(\xi_i,\eta_j,t_n),t_n)$ in (2.11) is denoted $\bar{E}(x(i,j,t_n),t_n)=(\bar{E}_1(x(i,j,t_n),t_n),\bar{E}_2(x(i,j,t_n),t_n))$. For $t_n\leqslant t\leqslant t_{n+1}$ the approximate trajectory is obtained as the solution to the system of equations

$$\begin{aligned}
&\frac{dx_1}{dt}=v_1,\quad x_1(t_n)=x_1(i,j,t_n)\\
&\frac{dv_1}{dt}=\bar{E}_1(x(i,j,t_n),t_n)-\beta v_1,\quad v_1(t_n)=v_1(i,j,t_n)\\
&\frac{dx_2}{dt}=v_2,\quad x_2(t_n)=x_2(i,j,t_n)\\
&\frac{dv_2}{dt}=\bar{E}_2(x(i,j,t_n),t_n)-\beta v_2,\quad v_2(t_n)=v_2(i,j,t_n)
\end{aligned}$$

These equations are integrated exactly as in [28], Section 2.2.3. Therefore, the equations for the particle trajectories given in vector notation are: let $x(i,j,0)=\xi_i,\ v(i,j,0)=\eta_j$. Then given $x(i,j,t_n)$, $v(i,j,t_n)$ and $\bar{E}(x(i,j,t_n),t_n)$ quantities at time t_{n+1} are

$$x(i,j,t_{n+1})=x(i,j,t_n)+\left(\frac{1-e^{-\beta\Delta t}}{\beta}\right)v(i,j,t_n)+\left(\frac{\Delta t}{\beta}-\frac{1-e^{-\beta\Delta t}}{\beta^2}\right)\bar{E}(x(i,j,t_n),t_n), \tag{3.19}$$

$$v(i,j,t_{n+1})=e^{-\beta\Delta t}v(i,j,t_n)+\left(\frac{1-e^{-\beta\Delta t}}{\beta}\right)\bar{E}(x(i,j,t_n),t_n). \tag{3.20}$$

3.2.4. Approximation of the first partial derivative equations (2.14) and the coefficients $c_1,\dots,c_{10}$

For an exact trajectory with initial point $x(\xi_i,\eta_j,0)=\xi_i,\ v(\xi_i,\eta_j,0)=\eta_j$ the first partial derivatives with respect to ξ,η can be written $\frac{\partial x_l}{\partial\xi_k}(\xi_i,\eta_j,t)$, $\frac{\partial v_l}{\partial\xi_k}(\xi_i,\eta_j,t)$, $\frac{\partial x_l}{\partial\eta_k}(\xi_i,\eta_j,t)$, $\frac{\partial v_l}{\partial\eta_k}(\xi_i,\eta_j,t)$ with $l=1,2$ and $k=1,2$. The system for first partial derivatives with respect to ξ_1 is given by (2.14). The approximation to the first partial derivatives at $t_n\in[0,T_1]$ are denoted $\frac{\partial x_l}{\partial\xi_k}(i,j,t_n)$, $\frac{\partial v_l}{\partial\xi_k}(i,j,t_n)$, $\frac{\partial x_l}{\partial\eta_k}(i,j,t_n)$, $\frac{\partial v_l}{\partial\eta_k}(i,j,t_n)$. As in [28], Section 2.2.4 the equations for these quantities are derived by differentiating (3.19) and (3.20) with respect to ξ,η. Let $\frac{\partial x_l}{\partial\xi_k}(i,j,t_n)=\frac{\partial x_l}{\partial\xi_k}(t_n)$ and similarly with other approximate partial derivatives. At $t_n=0$ let $\frac{\partial x_l}{\partial\xi_k}(0)=1$, $l=k$; $\frac{\partial x_l}{\partial\xi_k}(0)=0$, $l\neq k$; $\frac{\partial x_l}{\partial\eta_k}(0)=0$, and $\frac{\partial v_l}{\partial\xi_k}(0)=0$; $\frac{\partial v_l}{\partial\eta_k}(0)=1$, $l=k$; $\frac{\partial v_l}{\partial\eta_k}(0)=0$, $l\neq k$. Then given the values of $\frac{\partial x_l}{\partial\xi_k}(t_n)$, $\frac{\partial v_l}{\partial\xi_k}(t_n)$, $\frac{\partial x_l}{\partial\eta_k}(t_n)$, $\frac{\partial v_l}{\partial\eta_k}(t_n)$ the quantities at time t_{n+1} are computed as

$$\frac{\partial x_l}{\partial\xi_k}(t_{n+1})=\frac{\partial x_l}{\partial\xi_k}(t_n)+\left(\frac{1-e^{-\beta\Delta t}}{\beta}\right)\frac{\partial v_l}{\partial\xi_k}(t_n)+\left(\frac{\Delta t}{\beta}-\frac{1-e^{-\beta\Delta t}}{\beta^2}\right)\left(\frac{\partial\bar{E}_l}{\partial x_1}(x(t_n),t_n)\frac{\partial x_1}{\partial\xi_k}(t_n)+\frac{\partial\bar{E}_l}{\partial x_2}(x(t_n),t_n)\frac{\partial x_2}{\partial\xi_k}(t_n)\right) \tag{3.21}$$

$$\frac{\partial v_l}{\partial\xi_k}(t_{n+1})=e^{-\beta\Delta t}\frac{\partial v_l}{\partial\xi_k}(t_n)+\left(\frac{1-e^{-\beta\Delta t}}{\beta}\right)\left(\frac{\partial\bar{E}_l}{\partial x_1}(x(t_n),t_n)\frac{\partial x_1}{\partial\xi_k}(t_n)+\frac{\partial\bar{E}_l}{\partial x_2}(x(t_n),t_n)\frac{\partial x_2}{\partial\xi_k}(t_n)\right) \tag{3.22}$$

$$\frac{\partial x_l}{\partial\eta_k}(t_{n+1})=\frac{\partial x_l}{\partial\eta_k}(t_n)+\left(\frac{1-e^{-\beta\Delta t}}{\beta}\right)\frac{\partial v_l}{\partial\eta_k}(t_n)+\left(\frac{\Delta t}{\beta}-\frac{1-e^{-\beta\Delta t}}{\beta^2}\right)\left(\frac{\partial\bar{E}_l}{\partial x_1}(x(t_n),t_n)\frac{\partial x_1}{\partial\eta_k}(t_n)+\frac{\partial\bar{E}_l}{\partial x_2}(x(t_n),t_n)\frac{\partial x_2}{\partial\eta_k}(t_n)\right) \tag{3.23}$$

$$\frac{\partial v_l}{\partial\eta_k}(t_{n+1})=e^{-\beta\Delta t}\frac{\partial v_l}{\partial\eta_k}(t_n)+\left(\frac{1-e^{-\beta\Delta t}}{\beta}\right)\left(\frac{\partial\bar{E}_l}{\partial x_1}(x(t_n),t_n)\frac{\partial x_1}{\partial\eta_k}(t_n)+\frac{\partial\bar{E}_l}{\partial x_2}(x(t_n),t_n)\frac{\partial x_2}{\partial\eta_k}(t_n)\right) \tag{3.24}$$

The computation of the approximate electric field, $\bar{E}$, and its partial derivatives $\partial\bar{E}_l/\partial x_k$, $k,l=1,2$, is described in Section 3.2.6.

Given the first partial derivatives of the approximate trajectory $(x(i,j,t_n),v(i,j,t_n))$ the coefficients $c_1(i,j,t_n),\dots,c_{10}(i,j,t_n)$ in (3.4) can be derived. This involves approximating the solutions to systems (2.5). Thus, for each i,j at time t_n let

$$Q=\begin{pmatrix}
\frac{\partial x_1}{\partial\xi_1} & \frac{\partial x_1}{\partial\xi_2} & \frac{\partial x_1}{\partial\eta_1} & \frac{\partial x_1}{\partial\eta_2}\\
\frac{\partial x_2}{\partial\xi_1} & \frac{\partial x_2}{\partial\xi_2} & \frac{\partial x_2}{\partial\eta_1} & \frac{\partial x_2}{\partial\eta_2}\\
\frac{\partial v_1}{\partial\xi_1} & \frac{\partial v_1}{\partial\xi_2} & \frac{\partial v_1}{\partial\eta_1} & \frac{\partial v_1}{\partial\eta_2}\\
\frac{\partial v_2}{\partial\xi_1} & \frac{\partial v_2}{\partial\xi_2} & \frac{\partial v_2}{\partial\eta_1} & \frac{\partial v_2}{\partial\eta_2}
\end{pmatrix}. \tag{3.25}$$

Here $\frac{\partial x_1}{\partial\xi_1}=\frac{\partial x_1}{\partial\xi_1}(i,j,t_n)$ and similarly for all partial derivatives in Q. Let $\bar{u}_1=\left[\frac{\partial\xi_1}{\partial v_1},\frac{\partial\xi_2}{\partial v_1},\frac{\partial\eta_1}{\partial v_1},\frac{\partial\eta_2}{\partial v_1}\right]^T$ and $\bar{b}_1=[0,0,1,0]^T$. Let $\bar{u}_2=\left[\frac{\partial\xi_1}{\partial v_2},\frac{\partial\xi_2}{\partial v_2},\frac{\partial\eta_1}{\partial v_2},\frac{\partial\eta_2}{\partial v_2}\right]^T$ and $\bar{b}_2=[0,0,0,1]^T$. Then $\bar{u}_1,\bar{u}_2$ are the solutions to

$$Q\bar{u}_1=\bar{b}_1,\quad Q\bar{u}_2=\bar{b}_2. \tag{3.26}$$

Although the notation here is the same as in (2.5) the vectors $\bar{u}_1,\bar{u}_2$ represent approximate quantities, whereas, the vector $\bar{u}$ in (2.5) represents exact quantities. Solving the systems (3.26) for each i,j at time t_n the coefficients in (3.4) are: let $c_l(i,j,t_n)=c_l,\ l=1,\dots,10$, then

$$c_1=\sum_{k=1}^{2}\left(\frac{\partial\xi_1}{\partial v_k}\right)^2,\quad c_2=\sum_{k=1}^{2}\left(\frac{\partial\xi_2}{\partial v_k}\right)^2,\quad c_3=\sum_{k=1}^{2}\left(\frac{\partial\eta_1}{\partial v_k}\right)^2,\quad c_4=\sum_{k=1}^{2}\left(\frac{\partial\eta_2}{\partial v_k}\right)^2,\quad c_5=\sum_{k=1}^{2}\left(\frac{\partial\xi_1}{\partial v_k}\right)\left(\frac{\partial\xi_2}{\partial v_k}\right),$$
$$c_6=\sum_{k=1}^{2}\left(\frac{\partial\xi_1}{\partial v_k}\right)\left(\frac{\partial\eta_1}{\partial v_k}\right),\quad c_7=\sum_{k=1}^{2}\left(\frac{\partial\xi_1}{\partial v_k}\right)\left(\frac{\partial\eta_2}{\partial v_k}\right),\quad c_8=\sum_{k=1}^{2}\left(\frac{\partial\xi_2}{\partial v_k}\right)\left(\frac{\partial\eta_1}{\partial v_k}\right),\quad c_9=\sum_{k=1}^{2}\left(\frac{\partial\xi_2}{\partial v_k}\right)\left(\frac{\partial\eta_2}{\partial v_k}\right),$$
$$c_{10}=\sum_{k=1}^{2}\left(\frac{\partial\eta_1}{\partial v_k}\right)\left(\frac{\partial\eta_2}{\partial v_k}\right).$$

3.2.5. Approximation of the second partial derivative equations (2.15) and the coefficients $c_{11},\ldots,c_{14}$

To obtain the coefficients $c_{11},\ldots,c_{14}$ in (3.4) it is necessary to approximate the second partial derivatives with respect to ξ,η of the functions (2.10) which are the solutions to (2.11). There are ten second partial derivatives for each of the four functions of (2.10). The system of equations for derivatives with respect to ξ_1,ξ_2 is given by (2.15). As representative of the approximation of the second partials of (2.10) we therefore give the approximation of (2.15). This is done by further differentiating Eqs. (3.19) and (3.20). In (3.21) and (3.22) let us assume $k=2$ and differentiate with respect to ξ_1. Then for $l=1,2$ at $t_n=0$, $\frac{\partial^2 x_l}{\partial\xi_1\partial\xi_2}(0)=0$, $\frac{\partial^2 v_l}{\partial\xi_1\partial\xi_2}(0)=0$, and given values of $\frac{\partial x_l}{\partial\xi_1}(t_n)$, $\frac{\partial x_l}{\partial\xi_2}(t_n)$, $\frac{\partial^2 x_l}{\partial\xi_1\partial\xi_2}(t_n)$, $\frac{\partial^2 v_l}{\partial\xi_1\partial\xi_2}(t_n)$ quantities at time t_{n+1} are computed as

$$\begin{aligned}\frac{\partial^2 x_l}{\partial\xi_1\partial\xi_2}(t_{n+1})&=\frac{\partial^2 x_l}{\partial\xi_1\partial\xi_2}(t_n)+\left(\frac{1-e^{-\beta\Delta t}}{\beta}\right)\frac{\partial^2 v_l}{\partial\xi_1\partial\xi_2}(t_n)+\left(\frac{\Delta t}{\beta}-\frac{1-e^{-\beta\Delta t}}{\beta^2}\right)\left(\frac{\partial\overline{E}_l}{\partial x_1}(t_n)\frac{\partial^2 x_1}{\partial\xi_1\partial\xi_2}(t_n)+\frac{\partial\overline{E}_l}{\partial x_2}(t_n)\frac{\partial^2 x_2}{\partial\xi_1\partial\xi_2}(t_n)\right)\\&+\left(\frac{\Delta t}{\beta}-\frac{1-e^{-\beta\Delta t}}{\beta^2}\right)\left(\frac{\partial^2\overline{E}_l}{\partial x_1^2}(t_n)\left(\frac{\partial x_1}{\partial\xi_1}\right)\left(\frac{\partial x_1}{\partial\xi_2}\right)(t_n)+\frac{\partial^2\overline{E}_l}{\partial x_1\partial x_2}(t_n)\left(\frac{\partial x_1}{\partial\xi_1}\frac{\partial x_2}{\partial\xi_2}+\frac{\partial x_1}{\partial\xi_2}\frac{\partial x_2}{\partial\xi_1}\right)(t_n)\right.\\&\left.+\frac{\partial^2\overline{E}_l}{\partial x_2^2}(t_n)\left(\frac{\partial x_2}{\partial\xi_1}\right)\left(\frac{\partial x_2}{\partial\xi_2}\right)(t_n)\right),\end{aligned}\tag{3.27}$$

$$\begin{aligned}\frac{\partial^2 v_l}{\partial\xi_1\partial\xi_2}(t_{n+1})&=e^{-\beta\Delta t}\frac{\partial^2 v_l}{\partial\xi_1\partial\xi_2}(t_n)+\left(\frac{1-e^{-\beta\Delta t}}{\beta}\right)\left(\frac{\partial\overline{E}_l}{\partial x_1}(t_n)\frac{\partial^2 x_1}{\partial\xi_1\partial\xi_2}(t_n)+\frac{\partial\overline{E}_l}{\partial x_2}(t_n)\frac{\partial^2 x_2}{\partial\xi_1\partial\xi_2}(t_n)\right)\\&+\left(\frac{1-e^{-\beta\Delta t}}{\beta}\right)\left(\frac{\partial^2\overline{E}_l}{\partial x_1^2}(t_n)\left(\frac{\partial x_1}{\partial\xi_1}\right)\left(\frac{\partial x_1}{\partial\xi_2}\right)(t_n)+\frac{\partial^2\overline{E}_l}{\partial x_1\partial x_2}(t_n)\left(\frac{\partial x_1}{\partial\xi_1}\frac{\partial x_2}{\partial\xi_2}+\frac{\partial x_1}{\partial\xi_2}\frac{\partial x_2}{\partial\xi_1}\right)(t_n)\right.\\&\left.+\frac{\partial^2\overline{E}_l}{\partial x_2^2}(t_n)\left(\frac{\partial x_2}{\partial\xi_1}\right)\left(\frac{\partial x_2}{\partial\xi_2}\right)(t_n)\right).\end{aligned}\tag{3.28}$$

Here $\overline{E}_l(t_n)=\overline{E}_l(x(t_n),t_n)$. The computation of the second partial derivatives of $\overline{E}_l(t_n)$ is described in Section 3.2.6. Expressions for other approximate second partial derivatives of the functions (2.10) are the same form as (3.27) and (3.28) but with derivatives with respect to ξ_1,ξ_2 replaced by other second derivatives in terms of the variables $\xi_1,\xi_2,\eta_1,\eta_2$. All approximate second partial derivatives have initial value of zero at $t_n=0$.

Given the first and second partial derivatives of the approximate trajectory $(x(i,j,t_n),v(i,j,t_n))$ the coefficients $c_{11}(i,j,t_n),\ldots,c_{14}(i,j,t_n)$ in (3.4) can be derived. This is done by solving discrete versions of the system (2.6). For the indices i,j let $\frac{\partial^2 x_1}{\partial\xi_1^2}=\frac{\partial^2 x_1}{\partial\xi_1^2}(i,j,t_n)$ and similarly with the other nine second partial derivatives with respect to ξ,η of $x_1(i,j,t_n)$. Then

$$A_1=\begin{pmatrix}\frac{\partial^2 x_1}{\partial\xi_1^2} & \frac{\partial^2 x_1}{\partial\xi_1\partial\xi_2} & \frac{\partial^2 x_1}{\partial\xi_1\partial\eta_1} & \frac{\partial^2 x_1}{\partial\xi_1\partial\eta_2}\\ \cdots & \frac{\partial^2 x_1}{\partial\xi_2^2} & \frac{\partial^2 x_1}{\partial\xi_2\partial\eta_1} & \frac{\partial^2 x_1}{\partial\xi_2\partial\eta_2}\\ \cdots & & \frac{\partial^2 x_1}{\partial\eta_1^2} & \frac{\partial^2 x_1}{\partial\eta_1\partial\eta_2}\\ \cdots & & \cdots & \frac{\partial^2 x_1}{\partial\eta_2^2}\end{pmatrix}.$$

The lower triangular part of the matrix is obtained by symmetry. The 4×4 matrices A_2,A_3,A_4 are the same form as A_1 but with second partial derivatives of x_1 replaced with second partial derivatives with respect to ξ,η of x_2,v_1,v_2, respectively. Let $\overline{F}_1=[F_1,F_2,F_3,F_4]$ where $F_i=\bar{u}_1A_i\bar{u}_1^T$, $i=1,--,4$. Here $\bar{u}_1=\left[\frac{\partial\xi_1}{\partial v_1},\frac{\partial\xi_2}{\partial v_1},\frac{\partial\eta_1}{\partial v_1},\frac{\partial\eta_2}{\partial v_1}\right]$ is computed according to (3.26). Let $\bar{y}_1=\left[\frac{\partial^2\xi_1}{\partial v_1^2},\frac{\partial^2\xi_2}{\partial v_1^2},\frac{\partial^2\eta_1}{\partial v_1^2},\frac{\partial^2\eta_2}{\partial v_1^2}\right]$. Then the vector $\bar{y}_1$ is obtained as the solution to $Q\bar{y}_1=-\overline{F}_1$ in which the matrix Q is given by (3.25). Let $\bar{u}_2=\left[\frac{\partial\xi_1}{\partial v_2},\frac{\partial\xi_2}{\partial v_2},\frac{\partial\eta_1}{\partial v_2},\frac{\partial\eta_2}{\partial v_2}\right]$computed according to (3.26), and $\overline{F}_2=[F_1,F_2,F_3,F_4]$ where $F_i=\bar{u}_2A_i\bar{u}_2^T$, $i=1,--,4$. Let $\bar{y}_2=\left[\frac{\partial^2\xi_1}{\partial v_2^2},\frac{\partial^2\xi_2}{\partial v_2^2},\frac{\partial^2\eta_1}{\partial v_2^2},\frac{\partial^2\eta_2}{\partial v_2^2}\right]$. Then $\bar{y}_2$ is obtained as the solution to $Q\bar{y}_2=-\overline{F}_2$. The notation for vectors $\bar{y}_1,\bar{y}_2$ is the same as for $\bar{y}$ in (2.6). However, the understanding is that while $\bar{y}$ represents exact quantities $\bar{y}_1,\bar{y}_2$ represent approximate quantities computed on the basis of approximations to the first and second partial derivatives of the functions (2.10).

Having computed vectors $\bar{y}_1, \bar{y}_2$ the coefficients $c_{11}, \ldots, c_{14}$ are: let $c_l = c_l(i,j,t_n),\ l = 11, \ldots, 14$. Then

$$c_{11} = \sum_{k=1}^{2} \frac{\partial^2 \xi_1}{\partial v_k^2}, \quad c_{12} = \sum_{k=1}^{2} \frac{\partial^2 \xi_2}{\partial v_k^2}, \quad c_{13} = \sum_{k=1}^{2} \frac{\partial^2 \eta_1}{\partial v_k^2}, \quad c_{14} = \sum_{k=1}^{2} \frac{\partial^2 \eta_2}{\partial v_k^2}.$$

3.2.6. The approximate charge density and electric field

The description given here is a two-dimensional version of [28], Section 2.2.6. The approximate trajectory $(x(i,j,t_n), v(i,j,t_n)),\ t_n \in [0,T_1],\ n = 0,1,\ldots,N_g$ is considered to be the path of an element of charge $q_{i,j}$ in phase space. This element of charge is defined as $q_{i,j} = q_{i_1,i_2,j_1,j_2} = \bar{f}(x(i,j,t_n), v(i,j,t_n), t_n)\Delta A_{i,j}$ where $\bar{f}$ is the approximate distribution function, and $\Delta A_{i,j}$ is a differential of "volume" in four dimensional space associated with the i,j trajectory at time t_n. In terms of the parameters $\Delta\xi, \Delta u$ then

$$\Delta A_{i,j} = \frac{c^2 e^{-2\beta t_n} (\Delta u \Delta \xi)^2}{(1-u_{1,j_1}^2)^{3/2}(1-u_{2,j_2}^2)^{3/2}}.$$

On the time interval $[mT_1, (m+1)T_1],\ m = 0,1,\ldots,M-1$ then $\bar{f}(x(i,j,t_n), v(i,j,t_n), t_n) = e^{2\beta t_n} g_{i,j}^{m,n}$. Thus

$$q_{i,j}^{m,n} = e^{2\beta t_n} g_{i,j}^{m,n} \frac{c^2 e^{-2\beta t_n} (\Delta u \Delta \xi)^2}{\left(1-u_{1,j_1}^2\right)^{3/2}\left(1-u_{2,j_2}^2\right)^{3/2}} = \frac{c^2 g_{i,j}^{m,n} (\Delta u \Delta \xi)^2}{\left(1-u_{1,j_1}^2\right)^{3/2}\left(1-u_{2,j_2}^2\right)^{3/2}}. \tag{3.29}$$

A discrete electron charge density resulting from the charge elements $q_{i,j}^{m,n}$ is defined as

$$\tilde{\rho}_e(x,t) = \sum_{i,j} q_{i,j}^{m,n} \delta(x_1 - x_1(i,j,t_n)) \delta(x_2 - x_2(i,j,t_n)) \tag{3.30}$$

where $\delta(x)$ is the Dirac delta function.

We approximate the solution to

$$\begin{aligned} &\Delta_x \phi = -\rho(x,t) \\ &\phi(0,x_2,t) = \phi(L,x_2,t), \quad \phi(x_1,0,t) = \phi(x_1,L,t) \end{aligned} \tag{3.31}$$

by the particle and cell method in two dimensions. For the positive integer N_p let $\epsilon = L/N_p$. Then the region $[0,L] \times [0,L]$ is partitioned by a uniform rectangular grid as $x_{1,k_1} = k_1\epsilon,\ x_{2,k_2} = k_2\epsilon$ with k_1, k_2 integers such that $k_1, k_2 = 0,1,\ldots,N_p$. For $y \in R_1$ let $w(y)$ be a continuous function with compact support such that

$$\int_{-\infty}^{\infty} w(y)dy = 1, \ \sum_{i \in z} w(y-i) = 1, \quad z - \textit{integers}.$$

Let $w_\epsilon(y) = \frac{1}{\epsilon} w(\frac{y}{\epsilon})$. For $x = (x_1, x_2) \in R_2$ let $\bar{w}_\epsilon(x) = \bar{w}_\epsilon(x_1,x_2) = \frac{1}{\epsilon^2} w(\frac{x_1}{\epsilon}) w(\frac{x_2}{\epsilon})$. The grid charge density for electrons $\rho_\kappa^e(t_n),\ \kappa = (k_1,k_2),\ k_1,k_2 = 0,1,\ldots,N_p-1$ is determined by

$$\begin{aligned} \rho_\kappa^e(t_n) &= \int_0^L \int_0^L \bar{w}_\epsilon(x - x_\kappa) \tilde{\rho}_e(x,t_n) dx = \int_0^L \int_0^L w_\epsilon(x_1 - x_{1,k_1}) w_\epsilon(x_2 - x_{2,k_2}) \tilde{\rho}_e(x_1,x_2,t_n) dx_1 dx_2 \\ &= \sum_{i,j} q_{i,j}^{m,n} w_\epsilon(x_1(i,j,t_n) - x_{1,k_1}) w_\epsilon(x_2(i,j,t_n) - x_{2,k_2}). \end{aligned} \tag{3.32}$$

This formula can require some modification near the boundary to account for the periodicity, i.e., so that $\rho_{0,k_2}^e(t_n) = \rho_{N_p,k_2}^e(t_n)$ and $\rho_{k_1,0}^e(t_n) = \rho_{k_1,N_p}^e(t_n)$. Also, as a result of the normalization of $g_{i,j}^{m,n}$ discussed in Section 3.2.2 the grid charge density $\rho_\kappa^e(t_n)$ has the property that

$$\sum_{k_1=0}^{N_p-1} \sum_{k_2=0}^{N_p-1} \rho_\kappa^e(t_n) \epsilon^2 = K.$$

As for the background charge, $h(x)$, it is assumed that $\int_0^L \int_0^L h(x)dx = K$. This is necessary to preserve charge neutrality in the expression for $\rho(x,t)$ in (1.2). Let

$$\mu = \left(\sum_{k_1=0}^{N_p-1} \sum_{k_2=0}^{N_p-1} h(x_{1,k_1}, x_{2,k_2}) \epsilon^2 \right) \Big/ K.$$

The grid charge density for the background charge is then defined by $\rho_\kappa^b(t_n) = \frac{1}{\mu} h(x_{1,k_1}, x_{2,k_2})$ for $k_1, k_2 = 0,1,\ldots,N_p-1$, and it is also assumed that $\rho_{0,k_2}^b(t_n) = \rho_{N_p,k_2}^b(t_n)$ and $\rho_{k_1,0}^b(t_n) = \rho_{k_1,N_p}^b(t_n)$. The discrete function $\rho_\kappa^b(t_n)$ has the property

$$\sum_{k_1=0}^{N_p-1} \sum_{k_2=0}^{N_p-1} \rho_\kappa^b(t_n) \epsilon^2 = K. \tag{3.33}$$

The grid charge density for the discrete approximation to (1.2) is $\rho_\kappa(t_n) = \rho^e_\kappa(t_n) - \rho^b_\kappa(t_n)$. The grid function $\rho_\kappa(t_n)$ has the property

$$\sum_{k_1=0}^{N_p-1}\sum_{k_2=0}^{N_p-1}\rho_\kappa(t_n)\epsilon^2 = 0.$$

Thus, charge neutrality is preserved for the discrete problem.

The potential at grid points is then the solution to

$$\frac{\phi_{k_1+1,k_2} - 2\phi_{k_1,k_2} + \phi_{k_1-1,k_2}}{\epsilon^2} + \frac{\phi_{k_1,k_2+1} - 2\phi_{k_1,k_2} + \phi_{k_1,k_2-1}}{\epsilon^2} = -\rho_{k_1,k_2}(t_n), \tag{3.34}$$
$$k_1,k_2 = 0,1,\ldots,N_p-1, \quad \phi_{0,k_2} = \phi_{N_p,k_2}, \quad \phi_{k_1,0} = \phi_{k_1,N_p}.$$

Near the boundaries the formula (3.34) is modified by the periodicity. The solution to (3.34) is obtained by solving a linear system. A constant can be added to a solution of (1.2) and this still gives a solution. Therefore, the solution to (3.34) is obtained for which $\phi_{0,0} = 0$. We therefore solve for ϕ_{k_1,k_2}, $k_1,k_2 = 0,N_p-1$ with the assumption that $\phi_{0,0} = 0$ and $\phi_{0,k_2} = \phi_{N_p,k_2}$, $\phi_{k_1,0} = \phi_{k_1,N_p}$.

The linear system to be solved for ϕ_{k_1,k_2} is as follows: let $l = k_2N_p + k_1$, $k_1 = 0,1,\ldots,N_p-1$, $k_2 = 0,1,\ldots,N_p-1$. Let $u_l = \phi_{k_1,k_2}$ and $\rho_l = \rho_{k_1,k_2}(t_n)$, $l = 0,1,\ldots,N_p^2-1$. We need to determine the vector $\overline{\Phi} = [u_0,\ldots,u_{N_p^2-1}]$. This vector has N_p^2 components. However, from the previous consideration $u_0 = 0$. Thus, the unknown vector to be determined is $\bar{u} = [u_1,\ldots,u_{N_p^2-1}]$ with N_p^2-1 components. Let $\bar{\rho} = [\rho_1,\ldots,\rho_{N_p^2-1}]$. The system to be solved is

$$A\bar{u} = \bar{\rho} \tag{3.35}$$

where A is an $\left(N_p^2-1\right)\times\left(N_p^2-1\right)$ coefficient matrix. To obtain the matrix A we consider the $N_p^2\times N_p^2$ matrix B of the form

$$B = \begin{pmatrix} A_D & -I & \ddots & -I \\ -I & \ddots & \ddots & 0 \\ 0 & \ddots & \ddots & -I \\ -I & \ddots & -I & A_D \end{pmatrix}.$$

Here A_D is an $N_p\times N_p$ matrix such that $A_D(i,i) = 4$, $i = 1,\ldots,N_p$; $A_D(i,i+1) = -1$, $i = 1,\ldots,N_p-1$; $A_D(i-1,i) = -1$, $i = 2,\ldots,N_p$; $A_D(1,N_p) = -1$; $A_D(N_p,1) = -1$. All other elements in A_D are zero. The matrix $-I$ is $-I = (-1)I_{N_p}$ where I_{N_p} is an $N_p\times N_p$ identity matrix. Thus, B is a block tridiagonal matrix with the additional block, $-I$, in the upper right and bottom left corners. The matrix A is the $(N_p^2-1)\times(N_p^2-1)$ matrix obtained by eliminating the first row and first column of B. The matrix B is singular; however, A is nonsingular, and therefore the system (3.35) has a unique solution. The solution to (3.35) provides the values for ϕ_{k_1,k_2}, $k_1,k_2 = 0,1,\ldots,N_p-1$, and $(k_1,k_2)\neq(0,0)$. By assumption $\phi_{0,0} = 0$ and the values ϕ_{N_p,k_2}, $k_2 = 0,1,\ldots,N_p$ and ϕ_{k_1,N_p}, $k_1 = 0,1,\ldots,N_p$ are obtained by periodicity.

Having determined ϕ_{k_1,k_2} for $k_1,k_2 = 0,1,\ldots,N_p$ the electric field at the grid points at time t_n is determined as follows: for $k_2 = 0,\ldots,N_p-1$ and $k_1 = 1,\ldots,N_p-1$ then

$$E_1^n(\kappa) = E_1^n(k_1,k_2) = -\left(\frac{\phi_{k_1+1,k_2} - \phi_{k_1-1,k_2}}{2\epsilon}\right).$$

The exact field $E_1(x,t) = -\frac{\partial\phi}{\partial x_1}$ has the property that $\int_0^L E_1(x_1,x_2)dx_1 = -\int_0^L \frac{\partial\phi}{\partial x_1}dx_1 = 0$. Making use of this property for the discrete problem let $k_2 = 0,\ldots,N_p-1$ and $E_1^n(0,k_2) = -\sum_{k_1=1}^{N_p-1}E_1^n(k_1,k_2)$. For $k_1 = 0,\ldots,N_p-1$ and $k_2 = 1,\ldots,N_p-1$ then

$$E_2^n(\kappa) = E_2^n(k_1,k_2) = -\left(\frac{\phi_{k_1,k_2+1} - \phi_{k_1,k_2-1}}{2\epsilon}\right).$$

Also, as $\int_0^L E_2(x_1,x_2)dx_2 = 0$ the discrete analogue provides $E_2^n(k_1,0) = -\sum_{k_2=1}^{N_p-1}E_2^n(k_1,k_2)$. The quantities of $E_1^n(k_1,k_2), E_2^n(k_1,k_2)$ have now been obtained for $k_1,k_2 = 0,1,\ldots,N_p-1$. The values of E_1^n, E_2^n are extended to $k_2 = N_p$, $k_1 = 0,\ldots,N_p$ and $k_1 = N_p$, $k_2 = 0,\ldots,N_p$ by periodicity.

It is also necessary to compute approximate first and second partial derivatives of $E(x,t)$ at the grid points. For $l = 1,2$ and $k_1,k_2 = 1,\ldots,N_p$ then

$$D_1E_l^n(\kappa) = D_1E_l^n(k_1,k_2) = \frac{E_l^n(k_1+1,k_2) - E_l^n(k_1-1,k_2)}{2\epsilon},$$
$$D_2E_l^n(\kappa) = \frac{E_l^n(k_1,k_2+1) - E_l^n(k_1,k_2-1)}{2\epsilon},$$
$$D_1^2E_l^n(\kappa) = \frac{E_l^n(k_1+1,k_2) - 2E_l^n(k_1,k_2) + E_l^n(k_1-1,k_2)}{\epsilon^2},$$

$$D_2^2 E_l^n(\kappa) = \frac{E_l^n(k_1,k_2+1) - 2E_l^n(k_1,k_2) + E_l^n(k_1,k_2-1)}{\epsilon^2},$$
$$D_1 D_2 E_l^n(\kappa) = \big(E_l^n(k_1+1,k_2+1) - E_l^n(k_1+1,k_2-1) - E_l^n(k_1-1,k_2+1) + E_l^n(k_1-1,k_2-1)\big)/(4\epsilon^2).$$

These formulas are modified by the periodicity to obtain the values when $k_1 = 0$ or N_p or $k_2 = 0$ or N_p.

The approximate field $\bar{E}(x,t_n) = (\bar{E}_1(x,t_n), \bar{E}_2(x,t_n))$ and the first and second partial derivatives of $\bar{E}$ are defined as continuous functions of x as follows: let $\sum_{\kappa=0}^{N_p} = \sum_{k_1=0}^{N_p}\sum_{k_2=0}^{N_p}$ then for $l = 1,2$

$$\bar{E}_l(x,t_n) = \epsilon^2 \sum_{\kappa=0}^{N_p} E_l^n(\kappa)\bar{w}_\epsilon(x - x_\kappa) = \epsilon^2 \sum_{k_1=0}^{N_p}\sum_{k_2=0}^{N_p} E_l^n(k_1,k_2) w_\epsilon(x_1 - x_{1,k_1}) w_\epsilon(x_2 - x_{2,k_2}), \tag{3.36}$$

$$\frac{\partial \bar{E}_l(x,t_n)}{\partial x_1} = \epsilon^2 \sum_{\kappa=0}^{N_p} D_1 E_l^n(\kappa)\bar{w}_\epsilon(x - x_\kappa),$$
$$\frac{\partial \bar{E}_l(x,t_n)}{\partial x_2} = \epsilon^2 \sum_{\kappa=0}^{N_p} D_2 E_l^n(\kappa)\bar{w}_\epsilon(x - x_\kappa), \tag{3.37}$$

$$\frac{\partial^2 \bar{E}_l(x,t_n)}{\partial x_1^2} = \epsilon^2 \sum_{\kappa=0}^{N_p} D_1^2 E_l^n(\kappa)\bar{w}_\epsilon(x - x_\kappa),$$
$$\frac{\partial^2 \bar{E}_l(x,t_n)}{\partial x_2^2} = \epsilon^2 \sum_{\kappa=0}^{N_p} D_2^2 E_l^n(\kappa)\bar{w}_\epsilon(x - x_\kappa), \tag{3.38}$$
$$\frac{\partial^2 \bar{E}_l(x,t_n)}{\partial x_1 \partial x_2} = \epsilon^2 \sum_{\kappa=0}^{N_p} D_1 D_2 E_l^n(\kappa)\bar{w}_\epsilon(x - x_\kappa).$$

The particle to grid assignment function $w(y)$ that is used is the quadratic spline described in [28], Section 2.2.6. This function is of class C^1 and is given as

$$w(y) = \begin{cases} \frac{1}{2}\left(\frac{3}{2}+y\right)^2, & -\frac{3}{2} \leqslant y \leqslant -\frac{1}{2} \\ \frac{3}{4} - y^2, & -\frac{1}{2} \leqslant y \leqslant \frac{1}{2} \\ \frac{1}{2}\left(\frac{3}{2}-y\right)^2, & \frac{1}{2} \leqslant y \leqslant \frac{3}{2} \\ 0, & |y| > \frac{3}{2} \end{cases}. \tag{3.39}$$

With $\bar{w}_\epsilon(x)$ constructed from $w(y)$ given by (3.39) then in the formula (3.32) a charge $q_{i,j}^{m,n}$ is distributed to the nine nearest grid points. Similarly the field at a particle position which is obtained from (3.36) is derived from the field at the nine nearest grid points.

3.3. Regriding the solution

At the time $\tau_{m+1} = (m+1)T_1$, $m = 0,1,\ldots,M-1$ the solution along particle trajectories is interpolated onto the fixed grid given by (3.1) and (3.2). This provides a new initial function for (3.4). The particle method described in Section 3.2 is reinitialized with $t_n = 0$, and the particle computation of Section 3.2 is repeated for $(m+1)T_1 \leqslant t_n \leqslant (m+2)T_1$. We generalize to two dimensions the method of [28], Section 2.3 so that the regriding preserves the total charge, momentum, and kinetic energy of the solution.

At time $\tau_{m+1} = mT_1 + t_{N_g} = (m+1)T_1$ then the i',j' trajectory has coordinates in phase space $(x(i',j',t_{N_g}), v(i',j',t_{N_g}))$. Phase space is the set $\mathcal{A}$ defined for (1.1). This point in phase space corresponds to a point $(\bar{\xi},\bar{u})$ in Ω where $\bar{\xi} = (\bar{\xi}_1,\bar{\xi}_2) = x(i',j',t_{N_g}) = (x_1(i',j',t_{N_g}), x_2(i',j',t_{N_g}))$ and $\bar{u} = (\bar{u}_1,\bar{u}_2)$ with

$$\bar{u}_1 = \frac{v_1(i',j',t_{N_g})}{\sqrt{c^2 + (v_1(i',j',t_{N_g}))^2}}, \quad \bar{u}_2 = \frac{v_2(i',j',t_{N_g})}{\sqrt{c^2 + (v_2(i',j',t_{N_g}))^2}}.$$

The element of charge along the i',j' trajectory at time t_{N_g} is $q_{i',j'}^{m,N_g}$ as given by (3.29). Referring to the partition of Ω given by (3.1) and (3.2) it is assumed that there are indices $i = (i_1,i_2)$, $j = (j_1,j_2)$ such that $\xi_{1,i_1} \leqslant \bar{\xi}_1 \leqslant \xi_{1,i_1+1}$, $\xi_{2,i_2} \leqslant \bar{\xi}_2 \leqslant \xi_{2,i_2+1}$ and $u_{1,j_1} \leqslant \bar{u}_1 \leqslant u_{1,j_1+1}$, $u_{2,j_2} \leqslant \bar{u}_2 \leqslant u_{2,j_2+1}$. The charge $q_{i',j'}^{m,N_g}$ gets distributed over thirty six points of the partition of Ω. This is done in the following way. First, $\bar{\xi}$ is contained in the rectangle $\{(\xi_1,\xi_2)/\xi_{1,i_1} \leqslant \xi_1 \leqslant \xi_{1,i_1+1},\ \xi_{2,i_2} \leqslant \xi_2 \leqslant \xi_{2,i_2+1}\}$. Let $p_2 = (\bar{\xi}_1 - \xi_{1,i_1})/\Delta\xi$, $p_1 = 1 - p_2$; $d_2 = (\bar{\xi}_2 - \xi_{2,i_2})/\Delta\xi$, $d_1 = 1 - d_2$. Then let $w_{\kappa_1,\kappa_2} = p_{\kappa_1} d_{\kappa_2}$, $\kappa_1,\kappa_2 = 1,2$. Let $\bar{q} = q_{i',j'}^{m,N_g}$. The charge $\bar{q}$ is distributed linearly to the corner points of the rectangle. The charge at $(\xi_{1,i_1},\xi_{2,i_2})$ is $q_{1,1}$, at $(\xi_{1,i_1+1},\xi_{2,i_2})$ is $q_{2,1}$, at $(\xi_{1,i_1},\xi_{2,i_2+1})$ is $q_{1,2}$, at $(\xi_{1,i_1+1},\xi_{2,i_2+1})$ is $q_{2,2}$. These charges are $q_{1,1} = w_{1,1}\bar{q}$, $q_{2,1} = w_{2,1}\bar{q}$, $q_{1,2} = w_{1,2}\bar{q}$, $q_{2,2} = w_{2,2}\bar{q}$. Stated more concisely let $\kappa_1,\kappa_2 = 1,2$. Then the charge q_{κ_1,κ_2} given by $q_{\kappa_1,\kappa_2} = w_{\kappa_1,\kappa_2}\bar{q}$ is located at ξ coordinates given by $(\xi_{1,i_1+\kappa_1-1}, \xi_{2,i_2+\kappa_2-1})$. We note that $\sum_{\kappa_1=1}^{2}\sum_{\kappa_2=1}^{2} q_{\kappa_1,\kappa_2} = \bar{q}$.

Each of the four charges q_{κ_1,κ_2}, $\kappa_1,\kappa_2 = 1,2$ is then distributed over nine points in velocity space (the u domain) so as to conserve the total charge, momentum, and kinetic energy associated with the approximate distribution function. Let (u_{1,k_1}, u_{2,k_2}) be these points for indices k_1, k_2 to be specified. It is assumed that $u_{1,j_1} \leqslant \bar{u}_1 \leqslant u_{1,j_1+1}$, $u_{2,j_2} \leqslant \bar{u}_2 \leqslant u_{2,j_2+1}$. Let $b_1 = (\bar{u}_1 - u_{1,j_1})/\Delta u$, $b_2 = (\bar{u}_2 - u_{2,j_2})/\Delta u$. Let $\mathcal{K}_1$ be the set of k_1 indices. If $0 \leqslant b_1 \leqslant .5$ then $\mathcal{K}_1 = \{j_1 - 1, j_1, j_1 + 1\}$, i.e., k_1 has values $j_1 - 1, j_1, j_1 + 1$. If $.5 < b_1 \leqslant 1$ then $\mathcal{K}_1 = \{j_1, j_1 + 1, j_1 + 2\}$. Let $\mathcal{K}_2$ be the set of k_2 indices. If $0 \leqslant b_2 \leqslant .5$ then $\mathcal{K}_2 = \{j_2 - 1, j_2, j_2 + 1\}$, if $.5 < b_2 \leqslant 1$ then $\mathcal{K}_2 = \{j_2, j_2 + 1, j_2 + 2\}$. Let us consider the charge q_{κ_1,κ_2} at $(\xi_{1,i_1+\kappa_1-1}, \xi_{2,i_2+\kappa_2-1})$, $\kappa_1,\kappa_2 = 1,2$ and determine how the charge is distributed over points in velocity space. For each $k_1 \in \mathcal{K}_1$ and $k_2 \in \mathcal{K}_2$ then point $(\xi_{1,i_1+\kappa_1-1}, \xi_{2,i_2+\kappa_2-1}, u_{1,k_1}, u_{2,k_2}) \in \Omega$ corresponds to a point $(\xi_{1,i_1+\kappa_1-1}, \xi_{2,i_2+\kappa_2-1}, \eta_{1,k_1}, \eta_{2,k_2}) \in \mathcal{A}_0$ such that

$$\eta_{1,k_1} = \frac{cu_{1,k_1}}{\sqrt{1-(u_{1,k_1})^2}}, \quad \eta_{2,k_2} = \frac{cu_{2,k_2}}{\sqrt{1-(u_{2,k_2})^2}}.$$

Let $l_1 = 1,2,3$ count the indices in $\mathcal{K}_1$ in ascending order. Let us consider the case for $0 \leqslant b_1 \leqslant .5$. Then $l_1 = 1$ refers to $j_1 - 1$, $l_1 = 2$ to j_2, $l_1 = 3$ to $j_1 + 1$. Let $\gamma_{l_1} = y_{l_1} q_{\kappa_1,\kappa_2}$, $l_1 = 1,2,3$. Then $\gamma_1, \gamma_2, \gamma_3$ are the charges distributed to points in Ω with coordinates u_{1,k_1} and with coordinates u_{2,k_2} unspecified. The quantities $\gamma_1, \gamma_2, \gamma_3$ are obtained by multiplying q_{κ_1,κ_2} by the weight quantities y_1, y_2, y_3. Let $\bar{v} = (\bar{v}_1, \bar{v}_2) = (v_1(i', j', t_{N_g}), v_2(i', j', t_{N_g}))$, the v coordinates of the charge $\bar{q} = q^{m,N_g}_{i',j'}$. For $0 \leqslant b_1 \leqslant .5$ the weights y_1, y_2, y_3 are obtained as the solution to

$$\begin{aligned} &y_1 + y_2 + y_3 = 1 \\ &\eta_{1,j_1-1} y_1 + \eta_{1,j_1} y_2 + \eta_{1,j_1+1} y_3 = \bar{v}_1 \\ &(\eta_{1,j_1-1})^2 y_1 + (\eta_{1,j_1})^2 y_2 + (\eta_{1,j_1+1})^2 y_3 = \bar{v}_1^2. \end{aligned} \tag{3.40}$$

If $.5 < b_1 \leqslant 1$ the quantities $\eta_{1,j_1-1}, \eta_{1,j_1}, \eta_{1,j_1+1}$ in (3.40) are replaced with $\eta_{1,j_1}, \eta_{1,j_1+1}, \eta_{1,j_1+2}$.

Each charge γ_{l_1}, $l_1 = 1,2,3$ now gets distributed to points in Ω according to the coordinates u_{2,k_2}. Let us assume $0 \leqslant b_2 \leqslant .5$ then $\mathcal{K}_2 = \{j_2 - 1, j_2, j_2 + 1\}$. Let $\mu_{l_1,l_2} = z_{l_2}\gamma_{l_1}$. Then for $l_2 = 1,2,3$ μ_{l_1,l_2} is the charge distributed from γ_{l_1} to grid points (u_{1,k_1}, u_{2,k_2}) with k_1 fixed and $k_2 = j_2 - 1, j_2, j_2 + 1$, respectively. The weights z_{l_2} are obtained as the solution to

$$\begin{aligned} &z_1 + z_2 + z_3 = 1 \\ &\eta_{2,j_2-1} z_1 + \eta_{2,j_2} z_2 + \eta_{2,j_2+1} z_3 = \bar{v}_2 \\ &(\eta_{2,j_2-1})^2 z_1 + (\eta_{2,j_2})^2 z_2 + (\eta_{2,j_2+1})^2 z_3 = \bar{v}_2^2. \end{aligned} \tag{3.41}$$

If $.5 < b_2 \leqslant 1$ the quantities $\eta_{2,j_2-1}, \eta_{2,j_2}, \eta_{2,j_2+1}$ in (3.41) are replaced with $\eta_{2,j_2}, \eta_{2,j_2+1}, \eta_{2,j_2+2}$.

The redistribution of charge $\bar{q} = q^{m,N_g}_{i',j'}$ located at $(\bar{\xi}, \bar{u}) \in \Omega$ is summarized as follows: let m_1, m_2 be indices such that if $0 \leqslant b_1 \leqslant .5$ then $m_1 = 2$, if $.5 < b_1 \leqslant 1$ then $m_1 = 1$, if $0 \leqslant b_2 \leqslant .5$ then $m_2 = 2$, if $.5 < b_1 \leqslant 1$ then $m_2 = 1$. For $\kappa_1,\kappa_2 = 1,2$, $l_1 = 1,2,3$, $l_2 = 1,2,3$ the charge $\bar{q}$ is distributed to points in Ω given by

$$(\xi_{1,i_1+\kappa_1-1}, \xi_{2,i_2+\kappa_2-1}, u_{1,j_1+l_1-m_1}, u_{2,j_2+l_2-m_2}). \tag{3.42}$$

The distribution of charge to the (ξ_1, ξ_2) coordinates is determined by the weights w_{κ_1,κ_2}. The distribution of charge to the u_1 coordinates is determined by the weights $y_{l_1}, l_1 = 1,2,3$ given by the solution to (3.40). The distribution of charge to the u_2 coordinates is determined by the weights $z_{l_2}, l_2 = 1,2,3$ given by the solution to (3.41). Let $\alpha_{ij}(i\prime, j\prime)$ be the charge contributed to the i,j grid point in Ω from the charge $\bar{q} = q^{m,N_g}_{i',j'}$. Then the charge apportioned to the grid points given by (3.42) is

$$\alpha_{i_1+\kappa_1-1,i_2+\kappa_2-1,j_1+l_1-m_1,j_2+l_2-m_2}(i', j') = (w_{\kappa_1,\kappa_2} y_{l_1} z_{l_2})\bar{q}.$$

Summing the quantity $\alpha_{ij}(i', j')$ over all trajectories gives the total charge assigned to the i,j grid point in Ω, that is, $q^{m+1,0}_{ij} = \sum_{i',j'} \alpha_{ij}(i', j')$. Let

$$da_j = da_{j_1,j_2} = \frac{c^2(\Delta\xi\Delta u)^2}{(1-u_{1,j_1}^2)^{3/2}(1-u_{2,j_2}^2)^{3/2}}$$

which is the differential of "volume" associated with the i,j grid point in Ω at $t_n = 0$. Then $g^{m+1,0}_{ij} = q^{m+1,0}_{ij}/da_j$. The grid function $g^{m+1,0}_{ij}$ is then the initial data for (3.4) for the time interval $[(m+1)T_1, (m+2)T_2]$.

The grid function $g^{m+1,0}_{ij}$ has the property that

$$\begin{aligned} &\sum_{i,j} \frac{g^{m+1,0}_{ij} c^2(\Delta\xi\Delta u)^2}{(1-u_{1,j_1}^2)^{3/2}(1-u_{2,j_2}^2)^{3/2}} = \sum_{i,j} \frac{g^{m,N_g}_{ij} c^2(\Delta\xi\Delta u)^2}{(1-u_{1,j_1}^2)^{3/2}(1-u_{2,j_2}^2)^{3/2}}, \\ &\sum_{i,j} \frac{\eta_{1,j_1} g^{m+1,0}_{ij} c^2(\Delta\xi\Delta u)^2}{(1-u_{1,j_1}^2)^{3/2}(1-u_{2,j_2}^2)^{3/2}} = \sum_{i,j} \frac{v_1(i,j,t_{N_g}) g^{m,N_g}_{ij} c^2(\Delta\xi\Delta u)^2}{(1-u_{1,j_1}^2)^{3/2}(1-u_{2,j_2}^2)^{3/2}}, \end{aligned}$$

$$\sum_{i,j}\frac{\eta_{2,j_2}g_{i,j}^{m+1,0}c^2(\Delta\xi\Delta u)^2}{(1-u_{1,j_1}^2)^{3/2}(1-u_{2,j_2}^2)^{3/2}}=\sum_{i,j}\frac{v_2(i,j,t_{N_g})g_{i,j}^{m,N_g}c^2(\Delta\xi\Delta u)^2}{(1-u_{1,j_1}^2)^{3/2}(1-u_{2,j_2}^2)^{3/2}},$$

$$\sum_{i,j}\frac{(\eta_{1,j_1}^2+\eta_{2,j_2}^2)g_{i,j}^{m+1,0}c^2(\Delta\xi\Delta u)^2}{(1-u_{1,j_1}^2)^{3/2}(1-u_{2,j_2}^2)^{3/2}}=\sum_{i,j}\frac{[(v_1(i,j,t_{N_g}))^2+(v_2(i,j,t_{N_g}))^2]g_{i,j}^{m,N_g}c^2(\Delta\xi\Delta u)^2}{(1-u_{1,j_1}^2)^{3/2}(1-u_{2,j_2}^2)^{3/2}}.$$

Thus, the regriding process preserves the total charge, momentum, and kinetic energy associated with the approximate distribution function. The purpose of the regriding for the present two-dimensional problem, as well as in [28], is to improve significantly the long term stability and accuracy of the numerical method.

3.4. The solution on the time interval $[0,T]$

For $\bar{t}\in[0,T]$ the solution is represented here as in [28] by the electrostatic energy, kinetic energy, and free energy. For computations where the constant magnetic field is applied an additional quantity, the angular momentum, is introduced. This quantity clearly demonstrates the effect of a nonzero external magnetic field. Referring to the solution of (1.1) and (1.2) the electrostatic energy is defined as

$$ese(\bar{t})=\frac{1}{2}\int_0^L\int_0^L|E(x,\bar{t})|^2dx=\frac{1}{2}\int_0^L\int_0^L[(E_1(x,\bar{t}))^2+(E_2(x,\bar{t}))^2]dx_1dx_2.$$

For $\mathcal{A}$ the domain of (1.1) the kinetic energy is

$$ke(\bar{t})=\frac{1}{2}\int_{\mathcal{A}}|v|^2f(x,v,\bar{t})dvdx=\frac{1}{2}\int_{\mathcal{A}}(v_1^2+v_2^2)f(x,v,\bar{t})dvdx. \tag{3.43}$$

The entropy of the system is given by

$$ent(\bar{t})=-\int_{\mathcal{A}}f(x,v,\bar{t})ln(f(x,v,\bar{t}))dvdx.$$

As stated in [8] the free energy, $FE(\bar{t})$, is then defined as

$$FE(\bar{t})=ese(\bar{t})+ke(\bar{t})-q/\beta ent(\bar{t}). \tag{3.44}$$

For $mT_1\leqslant\bar{t}\leqslant(m+1)T_1$ and $t=\bar{t}-mT_1$ then as given by (2.20) $f(x,v,\bar{t})$ has the representation $f(x,v,\bar{t})=e^{2\beta t}g(\xi(x,v,t),u(\eta(x,v,t)),t)$ with $g(\xi,u,t)$ the solution to (2.9). In terms of the function $g(\xi,u,t)$ then

$$\begin{aligned}ke(\bar{t})&=\frac{1}{2}\int_\Omega(v(\xi,\eta(u),t))^2g(\xi,u,t)\frac{c^2}{(1-u_1^2)^{3/2}(1-u_2^2)^{3/2}}dud\xi\\&=\frac{1}{2}\int_\Omega[(v_1(\xi,\eta(u),t))^2+(v_2(\xi,\eta(u),t))^2]g(\xi,u,t)\frac{c^2}{(1-u_1^2)^{3/2}(1-u_2^2)^{3/2}}dud\xi\end{aligned}$$

and

$$ent(\bar{t})=-\int_\Omega g(\xi,u,t)ln(e^{2\beta t}g(\xi,u,t))\frac{c^2}{(1-u_1^2)^{3/2}(1-u_2^2)^{3/2}}dud\xi.$$

The Jacobian determinants for this change of integration variables are stated toward the end of Section 3.2.2.

The discrete versions of the kinetic energy and entropy are computed as follows: let $\bar{t}_k=\tau_m+t_n$ where $\tau_m=mT_1$ and $t_n=n\Delta t$ for $m=0,1,\ldots,M$; $n=0,1,\ldots,N_g$; and $k=mN_g+n$. Then in terms of approximate trajectories computed according to (3.19) and (3.20) and the normalized solution to (3.4)

$$\begin{aligned}ke(\bar{t}_k)&=\sum_{i,j}(v(i,j,t_n))^2g_{i,j}^{m,n}\frac{c^2(\Delta\xi\Delta u)^2}{(1-u_{1,j_1}^2)^{3/2}\left(1-u_{2,j_2}^2\right)^{3/2}}\\&=\sum_{i,j}\left[(v_1(i,j,t_n))^2+(v_2(i,j,t_n))^2\right]g_{i,j}^{m,n}\frac{c^2(\Delta\xi\Delta u)^2}{\left(1-u_{1,j_1}^2\right)^{3/2}\left(1-u_{2,j_2}^2\right)^{3/2}}\end{aligned} \tag{3.45}$$

and

$$ent(\bar{t}_k)=\sum_{i,j}g_{i,j}^{m,n}ln\left(e^{2\beta t_n}g_{i,j}^{m,n}\right)\frac{c^2(\Delta\xi\Delta u)^2}{(1-u_{1,j_1}^2)^{3/2}(1-u_{2,j_2}^2)^{3/2}}. \tag{3.46}$$

The electrostatic energy is computed from the electric field at grid points, $E_1^n(k_1,k_2)$, $E_2^n(k_1,k_2)$, obtained in Section 3.2.6. For $k_1,k_2 = 0,1,\ldots,N_p-1$ let

$$E_{1,av}^n(k_1,k_2) = (E_1^n(k_1,k_2) + E_1^n(k_1+1,k_2) + E_1^n(k_1,k_2+1) + E_1^n(k_1+1,k_2+1))/4,$$
$$E_{2,av}^n(k_1,k_2) = (E_2^n(k_1,k_2) + E_2^n(k_1+1,k_2) + E_2^n(k_1,k_2+1) + E_2^n(k_1+1,k_2+1))/4.$$

Then

$$ese(\bar{t}_k) = \frac{1}{2}\sum_{k_1=0}^{N_p-1}\sum_{k_2=0}^{N_p-1}[(E_{1,av}^n(k_1,k_2))^2 + (E_{2,av}^n(k_1,k_2))^2]\,\epsilon^2. \tag{3.47}$$

The discrete version of the free energy is

$$FE(\bar{t}_k) = ese(\bar{t}_k) + ke(\bar{t}_k) - q/\beta ent(\bar{t}_k). \tag{3.48}$$

3.5. Nonzero magnetic field

We outline the modifications needed to apply the numerical procedure of Sections 3.1–3.3 and 3.4 to the system (2.16) and (1.2) with $B_z = b \neq 0$. The main change to the numerical procedure to deal with B_z a nonzero constant is that the characteristic system of equations is now given by (2.17) rather than (2.11). This changes the approximation of particle trajectories, Section 3.2.3, the approximation of first partial derivatives, Section 3.2.4, and the approximation of second partial derivatives, Section 3.2.5. The remainder of the numerical procedure is essentially the same as for the case where $B_z = 0$. We modify the relevant sections of the numerical method of Section 3.

3.5.1. The approximation of (2.17), particle trajectories

The approximation to the solution of (2.17) which is denoted $(x(i,j,t_n), v(i,j,t_n))$ is now obtained as the solution to

$$\frac{dx_1}{dt} = v_1, \quad x_1(t_n) = x_1(i,j,t_n)$$
$$\frac{dv_1}{dt} = \bar{E}_1(x(i,j,t_n),t_n) + bv_2 - \beta v_1, \quad v_1(t_n) = v_1(i,j,t_n)$$
$$\frac{dx_2}{dt} = v_2, \quad x_2(t_n) = x_2(i,j,t_n)$$
$$\frac{dv_2}{dt} = \bar{E}_2(x(i,j,t_n),t_n) - bv_1 - \beta v_2, \quad v_2(t_n) = v_2(i,j,t_n).$$

With $\bar{E}_1, \bar{E}_2$ having fixed values at time t_n this system can be integrated exactly for $t_n \leqslant t \leqslant t_{n+1}$ to provide trajectory values at time t_{n+1}. Let $\lambda = (\beta, b)$, $|\lambda|^2 = \beta^2 + b^2$ and

$$d_1(\Delta t) = e^{-\beta\Delta t}sin(b\Delta t), \quad d_2(\Delta t) = e^{-\beta\Delta t}cos(b\Delta t),$$
$$d_3(\Delta t) = \frac{1}{|\lambda|^2}[bd_1(\Delta t) + \beta(1-d_2(\Delta t))], \quad d_4(\Delta t) = \frac{1}{|\lambda|^2}[b(1-d_2(\Delta t)) - \beta d_1(\Delta t)],$$
$$d_5(\Delta t) = \frac{1}{|\lambda|^2}[\beta(\Delta t - d_3(\Delta t)) + bd_4(\Delta t)], \quad d_6(\Delta t) = \frac{1}{|\lambda|^2}[b(\Delta t - d_3(\Delta t)) - \beta d_4(\Delta t)].$$

Let $(x_1(i,j,0), x_2(i,j,0)) = (\xi_{1,i_1}, \xi_{2,i_2})$ and $(v_1(i,j,0), v_2(i,j,0)) = (\eta_{1,j_1}, \eta_{2,j_2})$. Given $x_1(i,j,t_n), x_2(i,j,t_n), v_1(i,j,t_n), v_2(i,j,t_n)$ and $\bar{E}_1(x(i,j,t_n),t_n)$, $\bar{E}_2(x(i,j,t_n),t_n)$ quantities at time t_{n+1} are computed as follows: let $x_l(i,j,t_n) = x_l(t_n)$, $v_l(i,j,t_n) = v_l(t_n)$ and $\bar{E}_l(x(i,j,t_n),t_n) = \bar{E}_l(t_n)$, $l = 1,2$ then

$$x_1(t_{n+1}) = x_1(t_n) + d_3(\Delta t)v_1(t_n) + d_4(\Delta t)v_2(t_n) + d_5(\Delta t)\bar{E}_1(t_n) + d_6(\Delta t)\bar{E}_2(t_n), \tag{3.49}$$
$$v_1(t_{n+1}) = d_2(\Delta t)v_1(t_n) + d_1(\Delta t)v_2(t_n) + d_3(\Delta t)\bar{E}_1(t_n) + d_4(\Delta t)\bar{E}_2(t_n), \tag{3.50}$$
$$x_2(t_{n+1}) = x_2(t_n) - d_4(\Delta t)v_1(t_n) + d_3(\Delta t)v_2(t_n) - d_6(\Delta t)\bar{E}_1(t_n) + d_5(\Delta t)\bar{E}_2(t_n), \tag{3.51}$$
$$v_2(t_{n+1}) = -d_1(\Delta t)v_1(t_n) + d_2(\Delta t)v_2(t_n) - d_4(\Delta t)\bar{E}_1(t_n) + d_3(\Delta t)\bar{E}_2(t_n). \tag{3.52}$$

It can be verified that when $b = 0$ the trajectory formulas (3.49)–(3.51) and (3.52) become (3.19) and (3.20).

3.5.2. Approximation of the first partial derivative Eq. (2.14) with (2.19) and the coefficients $c_1,\ldots,c_{10}$

The first partial derivatives of the functions (2.18) with respect to ξ,η needed to derive the coefficients in (2.9) are obtained as solutions of systems of the type (2.14) in which the matrix A is given by (2.19). The approximation of these quantities follows the development of Section 3.2.4 except now one derives the equations for approximate first partial derivatives by differentiating the equations (3.49)–(3.51) and (3.52) with respect to ξ,η. For $l = 1,2$ and $k = 1,2$ the values of $\frac{\partial x_l}{\partial \xi_k}(0)$, $\frac{\partial v_l}{\partial \xi_k}(0)$, $\frac{\partial x_l}{\partial \eta_k}(0)$, $\frac{\partial v_l}{\partial \eta_k}(0)$ are as in Section 3.2.4. First partial derivatives with respect to ξ_k, $k = 1,2$ are obtained as follows: given the values of $\frac{\partial x_1}{\partial \xi_k}(t_n)$, $\frac{\partial v_1}{\partial \xi_k}(t_n)$, $\frac{\partial x_2}{\partial \xi_k}(t_n)$, $\frac{\partial v_2}{\partial \xi_k}(t_n)$ the quantities at time t_{n+1} are computed as

$$\frac{\partial x_1}{\partial \xi_k}(t_{n+1}) = \frac{\partial x_1}{\partial \xi_k}(t_n) + d_3(\Delta t)\frac{\partial v_1}{\partial \xi_k}(t_n) + d_4(\Delta t)\frac{\partial v_2}{\partial \xi_k}(t_n) + d_5(\Delta t)\left[\frac{\partial \bar{E}_1}{\partial x_1}(t_n)\frac{\partial x_1}{\partial \xi_k}(t_n) + \frac{\partial \bar{E}_1}{\partial x_2}(t_n)\frac{\partial x_2}{\partial \xi_k}(t_n)\right] + d_6(\Delta t)\left[\frac{\partial \bar{E}_2}{\partial x_1}(t_n)\frac{\partial x_1}{\partial \xi_k}(t_n) + \frac{\partial \bar{E}_2}{\partial x_2}(t_n)\frac{\partial x_2}{\partial \xi_k}(t_n)\right], \tag{3.53}$$

$$\frac{\partial v_1}{\partial \xi_k}(t_{n+1}) = d_2(\Delta t)\frac{\partial v_1}{\partial \xi_k}(t_n) + d_1(\Delta t)\frac{\partial v_2}{\partial \xi_k}(t_n) + d_3(\Delta t)\left[\frac{\partial \bar{E}_1}{\partial x_1}(t_n)\frac{\partial x_1}{\partial \xi_k}(t_n) + \frac{\partial \bar{E}_1}{\partial x_2}(t_n)\frac{\partial x_2}{\partial \xi_k}(t_n)\right] + d_4(\Delta t)\left[\frac{\partial \bar{E}_2}{\partial x_1}(t_n)\frac{\partial x_1}{\partial \xi_k}(t_n) + \frac{\partial \bar{E}_2}{\partial x_2}(t_n)\frac{\partial x_2}{\partial \xi_k}(t_n)\right], \tag{3.54}$$

$$\frac{\partial x_2}{\partial \xi_k}(t_{n+1}) = \frac{\partial x_2}{\partial \xi_k}(t_n) - d_4(\Delta t)\frac{\partial v_1}{\partial \xi_k}(t_n) + d_3(\Delta t)\frac{\partial v_2}{\partial \xi_k}(t_n) - d_6(\Delta t)\left[\frac{\partial \bar{E}_1}{\partial x_1}(t_n)\frac{\partial x_1}{\partial \xi_k}(t_n) + \frac{\partial \bar{E}_1}{\partial x_2}(t_n)\frac{\partial x_2}{\partial \xi_k}(t_n)\right] + d_5(\Delta t)\left[\frac{\partial \bar{E}_2}{\partial x_1}(t_n)\frac{\partial x_1}{\partial \xi_k}(t_n) + \frac{\partial \bar{E}_2}{\partial x_2}(t_n)\frac{\partial x_2}{\partial \xi_k}(t_n)\right], \tag{3.55}$$

$$\frac{\partial v_2}{\partial \xi_k}(t_{n+1}) = -d_1(\Delta t)\frac{\partial v_1}{\partial \xi_k}(t_n) + d_2(\Delta t)\frac{\partial v_2}{\partial \xi_k}(t_n) - d_4(\Delta t)\left[\frac{\partial \bar{E}_1}{\partial x_1}(t_n)\frac{\partial x_1}{\partial \xi_k}(t_n) + \frac{\partial \bar{E}_1}{\partial x_2}(t_n)\frac{\partial x_2}{\partial \xi_k}(t_n)\right] + d_3(\Delta t)\left[\frac{\partial \bar{E}_2}{\partial x_1}(t_n)\frac{\partial x_1}{\partial \xi_k}(t_n) + \frac{\partial \bar{E}_2}{\partial x_2}(t_n)\frac{\partial x_2}{\partial \xi_k}(t_n)\right]. \tag{3.56}$$

The equations for computing the approximate first partial derivatives with respect to $\eta_k,\ k = 1, 2$, are obtained by replacing ξ_k with η_k in (3.53)–(3.55) and (3.56).

To derive the coefficients $c_1(i, j, t_n), \ldots, c_{10}(i, j, t_n)$ in (3.4) the matrix Q given by (3.25) is formed on the basis of first partial derivatives computed from equations of type (3.53)–(3.55) and (3.56). The systems (3.26) are solved for vectors $\bar{u}_1, \bar{u}_2$. The coefficients $c_1, \ldots, c_{10}$ are then derived precisely as is done at the end of Section 3.2.4.

3.5.3. Approximation of the second partial derivative Eq. (2.15) with (2.19) and the coefficients $c_{11}, \ldots, c_{14}$

The second partial derivatives with respect to ξ, η of the functions (2.18) are needed for the coefficients $c_{11}, \ldots, c_{14}$ in (3.4). The second partial derivatives are obtained as solutions to systems of type (2.15) with the matrix A given by (2.19). The approximations of these quantities are obtained by further differentiating the Eqs. (3.49)–(3.51) and (3.52). As representative of this approximation we compute the second partial derivatives with respect to ξ_1, ξ_2. Let $k = 2$ in (3.53)–(3.55) and (3.56) and differentiate the equations with respect to ξ_1. At $t_n = 0$, $\frac{\partial^2 x_l}{\partial \xi_1 \partial \xi_2}(0) = 0$, $\frac{\partial^2 v_l}{\partial \xi_1 \partial \xi_2}(0) = 0$, $l = 1, 2$. Then given the values of $\frac{\partial x_l}{\partial \xi_1}(t_n)$, $\frac{\partial x_l}{\partial \xi_2}(t_n)$, $\frac{\partial^2 x_l}{\partial \xi_1 \partial \xi_2}(t_n)$, $\frac{\partial^2 v_l}{\partial \xi_1 \partial \xi_2}(t_n)$ quantities at time t_{n+1} are computed. Let

$$R_{1,1}(t_n) = \frac{\partial \bar{E}_1}{\partial x_1}(t_n)\frac{\partial^2 x_1}{\partial \xi_1 \partial \xi_2}(t_n) + \frac{\partial \bar{E}_1}{\partial x_2}(t_n)\frac{\partial^2 x_2}{\partial \xi_1 \partial \xi_2}(t_n),$$

$$R_{2,1}(t_n) = \frac{\partial \bar{E}_2}{\partial x_1}(t_n)\frac{\partial^2 x_1}{\partial \xi_1 \partial \xi_2}(t_n) + \frac{\partial \bar{E}_2}{\partial x_2}(t_n)\frac{\partial^2 x_2}{\partial \xi_1 \partial \xi_2}(t_n),$$

$$R_{1,2}(t_n) = \frac{\partial^2 \bar{E}_1}{\partial x_1^2}(t_n)\left(\frac{\partial x_1}{\partial \xi_1}\right)\left(\frac{\partial x_1}{\partial \xi_2}\right)(t_n) + \frac{\partial^2 \bar{E}_1}{\partial x_1 \partial x_2}(t_n)\left(\frac{\partial x_2}{\partial \xi_1}\frac{\partial x_1}{\partial \xi_2} + \frac{\partial x_1}{\partial \xi_1}\frac{\partial x_2}{\partial \xi_2}\right)(t_n) + \frac{\partial^2 \bar{E}_1}{\partial x_2^2}(t_n)\left(\frac{\partial x_2}{\partial \xi_1}\right)\left(\frac{\partial x_2}{\partial \xi_2}\right)(t_n),$$

$$R_{2,2}(t_n) = \frac{\partial^2 \bar{E}_2}{\partial x_1^2}(t_n))\left(\frac{\partial x_1}{\partial \xi_1}\right)\left(\frac{\partial x_1}{\partial \xi_2}\right)(t_n) + \frac{\partial^2 \bar{E}_2}{\partial x_1 \partial x_2}(t_n)\left(\frac{\partial x_2}{\partial \xi_1}\frac{\partial x_1}{\partial \xi_2} + \frac{\partial x_1}{\partial \xi_1}\frac{\partial x_2}{\partial \xi_2}\right)(t_n) + \frac{\partial^2 \bar{E}_2}{\partial x_2^2}(t_n)\left(\frac{\partial x_2}{\partial \xi_1}\right)\left(\frac{\partial x_2}{\partial \xi_2}\right)(t_n).$$

We note that $R_{k,l}(t_n) = R_{k,l}(x(i, j, t_n), t_n),\ k, l = 1, 2$, i.e., these qualities are evaluated along particle trajectories computed from (3.49)–(3.51) and (3.52). Then

$$\frac{\partial^2 x_1}{\partial \xi_1 \partial \xi_2}(t_{n+1}) = \frac{\partial^2 x_1}{\partial \xi_1 \partial \xi_2}(t_n) + d_3(\Delta t)\frac{\partial^2 v_1}{\partial \xi_1 \partial \xi_2}(t_n) + d_4(\Delta t)\frac{\partial^2 v_2}{\partial \xi_1 \partial \xi_2}(t_n) + d_5(\Delta t)R_{1,1}(t_n) + d_6(\Delta t)R_{2,1}(t_n) + d_5(\Delta t)R_{1,2}(t_n) + d_6(\Delta t)R_{2,2}(t_n), \tag{3.57}$$

$$\frac{\partial^2 v_1}{\partial \xi_1 \partial \xi_2}(t_{n+1}) = d_2(\Delta t)\frac{\partial^2 v_1}{\partial \xi_1 \partial \xi_2}(t_n) + d_1(\Delta t)\frac{\partial^2 v_2}{\partial \xi_1 \partial \xi_2}(t_n) + d_3(\Delta t)R_{1,1}(t_n) + d_4(\Delta t)R_{2,1}(t_n) + d_3(\Delta t)R_{1,2}(t_n) + d_4(\Delta t)R_{2,2}(t_n), \tag{3.58}$$

$$\frac{\partial^2 x_2}{\partial \xi_1 \partial \xi_2}(t_{n+1}) = \frac{\partial^2 x_2}{\partial \xi_1 \partial \xi_2}(t_n) - d_4(\Delta t)\frac{\partial^2 v_1}{\partial \xi_1 \partial \xi_2}(t_n) + d_3(\Delta t)\frac{\partial^2 v_2}{\partial \xi_1 \partial \xi_2}(t_n) - d_6(\Delta t)R_{1,1}(t_n) + d_5(\Delta t)R_{2,1}(t_n) - d_6(\Delta t)R_{1,2}(t_n) + d_5(\Delta t)R_{2,2}, \tag{3.59}$$

$$\frac{\partial^2 v_2}{\partial\xi_1\partial\xi_2}(t_{n+1}) = -d_1(\Delta t)\frac{\partial^2 v_1}{\partial\xi_1\partial\xi_2}(t_n) + d_2(\Delta t)\frac{\partial^2 v_2}{\partial\xi_1\partial\xi_2}(t_n) - d_4(\Delta t)R_{1,1}(t_n) + d_3(\Delta t)R_{2,1}(t_n) - d_4(\Delta t)R_{1,2}(t_n) + d_3(\Delta t)R_{2,2}(t_n). \tag{3.60}$$

The equations for the other approximate second partial derivatives of the functions (2.18) are of the same form as (3.57)–(3.60) with derivatives with respect to ξ_1, ξ_2 replaced with other second derivatives in terms of $\xi_1, \xi_2, \eta_1, \eta_2$. The computation of the approximate electric field $\bar{E}_l(t_n) = \bar{E}_l(x(i,j,t_n), t_n)$ and its first an second partial derivatives follow exactly the procedure of Section 3.2.6 in which the discrete charge density (3.30) is now based on approximate particle trajectories computed according to (3.49)–(3.51) and (3.52). It can be noted that the"volume" element $\Delta A_{i,j}$ and charge element $q_{i,j}^{m,n}$ have the same expression here as in Section 3.2.6. This is because the transformation of R_4 defined by solutions of (2.17) has the same Jacobian as the transformation of R_4 defined by solutions of (2.11).

To derive the coefficients $c_{11}(i,j,t_n), \ldots, c_{14}(i,j,t_n)$ in (3.4) the procedure of Section 3.2.5 is followed to compute the vector quantities $\bar{y}_1, \bar{y}_2$. In computing these vectors the matrix Q is formed from first partial derivatives computed in Section 3.5.2. The matrices $A_i,\ i = 1, \ldots, 4$ are formed from second partial derivatives computed from equations of type (3.57)–(3.59) and (3.60). The coefficients $c_{11}, \ldots, c_{14}$ are then derived from the formulas at the end of Section 3.2.5.

3.5.4. The solution on the time interval $[0, T]$

For $B_z \neq 0$ some modifications are also needed for Section 3.4 which are now given. With the nonzero magnetic field included expressions for the kinetic energy and electrostatic energy are the same form as in Section 3.4. The approximation of the kinetic energy is given by (3.45), the approximate electrostatic energy by (3.47). As defined in [8] the free energy is $FE(\bar{t}) = U(\bar{t}) - q/\beta ent(\bar{t})$ where $U(\bar{t})$ is the total energy and $ent(\bar{t})$ is the physical entropy of the system. The energy in the magnetic field is included in $U(\bar{t})$. Thus

$$U(\bar{t}) = \frac{1}{2}\int_{\mathcal{A}} |v|^2 f(x,v,\bar{t})\,dv\,dx + \frac{1}{2}\int_0^L\int_0^L |E(x,\bar{t})|^2\,dx + \frac{1}{2}\int_0^L\int_0^L |B_z(x,\bar{t})|^2\,dx.$$

As $B_z(x,t) = b$ and $\frac{1}{2}\int_0^L\int_0^L |B_z(x,\bar{t})|^2\,dx = (b^2L^2)/2$ then $U(\bar{t}) = ke(\bar{t}) + ese(\bar{t}) + (b^2L^2)/2$. The expression for the free energy is $FE(\bar{t}) = ke(\bar{t}) + ese(\bar{t}) + (b^2L^2)/2 - q/\beta ent(\bar{t})$. The approximation to the physical entropy is computed from (3.46). Thus with nonzero magnetic field

$$FE(\bar{t}_k) = ese(\bar{t}_k) + \frac{1}{2}b^2L^2 + ke(\bar{t}_k) - q/\beta ent(\bar{t}_k). \tag{3.61}$$

In computing quantities (3.45)–(3.47) the particle trajectories are computed according to Section 3.5.1. The grid function $g_{i,j}^{m,n}$ is obtained from the solution to (3.4) with the coefficients derived on the basis of approximate first and second partial derivatives computed according to Sections 3.5.2 and 3.5.3.

In approximating the system (2.16) and (1.2) with $B_z = b \neq 0$ it is useful to include the angular momentum as an additional quantity representative of the solution. The angular momentum is defined as

$$ang(\bar{t}) = \int_{\mathcal{A}} (x_1 v_2 - x_2 v_1) f(x,v,\bar{t})\,dv\,dx. \tag{3.62}$$

This quantity clearly distinguishes the solutions for which $B_z = b \neq 0$ from those for which $B_z = 0$. This is demonstrated with some computational examples in Section 4.

For $\bar{t}_k = \tau_m + t_n$ with $\tau_m = mT_1$ and $t_n = n\Delta t,\ m = 0, 1 \ldots, M;\ n = 0, 1, \ldots, N_g$; and $k = mN_g + n$ the approximation to angular momentum is denoted $ang(\bar{t}_k)$. Following the expression (3.45) for $ke(\bar{t}_k)$ one can consider computing $ang(\bar{t}_k)$ as

$$ang(\bar{t}_k) = \sum_{ij}(x_1(t_n)v_2(t_n) - x_2(t_n)v_1(t_n))g_{ij}^{m,n}\frac{c^2(\Delta\xi\Delta u)^2}{\left(1-u_{1,j_1}^2\right)^{3/2}\left(1-u_{2,j_2}^2\right)^{3/2}}. \tag{3.63}$$

Here $x_l(t_n) = x_l(i,j,t_n),\ v_l(t_n) = v_l(i,j,t_n),\ l = 1,2$. The problem with the formula (3.63) is that the expression $x_1(i,j,t_n)v_2(i,j,t_n) - x_2(i,j,t_n)v_1(i,j,t_n)$ becomes discontinuous as the $x_l(i,j,t_n)$ components of a trajectory cross a boundary $x_1 = 0$ or $x_1 = L, x_2 = 0$ or $x_2 = L$ and by periodicity re-enter the domain at $x_1 = L$ or $x_1 = 0, x_2 = L$ or $x_2 = 0$. As a result of this discontinuity the quantity $ang(\bar{t}_k)$ is not easily computed according to the formula (3.63).

For an alternative way to compute the angular momentum let

$$\zeta_1(x) = \int_{-\infty}^{\infty}\int_{-\infty}^{\infty} v_1 f(x,v,t)\,dv_1\,dv_2,\ \ \zeta_2(x) = \int_{-\infty}^{\infty}\int_{-\infty}^{\infty} v_2 f(x,v,t)\,dv_1\,dv_2.$$

Then

$$ang(\bar{t}) = \int_0^L\int_0^L (x_1\zeta_2(x) - x_2\zeta_1(x))\,dx_1\,dx_2. \tag{3.64}$$

Considering $ang(\bar{t})$ in the form (3.64) then $\zeta_1(x), \zeta_2(x)$ are approximated by the particle-in-cell method in the same way that the electron charge density is approximated in Section 3.2.6. Thus, given the approximate trajectories $(x(i,j,t_n), v(i,j,t_n)), t_n \in [0,T_1],\ n = 0,1,\ldots,N_g$ and charge elements $q_{i,j}^{m,n}$ given by (3.29) then the discrete velocity moments can be defined for $l = 1,2$ as

$$\tilde{\zeta}_l(x,t_n) = \sum_{i,j} v_l(i,j,t_n) q_{i,j}^{m,n} \delta(x_1 - x_1(i,j,t_n)) \delta(x_2 - x_2(i,j,t_n)).$$

The uniform rectangular grid and particle to grid assignment function $w(y)$ are as in Section 3.2.6. Velocity moments on the grid at time t_n are then defined for $l = 1,2$ and $\kappa = (k_1,k_2),\ k_1,k_2 = 0,1,\ldots,N_p - 1$ as

$$\zeta_l^n(k_1,k_2) = \int_0^L \int_0^L \bar{w}_\epsilon(x - x_\kappa) \tilde{\zeta}_l(x,t_n) dx = \sum_{i,j} v_l(i,j,t_n) q_{i,j}^{m,n} w_\epsilon(x_1(i,j,t_n) - x_{1,k_1}) w_\epsilon(x_2(i,j,t_n) - x_{2,k_2}).$$

Quantities $\zeta_l^n(k_1,k_2),\ k_2 = N_p,\ k_1 = 0,1,\ldots,N_p$ and $k_1 = N_p,\ k_2 = 0,1,\ldots,N_p$ are obtained by periodicity. Thus $\zeta_l^n(k_1,k_2)$ are defined at the grid points of Section 3.2.6 given by $x_{1,k_1},\ x_{2,k_2},\ k_1,k_2 = 0,1,\ldots,N_p$.

Let $\epsilon = L/N_p$ as defined in Section 3.2.6. For $k_1 = 1,\ldots,N_p,\ k_2 = 1,\ldots,N_p$ let $\bar{x}_{1,k_1} = (k_1 - .5)\epsilon$, $\bar{x}_{2,k_2} = (k_2 - .5)\epsilon$ and for $l = 1,2$

$$\zeta_{l,av}^n(\kappa) = \zeta_{l,av}^n(k_1,k_2) = (\zeta_l^n(k_1 - 1, k_2 - 1) + \zeta_l^n(k_1 - 1, k_2) + \zeta_l^n(k_1, k_2 - 1) + (\zeta_l^n(k_1,k_2))/4.$$

Then

$$ang(\bar{t}_k) = \sum_{k_1=1}^{N_p} \sum_{k_2=1}^{N_p} (\bar{x}_{1,k_1} \zeta_{2,av}^n(\kappa) - \bar{x}_{2,k_2} \zeta_{1,av}^n(\kappa)) \epsilon^2. \tag{3.65}$$

3.6. Summary of the numerical method

This section summarizes the numerical procedure in two dimensions similarly to [28], Section 2.4.1 for the one dimensional problem. For positive integers N_x, N_v let $\Delta\xi = L/N_x,\ \Delta u = 2/(N_v + 1)$. For multiindicies $i = (i_1,i_2)$ and $j = (j_1,j_2)$ then the domain Ω is partitioned as

$$\begin{aligned} &\xi_{1,i_1} = (i_1 - 1)\Delta\xi, \quad \xi_{2,i_2} = (i_2 - 1)\Delta\xi, \quad i_1,i_2 = 1,\ldots,N_x, \\ &u_{1,j_1} = -1 + j_1\Delta u, \quad u_{2,j_2} = -1 + j_2\Delta u, \quad j_1,j_2 = 1,\ldots,N_v. \end{aligned}$$

For $(\xi_i,u_j) \in \Omega$ there corresponds $(\xi_i,\eta_j) \in \mathcal{A}_0$ such that $\eta_j = (\eta_{1,j_1},\eta_{2,j_2})$ and

$$\eta_{1,j_1} = \frac{cu_{1,j_1}}{\sqrt{1 - u_{1,j_1}^2}}, \quad \eta_2 = \frac{cu_{2,j_2}}{\sqrt{1 - u_{2,j_2}^2}}.$$

For the partition of the time interval $[0,T]$ let $T_1 > 0$ be such that $T/T_1 = M$ an integer. Thus $[0,T]$ is divided into M subintervals of length T_1. For positive integer N_g let $\Delta t = T_1/N_g$. Then $t_n = n\Delta t,\ n = 0,1,\ldots,N_g$; $\tau_m = mT_1,\ m = 0,1,\ldots,M$; and $\bar{t}_k = \tau_m + t_n$ for $k = mN_g + n$. The time t_n is the partition of the time interval $[0,T_1]$ for the particle method, the regriding is done at times τ_m, and $\bar{t}_k$ is the actual time of the discrete approximation.

For positive integer N_p let $\epsilon = L/N_p$. The partition of the region $[0,L] \times [0,L]$ for the particle-in-cell computation is $x_{1,k_1} = k_1\epsilon,\ x_{2,k_2} = k_2\epsilon,\ k_1,k_2 = 0,1,\ldots,N_p$.

The numerical method proceeds as follows:

(1) at $m = 0,\ n = 0$, that is $\tau_m = 0,\ t_n = 0$:

$$\bar{g}_{i,j}^0 = f_0(\xi_i,\eta(u_j)) = f_0\left(\xi_{1,i_1},\xi_{2,i_2},\frac{cu_{1,j_1}}{\sqrt{1 - u_{1,j_1}^2}},\frac{cu_{2,j_2}}{\sqrt{1 - u_{2,j_2}^2}}\right), \quad \lambda = \frac{1}{K}\sum_{i,j} \bar{g}_{i,j}^0 \frac{c^2(\Delta u\Delta\xi)^2}{\left(1 - u_{1,j_1}^2\right)^{3/2}\left(1 - u_{2,j_2}^2\right)^{3/2}},$$

and $g_{i,j}^{0,0} = \bar{g}_{i,j}^0/\lambda$. Here K is the L_1 norm of $f_0(\xi,\eta)$.

(2) At $m \geqslant 0, n = 0$, that is $\tau_m = mT_1,\ t_n = 0$: $x_{i,j}(0) = \xi_i,\ v_{i,j}(0) = \eta_j$ where $\xi_i = (\xi_{1,i_1},\xi_{2,i_2}),\ \eta_j = (\eta_{1,j_1},\eta_{2,j_2})$. For $l,k = 1,2,\ \frac{\partial x_l}{\partial\xi_k}(i,j,0) = 1,\ l = k; \frac{\partial x_l}{\partial\xi_k}(i,j,0) = 0,\ l \neq k; \frac{\partial v_l}{\partial\xi_k}(i,j,0) = 0; \frac{\partial x_l}{\partial\eta_k}(i,j,0) = 0; \frac{\partial v_l}{\partial\eta_k}(i,j,0) = 1,\ l = k; \frac{\partial v_l}{\partial\eta_k}(i,j,0) = 0,\ l \neq k$. For the coefficients $c_1,\ldots,c_{10}$ of (3.4) $c_3 = 1,\ c_4 = 1$ and $c_k = 0,\ k = 1,2,5,--,10$. For $l = 1,2;\ 0 \leqslant r_1,r_2,s_1,s_2 \leqslant 2,\ r_1 + r_2 + s_1 + s_2 = 2,\ \frac{\partial^2 x_l}{\partial\xi_1^{r_1}\partial\xi_2^{r_2}\partial\eta_1^{s_1}\partial\eta_2^{s_2}}(i,j,0) = 0,\ \frac{\partial^2 v_l}{\partial\xi_1^{r_1}\partial\xi_2^{r_2}\partial\eta_1^{s_1}\partial\eta_2^{s_2}}(i,j,0) = 0$, coefficient $c_{11},c_{12},c_{13},c_{14} = 0$. The values of $g_{i,j}^{m,0}$ are given from (1) if $m = 0$ and from (4) if $m > 0$. The i,j^{th} charge is

$$q_{i,j}^{m,0} = g_{i,j}^{m,0} \frac{c^2(\Delta u\Delta\xi)^2}{(1 - u_{1,j_1}^2)^{3/2}(1 - u_{2,j_2}^2)^{3/2}}.$$

(3) For given time $\tau_m = mT_1,\ m = 0,1,\ldots,M-1$: For $t_n,\ n = 0,1,\ldots,N_g-1$ we assume values for $g_{ij}^{m,n}, x(i,j,t_n), v(i,j,t_n); \frac{\partial x_l}{\partial \xi_k}(i,j,t_n), \frac{\partial v_l}{\partial \xi_k}(i,j,t_n), \frac{\partial x_l}{\partial \eta_k}(i,j,t_n), \frac{\partial v_l}{\partial \eta_k}(i,j,t_n),\ k,l = 1,2;\ c_1(i,j,t_n),\ldots,c_{10}(i,j,t_n);\ \frac{\partial^2 x_l}{\partial \xi_1^{r_1}\partial \xi_2^{r_2}\partial \eta_1^{s_1}\partial \eta_2^{s_2}}(i,j,t_n), \frac{\partial^2 v_l}{\partial \xi_1^{r_1}\partial \xi_2^{r_2}\partial \eta_1^{s_1}\partial \eta_2^{s_2}}(i,j,t_n),\ l = 1,2,\ 0 \leqslant r_1,r_2,s_1,s_2 \leqslant 2,\ r_1+r_2+s_1+s_2 = 2;\ c_{11}(i,j,t_n),\ldots,c_{14}(i,j,t_n)$; and $q_{ij}^{m,n}$. The solution to the Poisson equation is approximated by the particle-in-cell method of Section 3.2.6. The background charge is normalized according to (3.33) so that charge neutrality is preserved. At the particle positions the electric field, $\bar{E}_l(x,t_n),\ l = 1,2$ is obtained from (3.36), the first partial derivatives, $\frac{\partial \bar{E}_l}{\partial x_k}(x,t_n),\ k,l = 1,2$, are obtained from(3.37), the second partial derivatives $\frac{\partial^2 \bar{E}_l}{\partial x_1^r \partial x_2^s}(x,t_n),\ l = 1,2,\ r,s = 0,1,2,\ r+s = 2$, are obtained from (3.38). For $\bar{t}_k = mT_1 + t_n,\ k = mN_g + n$, the values $ese(\bar{t}_k), ke(\bar{t}_k), FE(\bar{t}_k)$ are computed according to (3.47), (3.45) and (3.48). The quantity $ang(\bar{t}_k)$ is computed from (3.65) for problems involving $B_z = b \neq 0$. Then at time t_{n+1}

(i) $\bar{g}_{ij}^{n+1}$ is computed by solving (3.4),

$$\lambda = \frac{1}{K}\sum_{ij}\bar{g}_{ij}^{n+1}\frac{c^2(\Delta u\Delta\xi)^2}{(1-u_{1,j_1}^2)^{3/2}(1-u_{2,j_2}^2)^{3/2}},$$

and $g_{ij}^{m,n+1} = \bar{g}_{ij}^{n+1}/\lambda$.

(ii) $x(i,j,t_{n+1}),\ v(i,j,t_{n+1})$ are computed from (3.19) and (3.20) if $B_z = 0$ or from (3.49)–(3.51) and (3.52) if $B_z = b \neq 0$.

(iii) $\frac{\partial x_l}{\partial \xi_k}(i,j,t_{n+1}), \frac{\partial v_l}{\partial \xi_k}(i,j,t_{n+1}), \frac{\partial x_l}{\partial \eta_k}(i,j,t_{n+1}), \frac{\partial v_l}{\partial \eta_k}(i,j,t_{n+1}),\ k,l = 1,2$ are computed from (3.21)–(3.23) and (3.24) if $B_z = 0$ or from equations of type (3.53)–(3.55) and (3.56) if $B_z = b \neq 0$. Systems (3.26) are solved for each i,j and coefficients $c_1(i,j,t_{n+1}),\ldots,c_{10}(i,j,t_{n+1})$ are computed.

(iv) $\frac{\partial^2 x_l}{\partial \xi_1^{r_1}\partial \xi_2^{r_2}\partial \eta_1^{s_1}\partial \eta_2^{s_2}}(i,j,t_{n+1}),\ \frac{\partial^2 v_l}{\partial \xi_1^{r_1}\partial \xi_2^{r_2}\partial \eta_1^{s_1}\partial \eta_2^{s_2}}(i,j,t_{n+1}),\ l = 1,2,\ 0 \leqslant r_1,r_2,s_1,s_2 \leqslant 2, r_1+r_2+s_1+s_2 = 2$ are computed from equations of type (3.27) and (3.28) if $B_z = 0$ or from equations of type (3.57)–(3.59) and (3.60) if $B_z = b \neq 0$. Coefficients $c_{11}(i,j,t_{n+1}),\ldots,c_{14}(i,j,t_{n+1})$ are derived according to the procedure of Section 3.2.5.

(v) The charge at the i,j trajectory is

$$q_{ij}^{m,n+1} = g_{ij}^{m,n+1}\frac{c^2(\Delta u\Delta\xi)^2}{(1-u_{1,j_1}^2)^{3/2}(1-u_{2,j_2}^2)^{3/2}}.$$

(4) For $n = N_g,\ t_{N_g} = T_1$:

For given $m = 0,1,\ldots,M-1$ then $\bar{t}_k = mT_1 + t_{N_g} = (m+1)T_1 = \tau_{m+1}$ with $k = (m+1)N_g$. Following the procedure of Section 3.3 the solution along particle trajectories is interpolated onto the fixed grid in Ω given by (3.1) and (3.2). This provides the initial function $g_{ij}^{m+1,0}$ for (3.4) at time τ_{m+1}. If $m+1 < M$ then the computation returns to step (2). The cycle from (2) to (4) is repeated to compute the solution to (1.1) and (1.2) or (2.16) and (1.2) for $\bar{t}_k \in [(m+1)T_1,(m+2)T_1]$. If $m+1 = M$ then $k = MN_g = N_t$ and $g_{ij}^{m+1,0} = g_{ij}^{M,0}$ gives the approximate solution to (1.1) and (1.2) or (2.16) and (1.2) at time $\bar{t}_{N_t} = T$. The quantities ese, ke, FE and ang are computed at time T from the function $g_{ij}^{M,0}$, and the computational cycle is ended.

4. Computational examples

To demonstrate the effectiveness of the numerical method for solving (1.1) and (1.2) or (2.16) and (1.2) some computations are carried out to show the convergence to the steady state solution. It can be determined that the steady state solution for (1.1) and (1.2) is

$$f_s(x,v) = \frac{K}{2\pi q/\beta}\frac{\exp\left(-\frac{|v|^2/2+\phi(x)}{q/\beta}\right)}{\left(\int_0^L\int_0^L \exp\left(-\frac{\phi(x)}{q/\beta}\right)dx\right)} \tag{4.1}$$

where $K = \int_{\mathcal{A}} f_0(x,v)dvdx$. The function $\phi(x)$ is the solution to

$$\Delta_x\phi = -\left(K\frac{\exp\left(-\frac{\phi(x)}{q/\beta}\right)}{\int_0^L\int_0^L \exp\left(-\frac{\phi(x)}{q/\beta}\right)dx} - h(x)\right) \tag{4.2}$$

with

$$\phi(0,x_2) = \phi(L,x_2), \quad \phi(x_1,0) = \phi(x_1,L).$$

The function $h(x)$ is such that $\int_0^L\int_0^L h(x)dx = K$. The solution to (4.2) is not unique so that if $\phi(x)$ is a solution so is $\phi(x)+c$ for a constant c. However, the steady state solution (4.1) is unchanged if $\phi(x)$ is replaced by $\phi(x)+c$.

For a proof that the solution to (1.1) and (1.2) converges to a steady state of the form given by (4.1) and (4.2) we refer to [8], (Theorem B, p. 492). This proof in [8] is, however, for an initial value problem in a three dimensional space. The functions $f_s(x,v), \phi(x)$ defined by (4.1) and (4.2) are the adaptation to the present two-dimensional periodic problem of the steady state solution [8], (2.14) and (2.15). Another reference on the time asymptotic behavior of solutions to the Vlasov–Poisson–Fokker–Planck system of the form (1.1) and (1.2) is [6].

Another point to make is that the functions given by (4.1) and (4.2) also provide a time independent solution to (2.16) and (1.2). This is because $v_2 \frac{\partial f_s}{\partial v_1} - v_1 \frac{\partial f_s}{\partial v_2} = 0$. We do not provide a complete proof as in [8] that the solution to (1.1) and (1.2) or (2.16) and (1.2) converges to the functions given by (4.1) and (4.2) as $t \to \infty$. However, a key component of the proof in [8] is to show that the free energy, $FE(\bar{t})$, $\bar{t} \geqslant 0$ is a monotonically decreasing function bounded from below. The monotonic decrease of free energy is derived as [8], (2.46). Within the present 2-D context this result is written for $\bar{t} \in [0,T]$ as

$$\frac{d(FE(\bar{t}))}{d\bar{t}} = -\beta \int_{\mathcal{A}} \left| v\sqrt{f} + 2q/\beta \nabla_v \sqrt{f} \right|^2 (\bar{t}) dv dx. \tag{4.3}$$

The derivative with respect to $\bar{t}$ being negative the function $FE(\bar{t})$ is therefore decreasing. Following the derivation of [8] one can readily show that expression (4.3) can be derived from f as a solution to (1.1) and (1.2). The same expression can be derived from f as a solution to (2.16) and (1.2). That the free energy is bounded from below and therefore converges to a limit is proved in the present context similarly as in [8, p. 499]. This monotonic decrease of the free energy to a limiting value either for the solution of (1.1) and (1.2) or (2.16) and (1.2) is demonstrated in the computational examples to follow. It is our assumption that other aspects of the analysis of [8] can be adapted to prove the convergence of the solution of (1.1) and (1.2) to the steady state solution (4.1) and (4.2) as $\bar{t} \to \infty$. We will assume that the solution to (2.16) and (1.2) also converges to this same steady state solution. The focus at this point is to show this convergence computationally.

In demonstrating the convergence to the steady state representative quantities that are computed are the kinetic energy, electrostatic energy, free energy, and if $B_z \neq 0$ the angular momentum. One can determine analytically an exact expression for the steady state value of kinetic energy. For $f_s(x,v)$ given by (4.1) then $1/2 \int_{\mathcal{A}} |v|^2 f_s(x,v) dv dx = Kq/\beta$. Thus with $ke(\bar{t})$ defined by (3.43) as $\bar{t} \to \infty$ then

$$ke(\bar{t}) \to \frac{Kq}{\beta}. \tag{4.4}$$

Also by replacing $f(x,v,\bar{t})$ by $f_s(x,v)$ in (3.62) it is determined that $ang(\bar{t}) \to 0$ as $\bar{t} \to \infty$. The steady state values for the electrostatic energy and free energy depend on the function $\phi(x)$. Unless $\phi(x)$ is known exactly one cannot obtain exact values for the steady state *ese* and *FE*.

4.1. The order of accuracy of the deterministic particle method

Some computations are carried out similar to those in [28] to determine the order of accuracy of the numerical method of Section 3. In [30] an analysis is carried out that shows that as applied to a 1-D linear initial value problem the deterministic particle method has accuracy that is $O((\Delta x)^2 + (\Delta v)^2 + \Delta t + \varepsilon)$. Here $\Delta x, \Delta v$ are discretization parameters on phase space, Δt the discretization parameter in time, and ε provides a contribution to the error due to restriction of the approximation to a finite domain. If the domain of approximation is sufficiently large, and thus ε is sufficiently small then the error follows an estimate that is first order in Δt and second order in the spatial small parameters. It is then demonstrated computationally in [30] that a similar estimate that is first order in Δt and second order in the spatial small parameters can apply to the periodic boundary value problem. A result of this type is also demonstrated in [28] for the numerical approximation of the nonlinear Vlasov–Poisson–Fokker–Planck system in one dimension.

We determine computationally that the results on the order of accuracy in 1-D generalize in a consistent way to the approximation of (1.1) and (1.2) by the numerical method of Section 3. For this purpose a test problem is constructed. In (4.1) and (4.2) we let $L = 1$ and

$$\phi(x) = -q/\beta cos(2\pi x_1) cos(2\pi x_2). \tag{4.5}$$

Also,

$$K = 2\pi q/\beta \int_0^1 \int_0^1 \exp\left(-\frac{\phi(x)}{q/\beta}\right) dx,$$

and

$$h(x) = 2\pi q/\beta \exp(cos(2\pi x_1) cos(2\pi x_2)) + 2q/\beta (2\pi)^2 cos(2\pi x_1) cos(2\pi x_2).$$

With this an exact time independent solution to (1.1) and (1.2) is

$$f(x,v) = \exp(cos(2\pi x_1) cos(2\pi x_2)) \exp\left(-\frac{|v|^2}{2q/\beta}\right) \tag{4.6}$$

with $\phi(x)$ in (4.2) given by (4.5). The electric field for this solution is

$$E_1(x) = -\frac{\partial \phi}{\partial x_1} = -q/\beta(2\pi) sin(2\pi x_1) cos(2\pi x_2), \tag{4.7}$$

$$E_2(x) = -\frac{\partial \phi}{\partial x_2} = -q/\beta(2\pi) sin(2\pi x_2) cos(2\pi x_1). \tag{4.8}$$

The approximation to (1.1) and (1.2) is computed by the numerical method of Section 3 with initial data $f_0(x,v) = f(x,v)$ with $f(x,v)$ defined by (4.6). Regarded now as a time dependent solution the function (4.6) is the exact solution for the phase space distribution function, and (4.7) and (4.8) are the exact components of the electric field.

To determine the order of accuracy we consider the discrete relative L_2 error in the electric field. The partition of the Poisson mesh given in Section 3.2.6 is $x_{1,k_1}, x_{2,k_2},\ k_1,k_2 = 0,1,\ldots,N_p$. The partition of the time interval $[0,T]$ is given in terms of $\bar{t}_k,\ k = 0,1,\ldots,N_t$ as described in Section 3.1. The exact value of the electric field at the points (x_{1,k_1}, x_{2,k_2}) at time $\bar{t}_k$ is

$$E_1(x_{1,k_1}, x_{2,k_2}, \bar{t}_k) = -q/\beta(2\pi) sin(2\pi x_{1,k_1}) cos(2\pi x_{2,k_2}),$$
$$E_2(x_{1,k_1}, x_{2,k_2}, \bar{t}_k) = -q/\beta(2\pi) sin(2\pi x_{2,k_2}) cos(2\pi x_{1,k_1}).$$

For $\bar{t}_k$ in the subinterval $[mT_1,(m+1)T_1]$ then $\bar{t}_k = \tau_m + t_n$ where $\tau_m = mT_1$ and $t_n = n\Delta t,\ m = 0,1,\ldots,M-1,$ $n = 0,1,\ldots,N_g$. The approximation to the components of the electric field at the Poisson mesh points at the time t_n is computed in Section 3.2.6 and is denoted $E_1^n(k_1,k_2), E_2^n(k_1,k_2)$. Let $dif(E_1(k_1,k_2,\bar{t}_k)) = E_1(x_{1,k_1}, x_{2,k_2}, \bar{t}_k) - E_1^n(k_1,k_2)$ and $dif(E_2(k_1,k_2,\bar{t}_k)) = E_2(x_{1,k1}, x_{2,k_2}, \bar{t}_k) - E_2^n(k_1,k_2)$. The discrete relative L_2 error in the electric field is then given by

$$e_{rel}(\bar{t}_k) = \frac{\sqrt{\sum_{k_1=1}^{N_p}\sum_{k_2=1}^{N_p}\left[(dif(E_1(k_1,k_2,\bar{t}_k)))^2 + (dif(E_2(k_1,k_2,\bar{t}_k)))^2\right]}}{\sqrt{\sum_{k_1=1}^{N_p}\sum_{k_2=1}^{N_p}\left[(E_1(x_{1,k_1},x_{2,k_2},\bar{t}_k))^2 + (E_2(x_{1,k_1},x_{2,k_2},\bar{t}_k))^2\right]}} \tag{4.9}$$

The parameter, c, in (3.3) controls the extent of the domain in velocity space for the discrete approximation. This parameter is made sufficiently large so that error due to truncating velocity space to a finite domain is made negligibly small. Also, for all computations of Section 4 $N_p = N_x$ so the discretization parameter on the Poisson mesh, ϵ, is such that $\epsilon = \Delta\xi$. With this the assumption is made that $e_{rel}(\bar{t}_k)$ has a bound in terms of discretization parameters $\Delta\xi, \Delta u, \Delta t$ of the type

$$e_{rel}(\bar{t}_k) \leqslant K(\bar{t}_k)((\Delta\xi)^2 + (\Delta u)^2 + \Delta t) \tag{4.10}$$

in which $K(\bar{t})$ is a continuous function of time. The goal is to verify computationally the error estimate (4.10).

For the computation of relative L_2 error we let $\beta = .1,\ q = .01$ in (1.1) with $f_0(x,v) = f(x,v)$ given by (4.6). Computations are done with (1) $N_x = N_v = 16,\ \Delta\xi = 1/16, \Delta u = 2/17, \Delta t = .004$, (2) $N_x = N_v = 24,\ \Delta\xi = 1/24, \Delta u = 2/25, \Delta t = .002$, (3) $N_x = N_v = 32,\ \Delta\xi = 1/32, \Delta u = 2/33, \Delta t = .001$. The parameter, c, in (3.3) is $c = 1$. The computations are carried out for $0 \leqslant \bar{t}_k \leqslant T,\ T = 2$. For (1) the regrid parameter is $N_g = 25$, for (2) $N_g = 50$, for (3) $N_g = 100$. Thus regriding occurs for each computation at time intervals $\Delta\tau = .1$. Fig. 1 shows the graphs of $e_{rel}(\bar{t}_k)$ for computations (1)–(3), the solid line is from (3), the dashed line from (2), and the dashdot line from (1). Clearly $e_{rel}(\bar{t}_k)$ decreases as N_x, N_v increase and Δt decreases. We want to determine if the error conforms to the estimate (4.10).

If the function $K(\bar{t})$ in (4.10) is known precisely enough then we can assume $e_{rel}(\bar{t}_k) \approx K(\bar{t}_k)((\Delta\xi)^2 + (\Delta u)^2 + \Delta t)$. On the basis of this assumption from computation (3) with $\Delta\xi_3 = 1/32, \Delta u_3 = 2/33, \Delta t_3 = .001$ the function $K(\bar{t}_k)$ is approximated. Let $e_{rel,3}(\bar{t}_k)$ be the discrete relative L_2 error in the electric field computed from (4.9) with parameters $\Delta\xi_3, \Delta u_3, \Delta t_3$. Let $\Delta_3 = (\Delta\xi_3)^2 + (\Delta u_3)^2 + \Delta t_3$. Then

$$K(\bar{t}_k) \approx \frac{e_{rel,3}(\bar{t}_k)}{\Delta_3}. \tag{4.11}$$

We now determine if the discrete relative L_2 error from computations (1) and (2) conforms to expression (4.10) with $K(\bar{t}_k)$ given by (4.11). The L_2 error (4.9), obtained from computation (1) with $\Delta\xi_1 = 1/16, \Delta u_1 = 2/17, \Delta t_1 = .004$ is denoted $e_{rel,1}(\bar{t}_k)$, and the L_2 error from computation (2) with $\Delta\xi_2 = 1/24, \Delta u_2 = 2/25, \Delta t_2 = .002$ is denoted $e_{rel,2}(\bar{t}_k)$. For $\Delta_1 = (\Delta\xi_1)^2 + (\Delta u_1)^2 + \Delta t_1$ and $\Delta_2 = (\Delta\xi_2)^2 + (\Delta u_2)^2 + \Delta t_2$ let $est_1(\bar{t}_k) = K(\bar{t}_k)\Delta_1,\ est_2(\bar{t}_k) = K(\bar{t}_k)\Delta_2$ be the error estimates for computations (1) and (2). Expression (4.10) is valid if $e_{rel,2}(\bar{t}_k) \leqslant est_2(\bar{t}_k),\ e_{rel,1}(\bar{t}_k) \leqslant est_1(\bar{t}_k)$. Fig.2 shows the graphs of $e_{rel,l}(\bar{t}_k)$ compared with $est_l(\bar{t}_k),\ l = 1,2; e_{rel,1}$ is the thin line, $e_{rel,2}$ the solid line, est_1 the dashed line, est_2 the dashdot line. For the computation (2) with $N_x = N_v = 24, \Delta t = .002,\ e_{rel,2}(\bar{t}_k) \approx est_2(\bar{t}_k)$. For the computation (1) with $N_x = N_v = 16, \Delta t = .004,\ e_{rel,1}(\bar{t}_k) \approx est_1(\bar{t}_k)$ up to time $t \approx .4$. Then $e_{rel,1}(\bar{t}_k) < est_1(\bar{t}_k)$. Thus, the estimate (4.10) holds for computations (1) and (2) with $K(\bar{t}_k)$ computed from (4.11). This then provides some confirmation that the order of accuracy of the deterministic particle method of Section 3 is given by an expression of type (4.10).

Another computation is done involving the electrostatic energy to further clarify the order of accuracy estimate. From the expression for the field (4.7) and (4.8) an exact value of the electrostatic energy is

$$ese_{exact}(\bar{t}_k) = \frac{1}{2}\int_0^1\int_0^1 (|E_1|^2 + |E_2|^2)dx_1dx_2 = .098696\cdots.$$

Then let $\delta ese(\bar{t}_k) = |ese_{exact}(\bar{t}_k) - ese(\bar{t}_k)|$ in which $ese(\bar{t}_k)$ is the approximate value computed from (3.47). Assuming a bounded continuous function $\overline{K}(\bar{t})$ is known precisely then it is further assumed that the error $\delta ese(\bar{t}_k)$ is given by

$$\delta ese(\bar{t}_k) = \overline{K}(\bar{t}_k)((\Delta\xi)^2 + (\Delta u)^2 + \Delta t). \tag{4.12}$$

For $l = 1, 2, 3$ let $\Delta_l = (\Delta\xi_l)^2 + (\Delta u_l)^2 + \Delta t_l$, $ese_l(\bar{t}_k)$, and $\delta ese_l(\bar{t}_k) = |ese_{exact}(\bar{t}_k) - ese_l(\bar{t}_k)|$ be quantities corresponding to computations (1)–(3). Thus $\delta ese_l(\bar{t}_k) = \overline{K}(\bar{t}_k)\Delta_l$. Let $r_1 = \Delta_3/\Delta_1 \approx .2598$ and $r_2 = \Delta_3/\Delta_2 \approx .5574$. Assuming the error is given by (4.12) then for $l = 1, 2$, $\delta ese_3(\bar{t}_k)/\delta ese_l(\bar{t}_k) = r_l$ or $\delta ese_3(\bar{t}_k) = r_l \delta ese_l(\bar{t}_k)$. Fig. 3 shows the graphs of $ese(\bar{t}_k)$ for computations (1)–(3) compared to $ese_{exact}(\bar{t}_k)$ for $0 \leqslant \bar{t}_k \leqslant 2$. Fig. 4 shows the graphs of $\delta ese_l(\bar{t}_k)$, $l = 1, 2, 3$; the dashed line is for $l = 1$, the thin line for $l = 2$, and the solid line for $l = 3$. Also plotted in Fig. 4 are the quantities $r_1 \delta ese_1(\bar{t}_k)$ (dashdot line) and

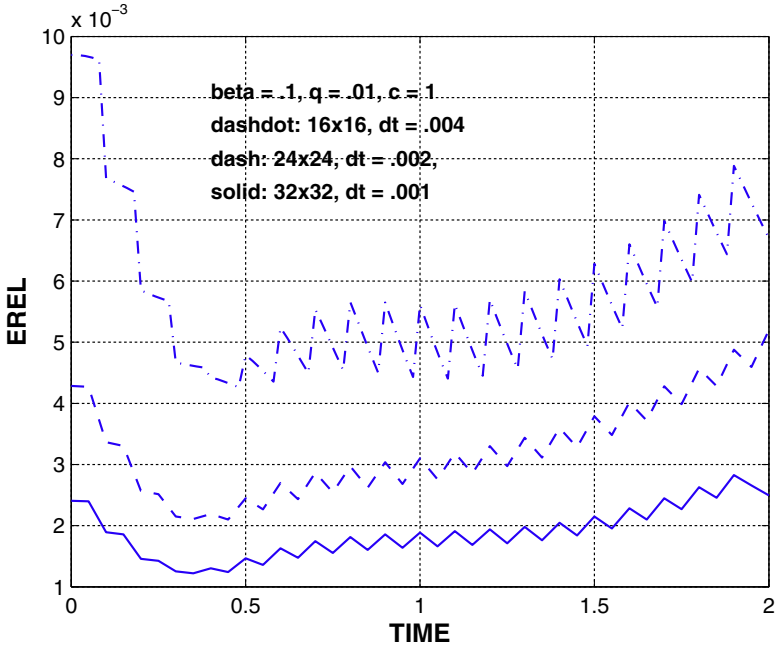

Fig. 1. Relative L_2 error in the electric field.

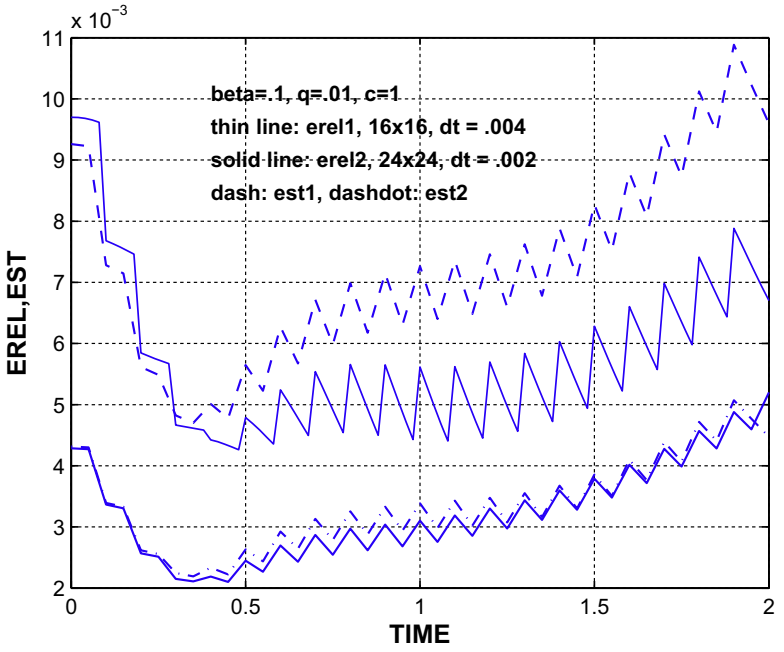

Fig. 2. Comparison of the relative L_2 error in the electric field with the error estimate (4.10).

$r_2\delta ese_2(\bar{t}_k)$ (dotted line with asterisks). The graphs of $r_l\delta ese_l(\bar{t}_k),\ l = 1,2$ are very close to the graph of $\delta ese_3(\bar{t}_k)$. It therefore appears that an expression for the error of the type (4.12) predicts rather precisely the error in the graphs of *ese*.

4.2. Approach to a steady state having a known exact solution

For the next example an exact analytical expression is obtained for the steady state solution. We begin by letting $B_z = 0$. The initial data for (1.1) and (1.2) is

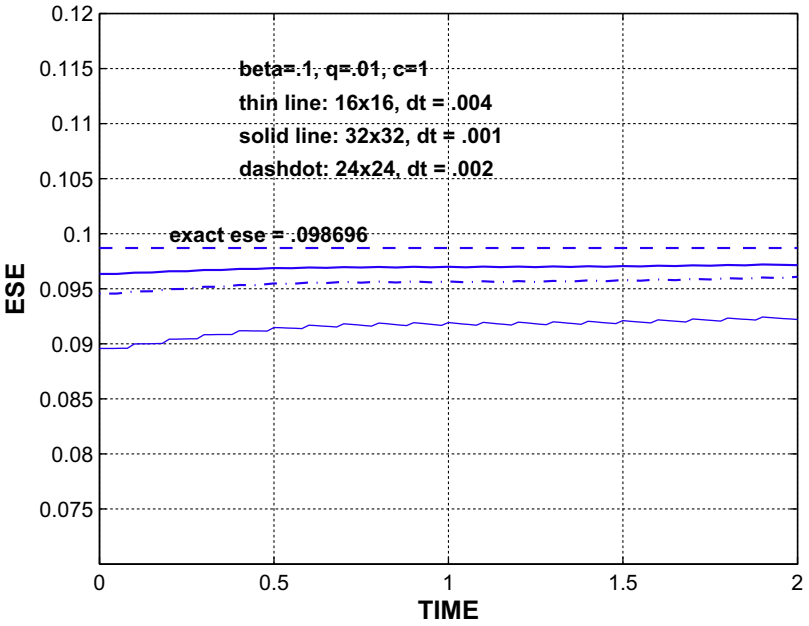

Fig. 3. Graphs of $ese(\bar{t}_k)$ compared to $ese_{exact}(\bar{t}_k)$.

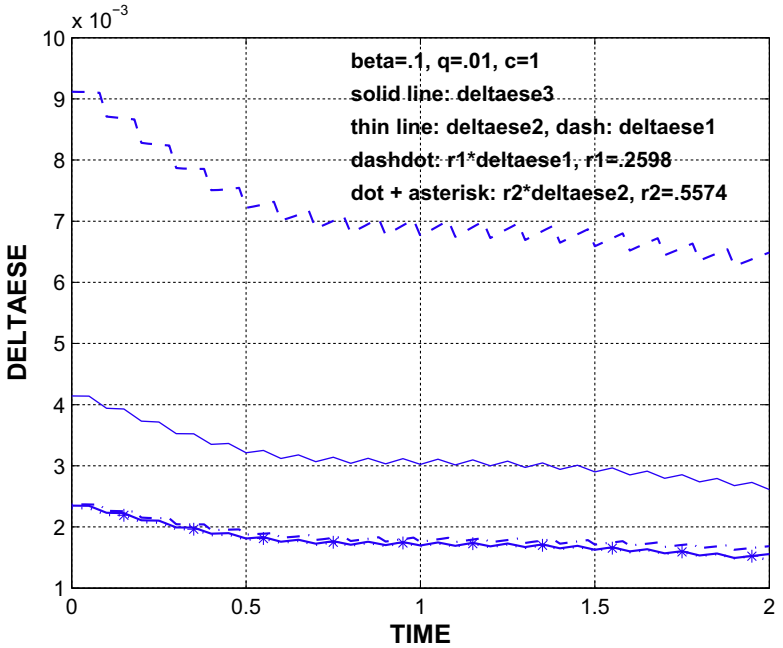

Fig. 4. Graphs of $\delta ese_l(\bar{t}_k), l = 1,2,3$. The graph $r_1\delta ese_1(\bar{t}_k), r_1 = \Delta_3/\Delta_1$, and the graph $r_2\delta ese_2(\bar{t}_k), r2 = \Delta_3/\Delta_2$, are compared to $\delta ese_3(\bar{t}_k)$.

$$f_0(x,v)=\frac{K}{2\pi v_{th}^2L^2}\left(1+2\epsilon\left(cos\left(\frac{2\pi x_1}{L}\right)+cos\left(\frac{2\pi x_2}{L}\right)\right)\right)\exp\left(-\frac{v_1^2+v_2^2}{2v_{th}^2}\right). \tag{4.13}$$

If $\beta=0,\ q=0$ in (1.1) which gives the collisionless Vlasov–Poisson system then initial data of the form (4.13) results in a solution that demonstrates Landau damping. Solving (1.1) and (1.2) with initial data (4.13) and β, q nonzero includes in the mathematical model effects of particle collisions. For this example the function, f, in (1.1) is assumed to be an electron distribution with $h(x)$ in (1.2) a fixed background density function for positive ions. The one dimensional form of (1.1) and (1.2) with initial data of type (4.13) is studied in [1,12,16]. The focus of the present computations is on the convergence of the solution to a steady state. The solution to (1.1) and (1.2) with initial data (4.13) has a limit function as $\bar{t}\to\infty$ that can be determined exactly. The L_1 norm of $f_0(x,v)$ is $\int_{\mathcal{A}}f_0(x,v)dvdx=K$. The background charge density in (1.2) is $h(x)=K/L^2$ so that $\int_0^L\int_0^L h(x)dx=K$. At the steady state $\phi(x)=0$. Therefore, as $\bar{t}\to\infty$ it follows from (4.1) that the solution to (1.1) and (1.2) or (2.16) and (1.2) converges to

$$f_s(x,v)=\frac{K}{(2\pi q/\beta)L^2}\exp(-|v|^2/(2q/\beta)). \tag{4.14}$$

Representative quantities that are computed converge to known steady state values. As $\bar{t}\to\infty$ the kinetic energy approaches the value given by (4.4). Since $\phi(x)=0$ then

$$ese(\bar{t})\to 0. \tag{4.15}$$

Also, using (4.14) in evaluating (3.44) it follows that

$$ent(\bar{t})\to -Kln\left(\frac{K}{(2\pi q/\beta)L^2}\right)+\frac{1}{q/\beta}\int_{\mathcal{A}}\frac{|v|^2}{2}f_s dvdx$$

and

$$FE(\bar{t})\to\frac{qK}{\beta}ln\left(\frac{K}{(2\pi q/\beta)L^2}\right). \tag{4.16}$$

For initial data given by (4.13) and $h(x)$ as given the approximation to (1.1) and (1.2) is computed by the deterministic particle method of Section 3. In (4.13) we let $L=1,\ K=3.5,\ \epsilon=.01,\ v_{th}=.3/\pi$. These parameters are the same as those used in the computations of [28], Figs. 8–11 for the 1-D system. In Eq. (1.1) $\beta=.1$. The diffusion parameter q is varied as $q=.0005$ and $q=.002$. For the computations $N_x=20, N_v=20$. Thus $\Delta\xi=1/N_x=1/20,\ \Delta u=2/(N_v+1)=2/21$. The parameter c in (3.3) is $c=.5$. For the time step $\Delta t=.01,\ t_n=n\Delta t, n=0,1,\ldots,N_g$ for $N_g=100$. Thus, the interval of the particle computation is $[0,T_1],\ T_1=1$. Regriding is done at time $\tau_m=mT_1=m,\ m=1,\ldots,M$, with $M=50$. The total number of time steps is $N_t=MN_g=5000$. The time of the computation is $\bar{t}_k=\tau_m+t_n,\ k=(m-1)N_g+n,\ m=1,\ldots,50; n=0,1,\ldots,100$. Thus $k=0,1,\ldots,5000$ and $0\leqslant\bar{t}_k\leqslant 50$.

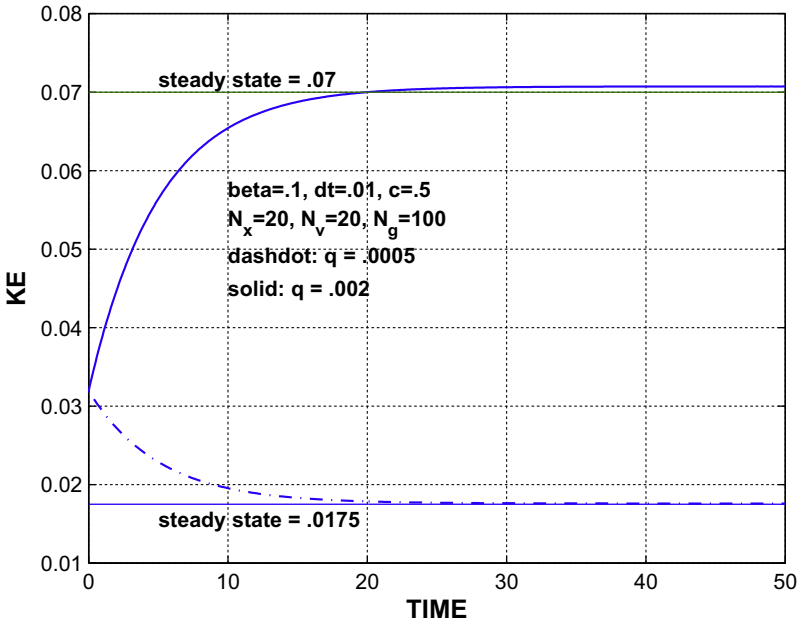

Fig. 5. Kinetic energy for Landau damping.

If $q = .0005$ then according to (4.4) $ke(\bar{t}) \to (3.5)(.0005)/.1 = .0175$. If $q = .002$ then $ke(\bar{t}) \to (3.5)(.002)/.1 = .07$. The approximation to kinetic energy is $ke(\bar{t}_k)$ computed according to (3.45). The graphs of $ke(\bar{t}_k)$ are shown in Fig. 5 compared to the exact steady state values. The electrostatic energy, $ese(\bar{t}_k)$, is computed from (3.47). The graphs of $ese(\bar{t}_k)$ are in Fig. 6. For both graphs $ese \to 0$ as expected; however, the approach to zero is faster for larger q. The free energy graphs are shown in Figs. 7 and 8. It is known from (4.3) that the free energy is a monotonically decreasing function of time. Letting $L = 1, K = 3.5, \beta = .1$ in (4.16) then if $q = .0005$, $FE \to .082481$ and if $q = .002$, $FE \to .232884$. The graph of $FE(\bar{t}_k)$ showing the convergence to the steady state value is in Fig. 8 for $q = .0005$ and in Fig. 7 for $q = .002$. The small discontinuities in the *FE* graphs are due to the regriding. The regriding preserves the continuity of the kinetic energy but not that of the entropy

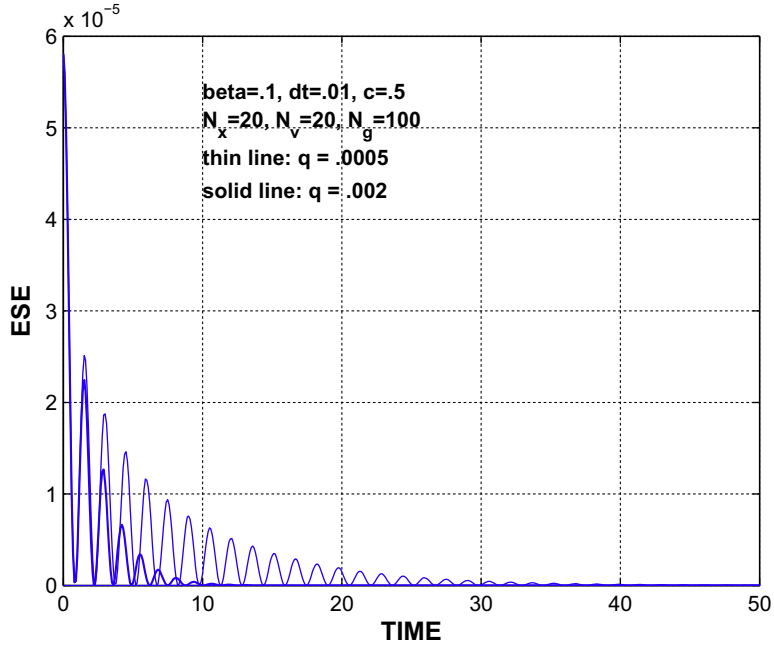

Fig. 6. Electrostatic energy for Landau damping.

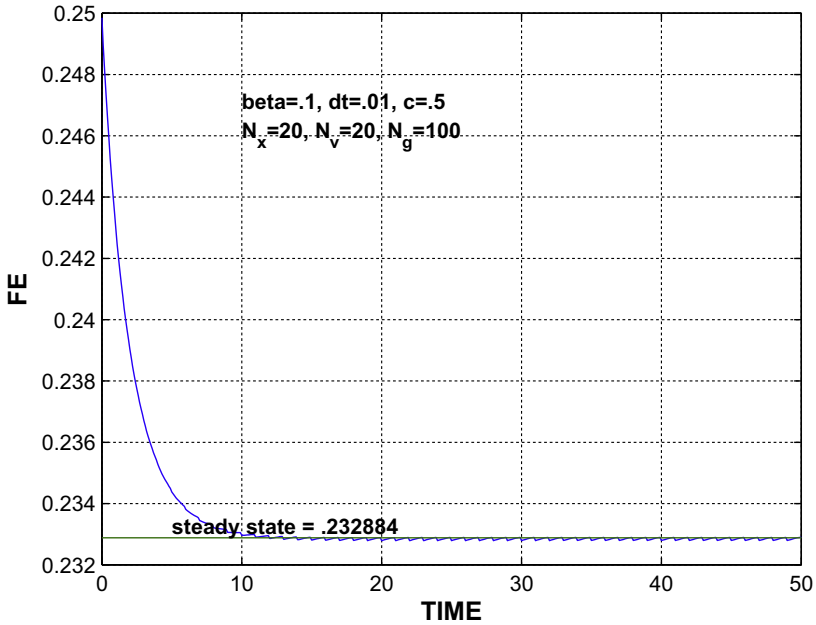

Fig. 7. Free energy for Landau damping, $q = .002$.

or free energy. The graphs in Figs. 5–8 demonstrate that the approach to the steady state of the computed values agrees well with the exact steady state values.

Some comments are provided at this point on how to set the parameters $T_1 = \Delta\tau$ and Δt giving the length of the interval and time step for the particle computation. This then determines the regrid parameter N_g. In general the parameter $\Delta\tau$ should be large relative to Δt so that many iterations of the particle method take place before regriding, but $\Delta\tau$ should be small relative to the total time of computation, T. The coefficients $c_l(i,j,t_n)$ in (3.4) increase with increasing t_n in the interval $[0,T_1]$, and the quantity $\Theta(t_n)$ following (3.5) also increases. The closer $\Theta(t_n)$ gets to one the more iterations are needed for convergence of the SOR algorithm for solving (3.4). So $\Delta\tau = T_1$ and the parameter N_g are made sufficiently small so as to limit

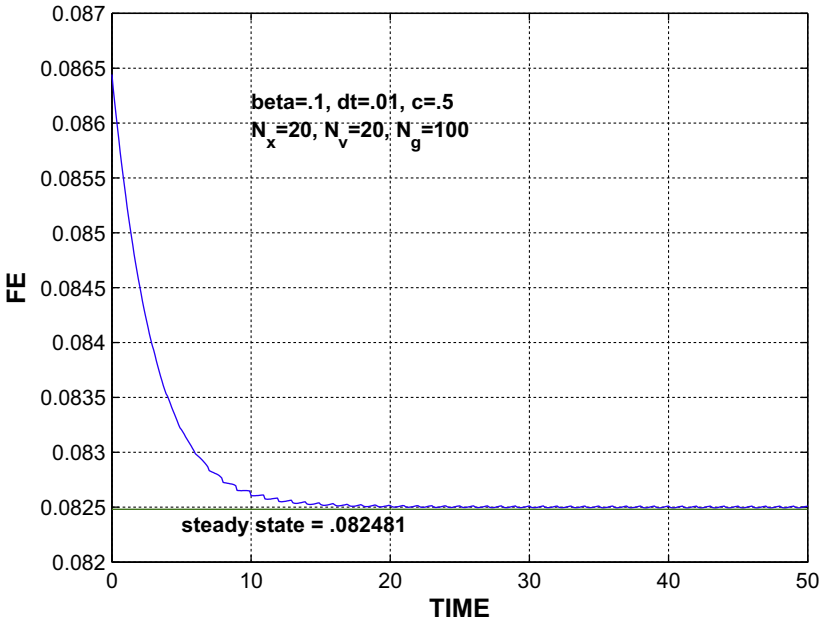

Fig. 8. Free energy for Landau damping, $q = .0005$.

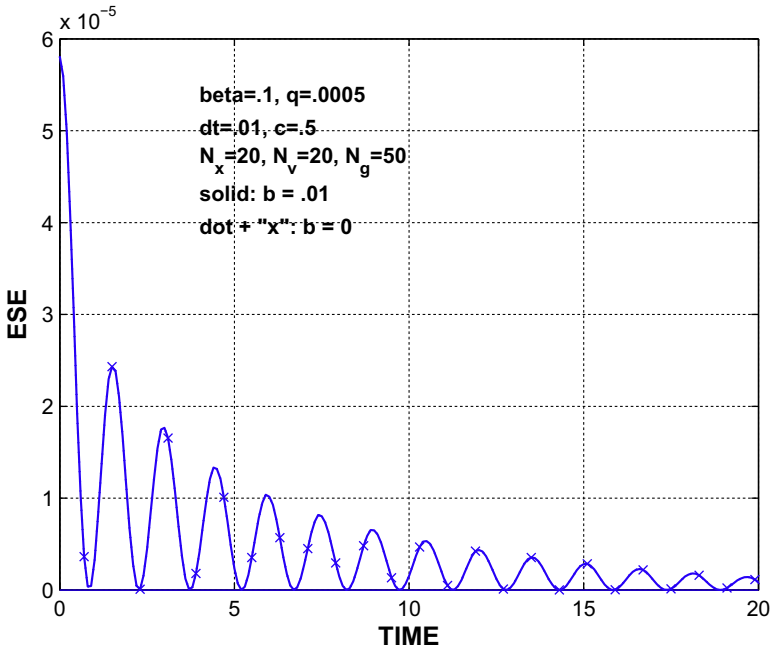

Fig. 9. Graphs of electrostatic energy for $b = 0$ and $b = .01$.

the number of iterations required for convergence of the SOR algorithm on the interval $[0, T_1]$. For example, for the computation of Figs. 5 and 6 for $\beta = .1,\ q = .002,\ T_1 = 1,\ N_g = 100$ the SOR method converges to a tolerance of 10^{-12} with 8 to 9 iterations at each time step on the interval $[0, T_1]$. Another reason for making T_1 relatively small is to keep discontinuities at the time of regriding from becoming too pronounced. Such discontinuities due to regriding are apparent in the free energy graphs, Figs. 7 and 8. Within limits the regrid parameter need not be specified very precisely. Regarding the solutions of Figs. 5 and 6 the regrid parameter is $N_g = 100$. There is little change in the solution if $N_g = 50$. However, without regriding the particle method becomes unstable and inaccurate for sufficiently large time. This happens regardless of whether the SOR method or Douglas–Rachford method is used for solving (3.4). For example, without regriding the *ese* graph of Fig. 6 for $\beta = .1, q = .002$ diverges away from zero and the solution becomes inaccurate after about 500 steps of the particle method alone. With regriding the solution is stable and accurate over an extended time interval. The main consideration in determining Δt, the time step of the particle method, is the accuracy of the solution. Our assumption based on the computations of Section 4.1 is that the accuracy of the method is $O((\Delta\xi)^2 + (\Delta u)^2 + \Delta t)$. Hence, it is assumed we should have $\Delta t \leqslant \Delta\xi, \Delta u$. Given this constraint Δt is then made sufficiently small so that the solution is not significantly changed by further reducing Δt. Some initial experimentation is needed to determine values for T_1 and Δt.

We now consider the effect of letting $B_z = b \neq 0$ in which case the equations to be approximated are (2.16) and (1.2). The initial data for (2.16) is maintained as (4.13). The parameters $L, K, \epsilon, v_{th}, \beta$ are as previously given. The parameter b is given the value $B_z = b = .01$. The parameter q is varied as $q = .0005$ and $q = .002$.

In applying the deterministic particle method of Section 3 to approximate (2.16) and (1.2) the computation of particle trajectories, first an second partial derivatives, and coefficients in (3.4) are carried out according to Sections 3.5.1, 3.5.2 and 3.5.3.

We compare the computation of kinetic energy, electrostatic energy, and free energy for $b = .01$ with the case previously computed for $b = 0$. What is observed is that the graphs of $ke(\bar{t}_k)$ and $ese(\bar{t}_k)$ for $b = .01$ and $b = 0$ are so close as to be indistinguishable. Also, the graph of $FE(\bar{t}_k)$ computed for $b = 0$ from (3.48) appears essentially the same as for $FE(\bar{t}_k) - 1/2b^2L^2$ computed from (3.61). To demonstrate this the graphs of $ese(\bar{t}_k)$ for $q = .0005$ with $b = 0$ and $b = .01$ are shown in Fig. 9 for $0 \leqslant \bar{t}_k \leqslant 20$. The graph for $b = .01$ is the solid line. The graph for $b = 0$ is a dotted line with x's at every eighth data point. The x's are visible, but otherwise the dotted line cannot be distinguished from the solid line.

A quantity that clearly distinguishes the solution with $b = .01$ from that with $b = 0$ is the angular momentum. The angular momentum, $ang(\bar{t})$, is defined by (3.62), and if $b = 0$ it can be determined analytically that if the initial data is (4.13) then $ang(\bar{t}) = 0,\ t \geqslant 0$. This is not the case if $b \neq 0$. Fig. 10 shows the graphs of the approximation to angular momentum, $ang(\bar{t}_k)$, computed according to (3.65) for the solution with $b = .01$. The solid line is for $q = .002$, the thin line for $q = .0005$. Thus, for $b = .01$ the angular momentum is a nonzero oscillating quantity which decays to zero as $\bar{t}_k$ gets large, the larger the value of q the faster the decay to zero. For $b = 0$ $ang(\bar{t}_k) \approx 0$. Fig. 10 also includes the graph $ang(\bar{t}_k)$ for $b = 0$ and $q = .0005$ given by a dashdot line. For this graph $|ang(\bar{t}_k)| \leqslant 10^{-10}$, so the graph essentially coincides with the t axis. The graph of angular momentum for $b = 0,\ q = .002$ is similarly close to zero. For all computations $ang(\bar{t}_k) \to 0$ for large $\bar{t}_k$. This is consistent with the fact that for f_s given by (4.14)

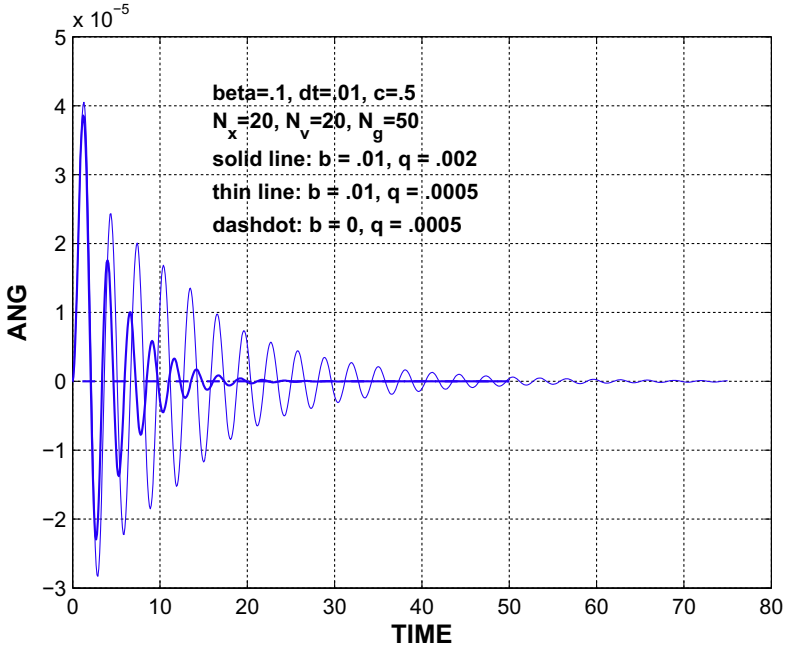

Fig. 10. Graphs of angular momentum for $b = 0$ and $b = .01$.

$$lim_{\bar{t}\to\infty} ang(\bar{t}) = \int_{\mathcal{A}} (x_1 v_2 - x_2 v_1) f_s(x, v) dv dx = 0.$$

We note that for the computations involving angular momentum the regrid parameter is $N_g = 50$. The more frequent regriding avoids some small discontinuities in the angular momentum graphs at points of regriding and otherwise has a negligible effect on the solution from that previously computed with $N_g = 100$.

We now take a closer look at the graphs of electrostatic energy given in Fig. 9 and determine that there is a difference between the *ese* graphs for $b = .01$ and $b = 0$. The graphs in Fig. 9 are for $q = .0005$. It can be determined that for f, ϕ the solution to (1.1) and (1.2) and $E = -\nabla\phi$ then

$$\frac{d}{d\bar{t}} \frac{1}{2} \int_0^L \int_0^L (|E_1|^2 + |E_2|^2) dx_2 dx_1 = -\int_{\mathcal{A}} (E_1 v_1 + E_2 v_2) f dv dx.$$

That is

$$\frac{d}{d\bar{t}} ese(\bar{t}) = -\int_{\mathcal{A}} (E \cdot v) f(x, v, \bar{t}) dv dx. \tag{4.17}$$

The same formula (4.17) is derived if f, ϕ are the solution to (2.16) and (1.2). Thus, let $ese(\bar{t})$ be the electrostatic energy associated with the solution to (1.1) and (1.2) and $ese_b(\bar{t})$ be the electrostatic energy associated with the solution to (2.16) and (1.2). Also, the distribution function and electric field for (1.1) and (1.2) are denoted $f(x, v, \bar{t})$ and $E(x, \bar{t}) = (E_1(x, \bar{t}), E_2(x, \bar{t}))$. The distribution function and field for (2.16) and (1.2) with $b \neq 0$ are denoted $f_b(x, v, \bar{t})$ and $E_b(x, \bar{t}) = (E_{b,1}(x, \bar{t}), E_{b,2}(x, \bar{t}))$. Then from (4.17) an equation for the difference $ese(\bar{t}) - ese_b(\bar{t})$ is

$$\frac{d}{d\bar{t}} (ese(\bar{t}) - ese_b(\bar{t})) = -\left[\int_{\mathcal{A}} (E \cdot v) f(x, v, \bar{t}) dv dx - \int_{\mathcal{A}} (E_b \cdot v) f_b(x, v, \bar{t}) dv dx\right]. \tag{4.18}$$

Let $I(\bar{t}) = \int_{\mathcal{A}} (E \cdot v) f dv dx$ and $I_b(\bar{t}) = \int_{\mathcal{A}} (E_b \cdot v) f_b dv dx$. Also, let $dese(\bar{t}) = ese(\bar{t}) - ese_b(\bar{t})$ and $dI(\bar{t}) = I(\bar{t}) - I_b(\bar{t})$. According to (4.18) the extreme values of $dese(\bar{t})$ occur at the zeros of $dI(\bar{t})$. This is demonstrated numerically. Let $ese(\bar{t}_k)$ be the *ese* graph for $b = 0$ and $ese_b(\bar{t}_k)$ the graph for $b \neq 0$. These graphs are in Fig. 9. Then the approximation to $dese(\bar{t})$ is $dese(\bar{t}_k) = ese(\bar{t}_k) - ese_b(\bar{t}_k)$. The approximation to $I(\bar{t})$ is computed from the formula

$$I(\bar{t}_k) = \sum_{k_1=1}^{N_p} \sum_{k_2=1}^{N_p} \left(E^n_{1,av}(\kappa) \zeta^n_{1,av}(\kappa) + E^n_{2,av}(\kappa) \zeta^n_{2,av}(\kappa)\right) \epsilon^2. \tag{4.19}$$

Here $\zeta^n_{1,av}$, $\zeta^n_{2,av}$ are precisely as in (3.65) and $E^n_{1,av}$, $E^n_{2,av}$ are as in formula (3.47). The approximation to $I_b(\bar{t})$, denoted $I_b(\bar{t}_k)$, is computed exactly as for (4.19) in which the field $E^n_b(\kappa)$ and moments $\zeta^n_1(\kappa)$, $\zeta^n_2(\kappa)$ are obtained by approximating (2.16) and (1.2) with $b \neq 0$. Thus, the approximation to $dI(\bar{t})$ is $dI(\bar{t}_k) = I(\bar{t}_k) - I_b(\bar{t}_k)$. Fig. 11 shows the graph of $dese(\bar{t}_k)$ and $-dI(\bar{t}_k)$ for

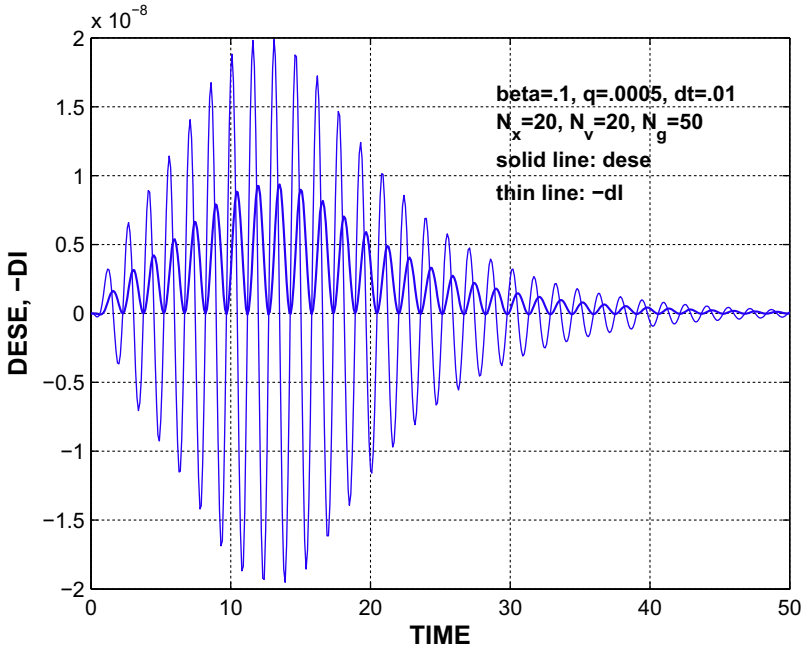

Fig. 11. Graphs of $dese(\bar{t}_k)$ and $-dI(\bar{t}_k)$ for $0 \leqslant \bar{t}_k \leqslant 50$.

the time interval $[0,T], T = 50$. The computational parameters are those of Fig. 9. Fig. 12 shows the graph for $0 \leqslant \bar{t}_k \leqslant 20$ in which it is more clearly seen that the relative maxima and minima of $dese(\bar{t}_k)$ are at the zeros of $dI(\bar{t}_k)$. This then is consistent with Eq. (4.18). The maximum value of $dese(\bar{t}_k)$ is $O(10^{-8})$. This difference between $ese(\bar{t}_k)$ and $ese_b(\bar{t}_k)$ is not apparent from the graphs in Fig. 9.

If the strength of the magnetic field is increased, that is the constant b in (2.16) is increased, then the angular momentum increases. Fig. 13 shows the result of computing the solution to (2.16) and (1.2) with $q = .0005$ and $b = .1$. The thin line is the angular momentum computed with $b = .1$ in comparison to that computed with $b = .01$ shown by the solid line. The quantity $dese(\bar{t}_k)$, shown in Fig. 11 for $b = .01$, similarly increases. If $b = .1$ the graphs of $dese(\bar{t}_k)$ and $dI(\bar{t}_k)$ have a similar form to the graphs in Fig. 11, but the maximum value of $dese(\bar{t}_k)$ is now $O(10^{-6})$. These graphs are not shown.

The graphs of angular momentum, Figs. 10 and 13, and the graph of $dese(\bar{t}_k)$, Fig. 11, demonstrate the difference in the solutions to (1.1) and (1.2) for $b = 0$ and (2.16) and (1.1) for $b \neq 0$. What is also observed is that representative quantities approach the same steady state values if $b = 0$ and (1.1) and (1.2) is solved or $b \neq 0$ and (2.16) and (1.2) is solved. Thus in Figs. 10 and 13 $ang(\bar{t}_k) \to 0$ and in Fig. 11 $dese(\bar{t}_k) \to 0$ as $\bar{t}_k$ gets large. This is consistent with our assumption that solutions to (1.1) and (1.2) and solutions to (2.16) and (1.2) with $b \neq 0$ approach the same steady state solution given by (4.1) and (4.2). However, for the present example it can be shown more precisely that the solutions with $b = 0$ and $b \neq 0$ both converge with increasing time to the same limit function.

For initial data (4.13) we demonstrate that the solutions to (1.1) and (1.2) with $b = 0$ and (2.16) and (1.2) with $b \neq 0$ converge in a pointwise sense to the exact steady state solution given by (4.14). The approximation to the distribution function, $f(x,v,t)$, is recovered on a fixed grid at the time of regriding. That is in Section 3.3 at time $\bar{t}_k = \tau_m = mT_1,\ t_n = 0, k = mN_g, n = 0$ the grid function $g^{m,0}_{i,j} \approx f(\xi_i, \eta_j, mT_1)$ where $f(x,v,t)$ is the solution to (1.1) and (1.2) if $b = 0$ or (2.16) and (1.2) if $b \neq 0$ and ξ_i, η_j are defined by (3.1) and (3.3). For $f_s(x,v)$ given by (4.14) let $f^e_{i,j} = f_s(\xi_i, \eta_j)$ be the exact steady state solution at grid points (ξ_i, η_j). At time $\bar{t}_k = \tau_m$ the maximal difference between $g^{m,0}_{i,j}$ and $f^e_{i,j}$ is computed as

$$difmx(\tau_m) = max_{i,j}|g^{m,0}_{i,j} - f^e_{i,j}| \tag{4.20}$$

for $m = 0, 1, \ldots, M$.

For $b = 0$ and the solution to (1.1) and (1.2) we consider the computations of Figs. 5–8. Here $\Delta t = .01,\ N_g = 100$ so $\Delta\tau = 1$ and $\tau_m = m$ for $m = 0, 1, \ldots, M$ with $M = 50$. The quantity $difmx(\tau_m)$ is computed for the solution with $\beta = .1,\ q = .002$ (the solid line in Figs. 5 and 6). The solid line in Fig. 14 shows the graph of $difmx(\tau_m)$ for $0 \leqslant \tau_m \leqslant 50$. For $\tau_m = 0,\ difmx(0) = 32.59$. The minimum of $difmx$ is at $\tau_m = 19$ and is $difmx(19) = .0306$. We note that $\tau_m = 19$ approximately corresponds to the point where the graph of ke, Fig. 5, takes on the exact steady state value. The quantity $difmx$ then increases somewhat to an approximately constant steady state value. At $\tau_m = 50$ the maximal difference (4.20) is at $i_1 = 16, i_2 = 5, j_1 = 10, j_2 = 11$ and is $difmx(50) = .3056$.

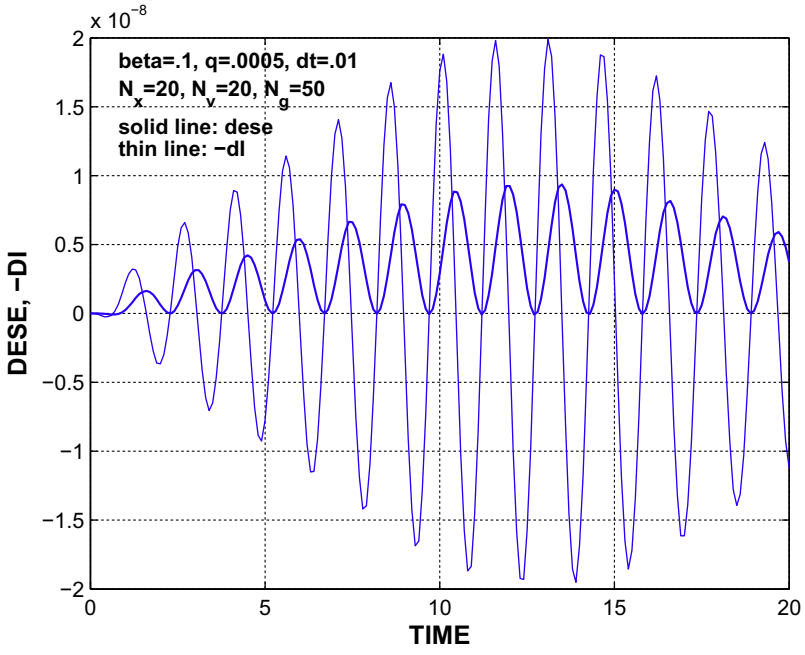

Fig. 12. Graphs of $dese(\bar{t}_k)$ and $-dI(\bar{t}_k)$ for $0 \leqslant \bar{t}_k \leqslant 20$.

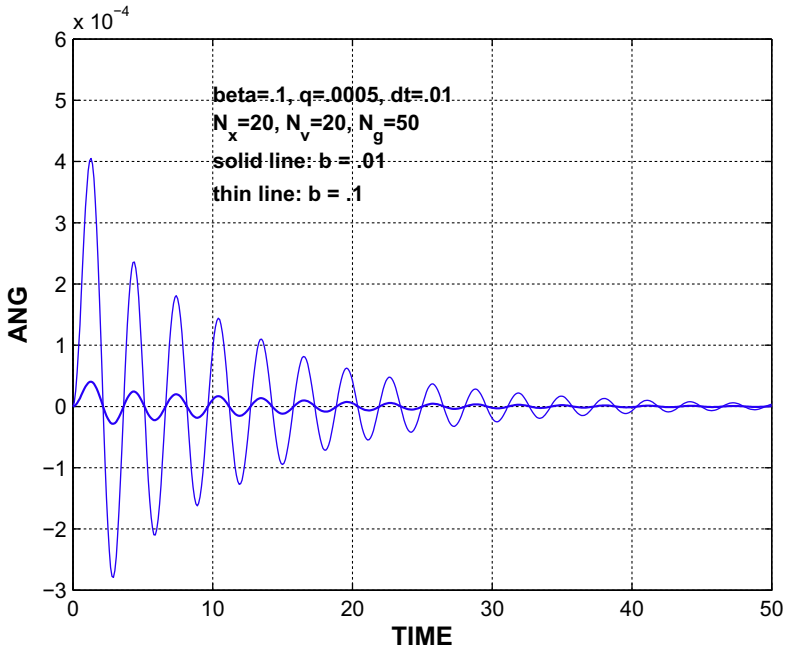

Fig. 13. Graphs of angular momentum for $b = .01$ and $b = .1$.

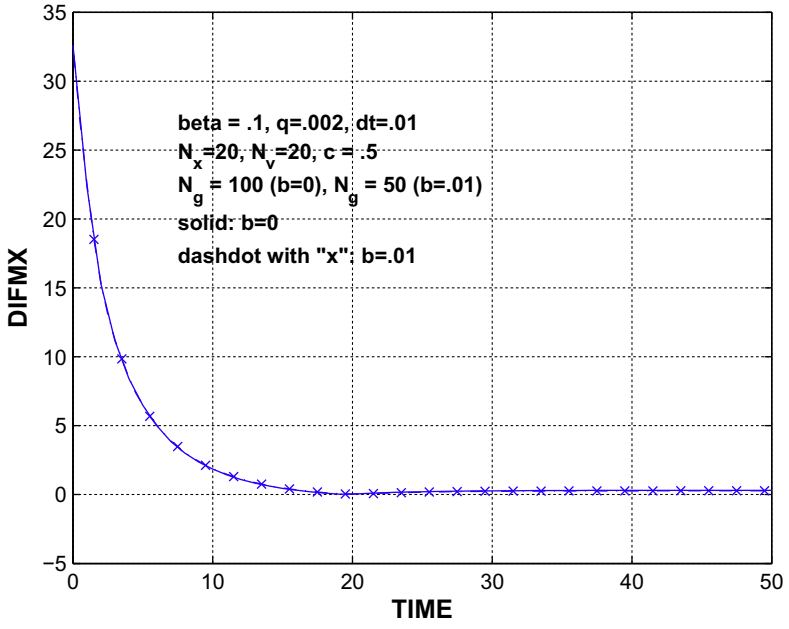

Fig. 14. Maximal difference between solutions to (1.1) and (1.2) and (2.16) and (1.2) and the exact steady state solution (4.14).

For $b \neq 0$ and the solution to (2.16) and (1.2) we consider the computation of Fig. 10 for which $b = .01$. Here $\Delta t = .01$, $N_g = 50$ so $\Delta\tau = .5$ and $\tau_m = .5m$ for $m = 0, 1, \ldots, M$ with $M = 100$. The quantity $difmx(\tau_m)$ is again computed for the solution with $\beta = .1$, $q = .002$ (the solid line in Fig. 10). The graph for $difmx(\tau_m)$ for $b = .01$ is a dashdot line in Fig. 14. There is a very close correspondence between this graph and the solid line graph of $b = 0$, so to distinguish the two graphs "x's" are plotted at every fourth data point on the dashdot graph for $b = .01$. For $b = .01$ the minimum of $difmx$ is at $\tau_m = 19.5$ and is $difmx(19.5) = .0451$. At $\tau_m = 50$ the maximal difference is at $i_1 = 5, i_2 = 5, j_1 = 11, j_2 = 11$ and is $difmx(50) = .2739$. The convergence of $difmx$ as $\bar{t}_k$ gets large is essentially the same for $b = 0$ and $b = .01$, and the conclusion is that the limit function for both of these solutions is (4.14).

In Fig. 15 a one dimensional profile of the solution for $b = 0$ is graphed that includes the point of maximal difference at $\tau_m = 50$. For the graphs in this Figure $i_1 = 16, i_2 = 5, j_2 = 11$ and $j_1 = 1, \ldots, N_v$, $N_v = 20$. The exact steady state solution is denoted $f^e_{j_1} = f_s(\xi_i, \eta_j)$ for $f_s(x, v)$ given by (4.14) and i_1, i_2, j_2 constant and j_1 variable. Similarly with i_1, i_2, j_2 constant and j_1 variable the approximate solution at $\tau_m = 50$ is $f^m_{j_1} = g^{m,0}_{i,j}$, $m = 50$. The initial function at $\tau_m = 0$ is denoted $f^i_{j_1} = g^{0,0}_{i,j}$. The grid function $g^{0,0}_{i,j}$ is defined in Section 3.2.1 for which the initial function $f_0(x, v)$ is given by (4.13). The quantities $f^m_{j_1}, f^e_{j_1}$ and $f^i_{j_1}$ are graphed as functions of η_{1,j_1} defined by (3.3). The dashed line in Fig. 15 is $f^i_{j_1}$, the solid line is $f^m_{j_1}$. The exact steady state solution, $f^e_{j_1}$, is given by a dashdot line; however, on this scale it cannot be seen against the solid line of $f^m_{j_1}$, so "x's" are plotted at the data points along the $f^e_{j_1}$ graph. Thus, at $T = 50$ this 1-D profile of the approximate solution $g^{m,0}_{i,j}$ is close to the profile of the steady state solution. The maximal difference of $difmx(50) = .3056$ occurs at $j_1 = 10$, i.e., $\eta_{1,j_1} \approx 0$. This is seen graphically on a fine scale in the inset to Fig. 15. The maximum of $f^e_{j_1}$ is 27.07, also occuring at $j_1 = 10$. The relative maximum error along the 1-D profile is $difmx(50)/max_{j_1} f^e_{j_1} = .0113$. For $b = .01$ similar graphs are obtained for a 1-D profile of the solution through the point of maximal difference at $\tau_m = 50$.

4.3. Approach to a steady state with $\phi(x) \neq 0$

Some computations are now done to verify the form of the steady state solution (4.1) and (4.2) in the case that $\phi(x) \neq 0$. In this case the steady state value of kinetic energy is known exactly from (4.4); however, $\phi(x)$ is in general not known exactly. Therefore, to obtain the steady state solution $f_s(x, v)$ given by (4.1) the function $\phi(x)$ must be approximated, and on this basis the steady state values of *ese* and *FE* are also computed.

The Eqs. (1.1) and (1.2) are approximated with $L = 1$ for the domain $\mathcal{A}$ and with initial data a shifted Maxwellian given as

$$f_0(x, v) = \frac{10}{\pi} \exp(-10[(v_1 - .75)^2 + (v_2 - .5)^2]). \tag{4.21}$$

Thus $\int_{\mathcal{A}} f_0(x, v) dv dx = 1$. The background charge $h(x)$ is

$$h(x) = 1 + sin(2\pi x_1) + sin(2\pi x_2). \tag{4.22}$$

As $\int_0^1 \int_0^1 h(x) dx = 1$ then for $f_0(x, v)$ and $h(x)$ as given the condition for charge neutrality is met. An example problem of this type in 1-D is considered in [25].

The solution to (1.1) and (1.2) with initial data (4.21) and background charge (4.22) converges to a steady state for which $\phi(x) \neq 0$. We determine that the steady state solution is given by (4.1) and (4.2) as follows: the solution to (1.1) and (1.2) is computed on a time interval $[0, T]$ such that at $t = T$ representative quantities, ke, ese, FE, have converged closely to time independent values. At this point the computation is stopped. At time $t = T$ the grid function ϕ_{k_1,k_2} given by the solution to (3.34) is used to approximate the steady state solution (4.1). This approximation to (4.1) is then used as initial data for the deterministic particle method to approximate the solution to (1.1) and (1.2) on a time interval $[0, \overline{T}]$. If the solution

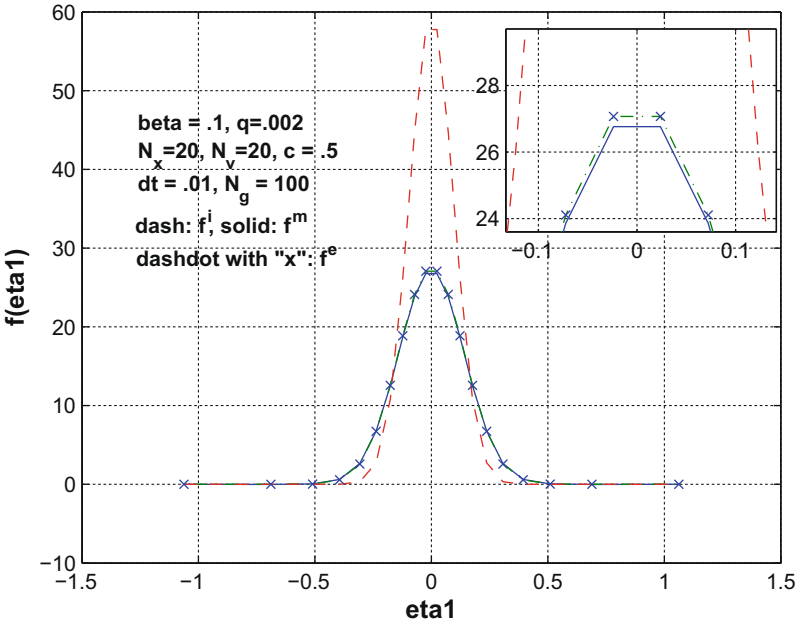

Fig. 15. 1-D profile of $f^e_{j_1}$ (exact), $f^i_{j_1}$ (initial), $f^m_{j_1} = g^{0,m}_{i,j}, m = 50$ (solution) vs. $\eta_{1,j_1}, j_1 = 1, 20$, with the inset showing the maximal difference between $f^e_{j_1}$ and $f^m_{j_1}$.

on $[0,T]$ has converged closely to the steady state given by (4.1) and (4.2) then the solution on $[0,\overline{T}]$ should be approximately constant and match the $[0,T]$ solution given at time $t=T$. With the grid function ϕ_{k_1,k_2} computed at time $t=T$ and referring to Section 3.2.1 the initial data for the computation on $[0,\overline{T}]$ is given by

$$f_0(\xi_i,\eta_j)=\frac{K}{2\pi(q/\beta)C}\exp\left(-\frac{|\eta_j|^2/2+\phi_{av}(i)}{q/\beta}\right),\quad i_1,i_2=1,\ldots,N_x,\quad j_1,j_2=1,\ldots,N_v,\quad N_p=N_x, \tag{4.23}$$

and where $\phi_{av}(i)=[\phi_{i_1-1,i_2-1}+\phi_{i_1,i_2-1}+\phi_{i_1-1,i_2}+\phi_{i_1,i_2}]/4$. The constant C is computed on the Poisson mesh of Section 3.2.6 and is

$$C=\sum_{k_1=1}^{N_p}\sum_{k_2=1}^{N_p}\exp\left(-\frac{\phi_{av}(\kappa)}{q/\beta}\right)\epsilon^2.$$

For initial data given by (4.21) and $h(x)$ given by (4.22) the numerical method of Section 3 is computed for the time interval $[0,T], T=30$. The computational parameters are $L=1,\ \beta=.1$. The constant q is varied as $q=.1,.2,.4$. The grid parameters are $N_x=30,\ N_v=30,\ N_p=30,\ \Delta t=.005$. Diffusion to higher velocities occurs more rapidly with higher q values. To adequately represent higher velocity particles the computational domain in velocity space is made wider for larger q. This is done by adjusting the constant c in (3.3). Thus, for $q=.1,\ c=2$, for $q=.2,\ c=4$, and for $q=.4,\ c=8$. The regrid parameter is $N_g=40$. Therefore, the particle computation is carried out on a time interval $[0,T_1], T_1=.2$. Regriding occurs at times $\tau_m=.2m,\ m=1,2,\ldots,150$.

For the computation for each value of q the grid function ϕ_{k_1,k_2} is taken at time $\bar{t}_k=30$ and used to determine the initial grid function, $f_0(\xi_i,\eta_j)$, given by (4.23). The constant K is $K=1$. With initial data (4.23) and background charge (4.22) the numerical method of Section 3 is computed on a time interval $[0,\overline{T}], \overline{T}=20$. All computational parameters are maintained the same as for the computation on $[0,T], T=30$. In graphing the results the solution for each value of q on $[0,\overline{T}]$ is shifted to the time interval $[T,T+\overline{T}]$ and matched to the solution on $[0,T]$ with initial data (4.21). Thus, the solution is graphed on the time interval $[0,T+\overline{T}]=[0,50]$. The solution on $[0,T]=[0,30]$ is computed with initial data (4.21), and the solution on $[T,T+\overline{T}]=[30,50]$ is computed with initial data (4.23).

Fig. 16 shows the graphs of kinetic energy. According to (4.4) with $\beta=.1,\ K=1$ if $q=.1$ then $ke\to 1$, if $q=.2$ then $ke\to 2$, and if $q=.4$ then $ke\to 4$. This convergence to the steady state values is demonstrated in Fig. 16. Also, the graphs on the interval $[30,50]$ computed with initial data (4.23) are approximately constant and match well at time $T=30$ to the graphs on [0,30] computed with initial data (4.21). On a fine scale one can perceive small discontinuities in the *ke* graphs at time $T=30$ where the solution with initial data (4.21) ends and the solution with initial data (4.23) begins.

Fig. 17 shows the graphs of electrostatic energy, and Fig. 18 shows the graphs of free energy. The solid line is for $q=.1$, the dashdot line for $q=.2$, and the dashed line for $q=.4$. Small discontinuities can be perceived mainly in the *ese* graphs at time $T=30$ where the solutions are restarted with initial data (4.23). Otherwise, there is a good match between the

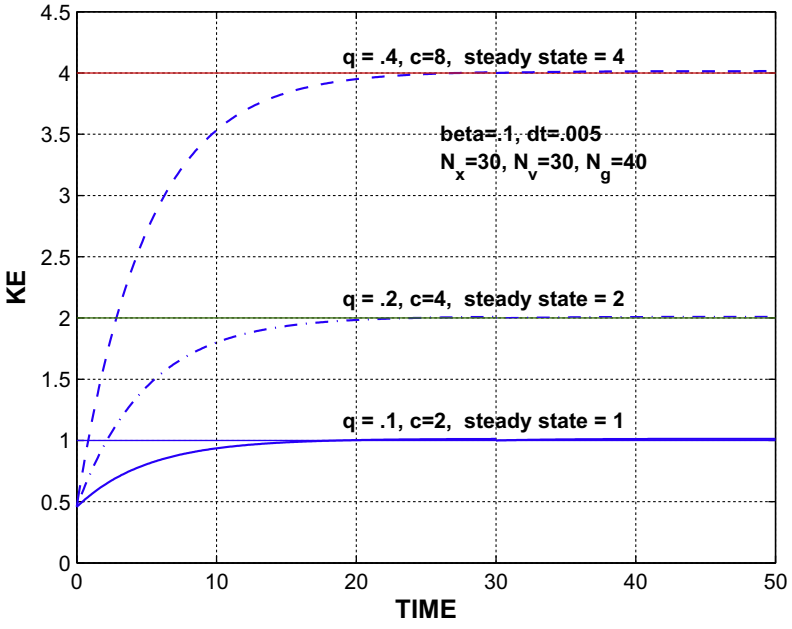

Fig. 16. Kinetic energy for shifted Maxwellian, time dependent and steady state solutions.

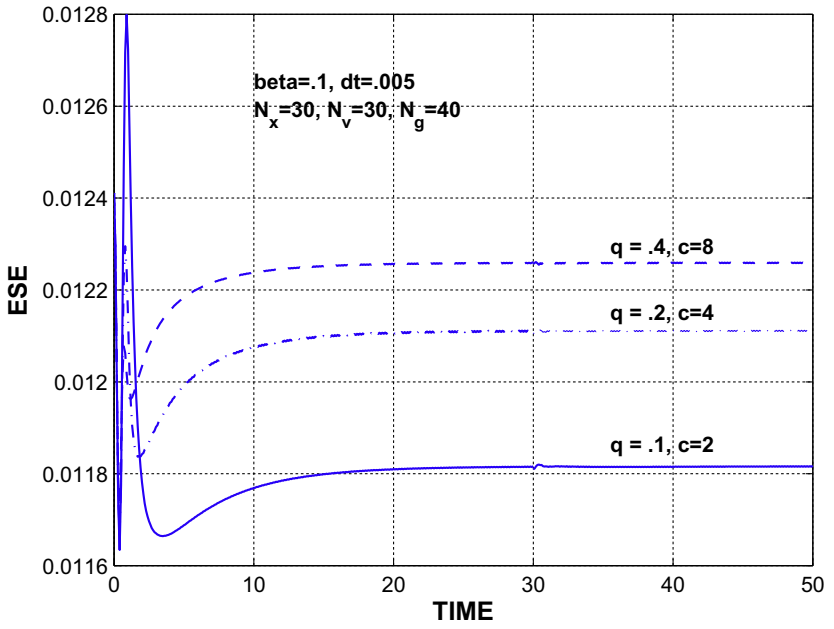

Fig. 17. Electrostatic energy for shifted Maxwellian, time dependent and steady state solutions.

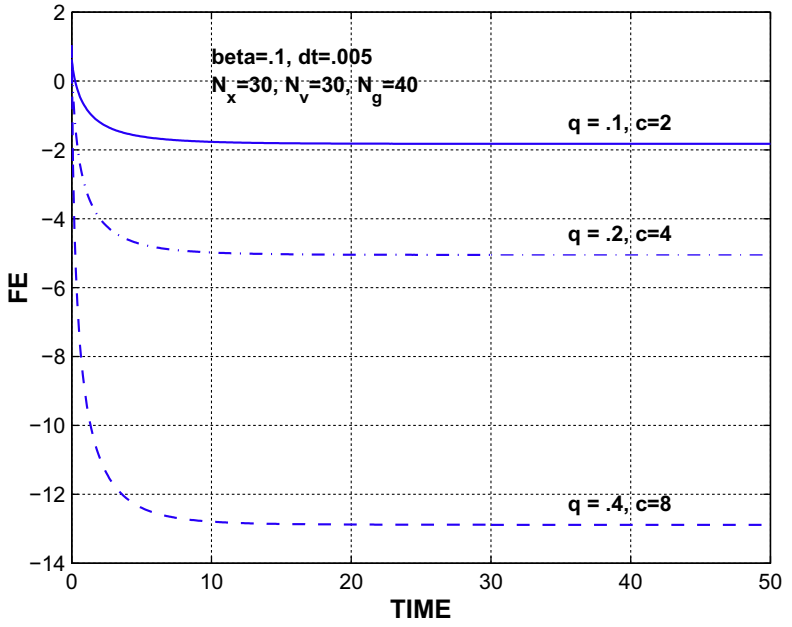

Fig. 18. Free energy for shifted Maxwellian, time dependent and steady state solutions.

approach to steady state computed on the interval [0,30] and the steady state solution graphed on the interval [30,50]. For the *ese* and *FE* a comparison is not made to exact values. As $\phi(x)$ is not known exactly at the steady state we are not able to determine analytically exact steady state values for *ese* and *FE*. None-the-less, the computations provide verification that the time dependent solution on $[0,T], T = 30$ converges to a time independent solution of the form (4.1) and (4.2).

To give a graphical demonstration of pointwise convergence to the steady state we show the evolution of a 1-D profile of the approximate solution at times of regriding. For this example $\Delta t = .005,\ N_g = 40$, so $T_1 = \Delta\tau = .2$, and regriding occurs at time $\tau_m = .2m,\ m = 1,2,\ldots,M,\ M = 150$. Thus, $0 \leqslant \tau_m \leqslant 30$. We consider the computation for $\beta = .1,\ q = .1$, the solid line in Figs. 16–18. The 1-D profile is obtained by letting $i_1 = 15, i_2 = 15, j_2 = 15$, and $j_1 = 1,2,\ldots,N_v,\ N_v = 30$. The grid function obtained from the regriding process of Section 3.3 at time $\bar{t}_k = \tau_m$ is denoted $g_{i,j}^{m,0}$ for $m = 1,2,\ldots,M$ where $M = 150$. We note

that $g_{i,j}^{m,0} \approx f(\xi_i, \eta_j, mT_1)$ for $f(x, v, t)$ the solution to (1.1) and (1.2) with initial data (4.21). For i_1, i_2, j_2 constant and j_1 variable let $f_{j_1}^m = g_{i,j}^{m,0}$. The initial profile at time $\tau_m = 0$ is denoted $f_{j_1}^i = g_{i,j}^{0,0}$ where $g_{i,j}^{0,0}$ is defined in Section 3.2.1 on the basis of the initial function $f_0(x, v)$ given by (4.21). There is not an exact analytical solution for the steady state for this example. A best approximation to the "exact" 1-D profile for the steady state solution is taken to be $f_{j_1}^e = f_0(\xi_i, \eta_j)$ where $f_0(\xi_i, \eta_j)$ is the approximation to (4.1) and (4.2) given by (4.23). Fig. 19 shows the graphs of $f_{j_1}^i$, $f_{j_1}^e$ and $f_{j_1}^m$ for $m = 25, 50$, and 150 plotted as functions of η_{1,j_1}. That is we plot the initial profile at $\tau_m = 0$, the evolution of the solution profile at times $\tau_m = 5, 10, 30$, and the"exact" steady state profile. The graph of $f_{j_1}^i$ is the dashed line, the graphs of $f_{j_1}^m$ for $\tau_m = 5, 10, 30$

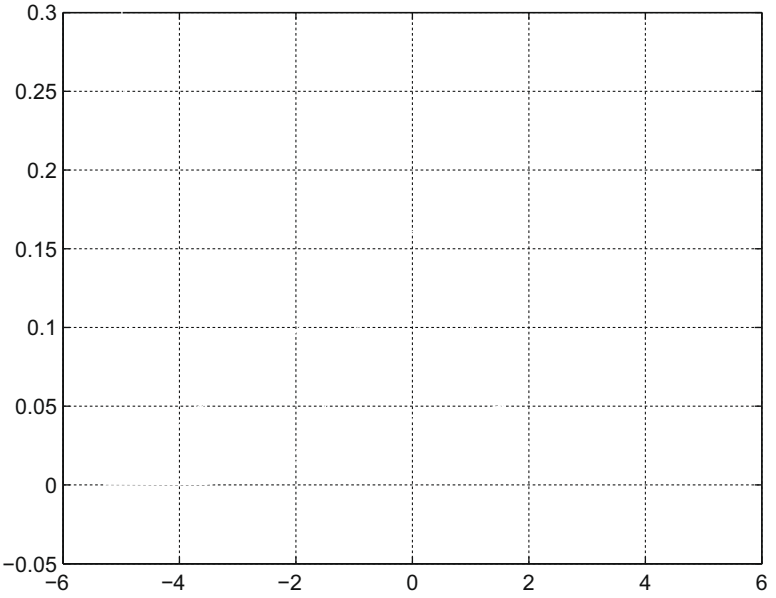

are given by solid lines, the graph of $f^e_{j_1}$ is a dashdot line. Thus, for $m = 150,\ \tau_m = 30$ the graph of $f^m_{j_1}$ has converged closely to the"exact" profile, $f^e_{j_1}$. For $m = 150$ the maximal difference between $f^m_{j_1}$ and $f^e_{j_1}$ is $max_{j_1}|f^m_{j_1} - f^e_{j_1}| = .0032$. The relative maximal difference is $\max_{j_1}|f^m_{j_1} - f^e_{j_1}|/\max_{j_1}(f^e_{j_1}) = .0201$.

For the computations up to this point the Eq. (3.4) has been solved by the iterative SOR method. Referring to Section 3.2.2 for the notation the iterative procedure (3.6) and (3.7) continues until $\|h^{k+1} - h^k\| < 10^{-12}$ at which point it is stopped and $\bar{g}^{n+1}_{i,j} = h^{k+1}_{i,j}$. As the diffusion parameter q is increased the number of iterations required for convergence of the SOR algorithm increases. This is because the quantity $\Theta(t_n)$ following (3.5) gets close to one for large q. Thus the number of iterations of the Jacobi method increases, and there is an increase in the number of iterations needed for the SOR procedure (3.6) and (3.7) as well. For q sufficiently large the more efficient method for solving (3.4) can be the direct Douglas–Rachford method (3.15)–(3.17) and (3.18). To demonstrate the use of the Douglas–Rachford method we consider initial data of the form (4.21) and compute the time dependent solution to (1.1) and (1.2) with $\beta = 1, q = 2$. The other computational parameters are the same as for $\beta = .1, q = .2$ in Figs. 16–18. If $\beta = .1, q = .2$ the SOR method requires on average 9–10 iterations to solve (3.4) to a tolerance of 10^{-12} in carrying out the particle computation on $[0, T_1], T_1 = .2$. If $\beta = 1, q = 2$ the number of iterations required of the SOR method to reach the tolerance of 10^{-12} is on average 20–21 on $[0, T_1], T_1 = .2$. In this case the more time efficient method for solving (3.4) is the Douglas–Rachford method. For $\beta = 1, q = 2$ we, therefore, solve (3.4) according to the procedure (3.15)–(3.17) and (3.18). We note that the steady state solution (4.1) and (4.2) depends only on the ratio q/β. Therefore, with other parameters the same the solution to (1.1) and (1.2) with $\beta = 1, q = 2$ converges to the same limiting solution as with $\beta = .1,\ q = .2$. However, the convergence to the limit is faster with the larger β, q values. The solution for $\beta = 1, q = 2$ is computed on the time interval $[0, T], T = 10$. Fig. 20 shows the graphs of kinetic energy, *ke*, for the solution with $\beta = 1, q = 2$ compared to the solution with $\beta = .1, q = .2$ (computed with the SOR algorithm). The dashdot line is for $\beta = 1, q = 2$, the solid line for $\beta = .1, q = .2$. As expected the two solutions converge to the same limit with the larger q, β values resulting in the faster convergence. From (4.4) the exact limiting value of *ke* is $ke \to 2$. Fig. 21 shows the *FE* graphs, the dashdot line for $\beta = 1, q = 2$, the solid line for $\beta = .1, q = .2$. The two graphs approach the same limit. In this case we do not have an exact *FE* value for comparison.

4.4. Computation on a parallel computer

In computing the numerical method of Section 3 an effort has been made to write a computer program to run on a parallel computer. At this point the process of parallelizing the algorithms is not complete although some progress has been made as will be described. Referring to Section 3.1 parallel computations are done for quantities given in terms of the four dimensional phase space variables (ξ_i, u_j) with indices $i = (i_1, i_2),\ j = (j_1, j_2)$. Within this context the most significant computation not yet parallelized is that to compute the solution to (3.4), i.e., the SOR algorithm (3.6) and (3.7) or the Douglas–Rachford method (3.15)–(3.17) and (3.18). The other relatively large computation that has not been parallelized is the regriding of Section 3.3. However, as the regriding is done relatively infrequently it does not account for much time in the overall computation. All other computations involving (ξ_i, u_j) with indices $i = (i_1, i_2),\ j = (j_1, j_2)$ have been adapted to run on a parallel

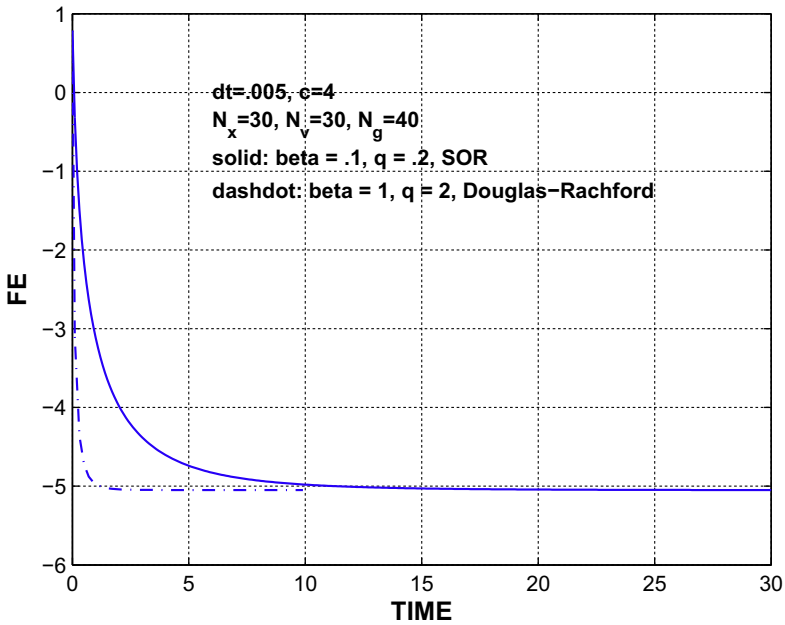

Fig. 21. Free energy for $\beta = .1, q = .2$ using the SOR method and $\beta = 1, q = 2$ using the Douglas–Rachford method.

multiprocessor system. Computations on a 2-D space involving only two indices are not parallelized and run simultaneously on each processor as needed. These computations are the solution to the Poisson equation (3.34) and computations involving the field at the Poisson mesh points.

The computer program is written in Fortran 77 for a parallel computer with MPI (multiprocessor interface). Our reference for writing the program is [22]. For computations involving indices $i_1, i_2 = 1, \ldots, N_x; j_1, j_2 = 1, \ldots, N_v$ division between processors is carried out on the basis of the index j_2. Let $N_v = n_a n_b$ for integers n_a, n_b. Then for $j_2 = 1, \ldots, N_v$ groups of n_a indices of j_2 are allocated to n_b processors. So on processor 0, $i_1, i_2 = 1, \ldots, N_x, j_1 = 1, \ldots, N_v$, and $j_2 = 1, \ldots, n_a$; on processor 1, i_1, i_2, j_1 are the same and $j_2 = n_a + 1, \ldots, 2n_a$; on processor $n_b - 1$, i_1, i_2, j_1 are the same and $j_2 = (n_b - 1)n_a + 1, \ldots, N_v$. The quantities in Section 3 that are computed according to this format are as follows: $\rho_\kappa(t_n)$ based on expression (3.32); the field $\bar{E}_l$ and the first and second partial derivatives of the field at particle positions (these quantities are obtained from expressions (3.36)–(3.38) in which $x_1 = x_1(i, j, t_n), x_2 = x_2(i, j, t_n)$); the kinetic energy based on (3.45) and entropy based on (3.46); the particle trajectories and first and second partial derivatives from Eqs. (3.19)–(3.24), (3.27) and (3.28); the coefficients $c_l(i, j, t_n), l = 1, \ldots, 10$, defined at the end of Section 3.2.4; the coefficients $c_l(i, j, t_n), l = 11, \ldots, 14$, defined at the end of Section 3.2.5.

To demonstrate the parallel computation we consider the example of Figs. 5 and 6 with $q = .0005$. Here the initial data is given by (4.13), grid parameters are $N_x = 20, N_v = 20$. The regrid parameter is $N_g = 100$. The number of processors used, n_b, is a factor of 20. Computations are done for $n_b = 1, 5, 10, 20$. The program is run on a 400 node Xeon-based 64-bit Linux, Beowulf cluster. One complete cycle of the numerical procedure of Section 3 is computed. That is, the grids are set up, 3.1, and initial data is computed, 3.2.1; then $N_g = 100$ steps of the deterministic particle method of Section 3.2 is carried out, i.e., 3.2.2,–,3.2.6, and included are the computations of *ese*, *ke*, *FE* of 3.4; when $n = N_g = 100$ the regriding of Section 3.3 is done and the computation is stopped. The results of the computation are given in Table 1. In Table 1 "Total" refers to the total time of the computation in seconds, "DP-Total" is the amount of time spent on the 100 steps of the deterministic particle (DP) method of Section 3.2, "DP-Pl" is the time spent on the parts of the DP method of Section 3.2 for which the computations are parallelized. Thus if 1 processor is used the total computation time is 228.21 seconds. The total time spent on the DP method is 225.61 seconds and of this 171.46 seconds are spent on computations that are parallelized. The parts of the DP method that are not parallelized are the computation of (3.4) (the SOR algorithm is used) and the computations on the 2-D grid. The 2-D computations are solving the Poisson equation (3.34), obtaining the field and its derivatives at the Poisson mesh points, and computing the *ese*. The 2-D computations account for a small amount of computing time. Most of the time in the nonparallel part of the DP method is taken up with the computation of (3.4). Thus, with 1 processor DP-Total-DP-Pl = 54.15 seconds. The total time computing (3.4) is 50.68 seconds. The difference between Total = 228.21 seconds and DP-Total = 225.61 seconds is mainly taken up with the regriding of Section 3.3.

If more than one processor is used the time for DP-Pl is significantly reduced and scales well with the number of processors used. Table 1 gives the results for 5, 10, and 20 processors. However, the quantity DP-Total-DP-Pl increases. This is due to the fact that (3.4) is computed on a single processor and the result needs to be broadcast to all the processors for subsequent computations. Also, the coefficients in (3.4) are obtained from parallel computations and need to be gathered onto a single processor for the computation of (3.4). The time for these gathering a broadcasting operations increases significantly with the number of processors being used. These effects are demonstrated in Table 2. In this table "DP-Total" is abbreviated "DP-T", so the time spent on the nonparallel part of the DP method is "DP-T-DP-Pl". The total time spent gathering coefficients, computing (3.4), and broadcasting the result is "Time (3.4)", and "% (3.4)" gives the ratio"Time (3.4)/(DP-T-DP-Pl)". Thus, if 1 processor is used 94% of time spent in the nonparallel part of the DP method is used in computing (3.4). If 5, 10, or 20 processors is used 88% to 90% of nonparallel computing time is used in the computations involving (3.4).

Referring to Table 1 it is clear that most of the computing time is spent on the deterministic particle (DP) method. The regriding which is the main component of "Total-DP-Total" is a small contribution to the total time of computation. The time

Table 1
Time in seconds, parallel program.

Processors	DP-Pl	DP-Total	Total
1	171.46	225.61	228.21
5	34.84	117.43	119.66
10	14.83	103.77	105.70
20	7.18	101.60	104.40

Table 2
Time for nonparallel computations.

Processors	DP-T-DP-Pl	Time (3.4)	% (3.4)
1	54.15	50.68	.94
5	82.59	73.01	.88
10	88.94	79.02	.89
20	94.42	84.71	.90

for the DP method, "DP-Total", is reduced from 225.61 seconds with 1 processor to 101.60 seconds with 20 processors. The total computation time reduces from 228.21 seconds with 1 processor to 104.40 seconds with 20 processors. This is a reduction in computing time of about 46%. To obtain a significant further reduction in computing time it is necessary to develop a parallel algorithm for solving (3.4) and to avoid the broadcasting and gathering operations that are presently being used. A parallel program for solving (3.4) can be based on the SOR method, (3.6) and (3.7), or the Douglas–Rachford method, (3.15)–(3.17) and (3.18).

The complete computation of the example of Figs. 5 and 6 with $q = .0005$ requires 5000 time steps and 50 cycles of the numerical method of Section 3. Using 10 processors a total run time of this computation was 5114.18 seconds or about 1 hour and 25 minutes. This is approximately what one could expect by taking the run time under "Total" of Table 1 for 10 processors and multiplying the number by 50.

5. Conclusion

It is shown in this paper that the numerical procedure of [28] for approximating the 1-D Vlasov–Poisson–Fokker–Planck system can be carried out for the system in two dimensions. The numerical approximation can be considered a type of deterministic particle method. In two dimensions various computations become more lengthy and somewhat more complicated, but otherwise there is a reasonably straight forward generalization of the components of the numerical method from 1-D to 2-D. Also, in two dimensions it becomes meaningful to consider the electrostatic problem with a constant, perpendicular magnetic field. The numerical approximation is easily adapted to include the constant magnetic field. The computational examples show that the numerical method is convergent and accurate on an extended time interval. The order of accuracy is demonstrated computationally to be first order in time and second order in the spatial small parameters. This is consistent with the order of accuracy found for the approximation in one dimension.

It is conjectured that the solution to (1.1) and (1.2) with zero magnetic field and the solution to (2.16) and (1.2) with constant, nonzero magnetic field both converge to the same steady state solution given by (4.1) and (4.2). There is not a complete analytical proof to guarantee this convergence; however, computational examples are given that demonstrate that the solution with both zero and nonzero magnetic field converge for large time to the same limit. The computational work, therefore, provides some verification for the assumption that solutions to (1.1) and (1.2) and (2.16) and (1.2) both converge as $t \to \infty$ to (4.1) and (4.2).

Parts of the numerical method are readily adapted to run on a parallel computer, and this parallelization significantly reduces the overall run time for the computer program. The main component of the numerical procedure that has not yet been parallelized is the approximation of the PDE (2.9). At present this is setting the limit on the reduction in computing time that is achieved by the parallel program.

Acknowledgements

We would like to acknowledge the help and support provided by the CUNY High Performance Computing Center that make the parallel computations possible. We would also like to thank the referees for useful suggestions that added to the paper.

References

[1] E.J. Allen, H.D. Victory Jr., A computational investigation of the random particle method for numerical solution of the kinetic Vlasov–Poisson–Fokker–Planck equations, Phys. A 209 (1994) 318–346.
[2] W.F. Ames, Numerical Methods for Partial Differential Equations, Barnes and Noble, Inc., New York, 1971.
[3] M. Asadzadeh, P. Kowalczyk, Convergence analysis of the streamline diffusion and discontinouous Galerkin methods for the Vlasov–Fokker–Planck system, Numer. Methods Partial Differ. Equat. 21 (2005) 472–495.
[4] M. Asadzadeh, A. Sopasakis, Convergence of a *hp*-streamline diffusion scheme for Vlasov–Fokker–Planck system, Math. Models Methods Appl. Sci. 17 (8) (2007) 1159–1182.
[5] A.R. Bell, A.P.L. Robinson, M. Sherlock, R.J. Kingham, W. Rozmus, Fast electron transport in laser-produced plasmas and the KALOS code for solution of the Vlasov–Fokker–Planck equation, Plasma Phys. Control. Fusion 48 (2006) R37–R57.
[6] L.L. Bonilla, J.A. Carrillo, J. Soler, Asymptotic behavior of an initial-boundary value problem for the Vlasov–Poisson–Fokker–Planck system, SIAM J. Appl. Math. 57 (1997) 1343–1372.
[7] C. Buet, S. Cordier, P. Degond, M. Lemou, Fast algorithms for numerical, conservative and entropy approximations of the Fokker–Planck–Landau equation, J. Comput. Phys. 133 (1997) 310–322.
[8] F. Bouchut, J. Dolbeault, On long time asymptotics of the Vlasov–Fokker–Planck equation and of the Vlasov–Poisson–Fokker–Planck system with coulombic and Newtonian potentials, Differ. Integral Equat. 8 (3) (1995) 487–514.
[9] J. Candy, R.E. Waltz, An Eulerian Gyrokinetic–Maxwell solver, J. Comput. Phys. 186 (2003) 545–581.
[10] S. Chandrasekhar, Stochastic problems in physics and astronomy, Rev. Mod. Phys. 15 (1943) 1–89.
[11] N. Crouseilles, F. Filbert, Numerical approximation of collisional plasmas by high order methods, J. Comput. Phys. 201 (2) (2004) 546–572.
[12] J. Denavit, B.W. Doyle, R.H. Hirsch, Nonlinear and collisional effects on Landau Damping, Phys. Fluids 11 (10) (1968) 2241–2250.
[13] J.M. Donoso, E. del Rio, Integral propagator solvers for Vlasov–Fokker–Planck equations, J. Phys. A: Math. Theor. 40 (2007) F449–F456.
[14] E.M. Epperlein, Fokker–Planck modeling of electron transport in laser-produced plasmas, Laser Part. Beams 12 (1994) 257–272.
[15] K.J. Havlak, H.D. Victory Jr., The numerical analysis of random particle methods applied to Vlasov–Poisson–Fokker–Planck kinetic equations, SIAM J. Numer. Anal. 33 (1996) 291–317.
[16] K.J. Havlak, H.D. Victory Jr., On deterministic particle methods for solving Vlasov–Poisson–Fokker–Planck systems, SIAM J. Numer. Anal. 35 (4) (1998) 1473–1519.

[17] F.L. Hinton, Collisional transport in plasma, in: M.N. Rosenbluth, R.Z. Sagdeev (Eds.), Handbook of Plasma Physics, vol. 1, North-Holland, Amsterdam, 1983.
[18] R.W. Hockney, J.W. Eastwood, Computer Simulation Using Particles, Adam Hilger, Bristol, 1988.
[19] R.J. Kingham, A.R. Bell, An implicit Vlasov–Fokker–Planck code to model non-local electron transport in 2-D with magnetic field, J. Comput. Phys. 194 (2004) 1–34.
[20] A. Lenard, I.B. Bernstein, Plasma oscillations with diffusion in velocity space, Phys. Rev. 112 (5) (1958) 1456–1459.
[21] E.M. Lifshitz, L.P. Pitaevskii, Physical Kinetics, Pergamon Press, Oxford, 1981.
[22] P.S. Pacheco, Parallel Programming with MPI, Morgan Kaufman Publishers, San Francisco, 1997.
[23] L. Pareschi, G. Russo, G. Toscani, Fast spectral methods for the Fokker–Planck–Landau collision operator, J. Comput. Phys. 165 (2000) 236–316.
[24] H. Risken, The Fokker–Planck Equation: Methods of Solution and Applications, Springer-Verlag, Berlin, 1989.
[25] J. Schaeffer, A difference scheme for the Vlasov–Poisson–Fokker–Planck system, Research Report No. 97-NA-004, Department of Mathematical Sciences, Carnegie Mellon University, 1997.
[26] M. Shoucri, R.R.J. Gagne, Numerical solution of a two-dimensional Vlasov equation, J. Comput. Phys. 25 (1977) 94–103.
[27] J.W. Thomas, Numerical Partial Differential Equations, Springer-Verlag, New York, 1995.
[28] S. Wollman, E. Ozizmir, Numerical approximation of the Vlasov–Poisson–Fokker–Planck system in one dimension, J. Comput. Phys. 202 (2005) 602–644.
[29] S. Wollman, E. Ozizmir, A numerical method for the Vlasov–Poisson–Fokker–Planck system in two dimensions, Proc. Neural Parallel Sci. Comput. 3 (2006) 44–47.
[30] S. Wollman, E. Ozizmir, A deterministic particle method for the Vlasov–Fokker–Planck equation in one dimension, J. Comput. Appl. Math. 213 (2008) 316–365.